Supporting Information

Mixed-linker solid solutions of functionalized pillared-layer MOFs - Adjusting structural flexibility, gas sorption, and thermal responsiveness

I. Schwedler,[a,b] S. Henke,[a,b,*] M. T. Wharmby,[b,c] S. Bajpe,[b] A. K. Cheetham[b,*] and R. A. Fischer[a,*]

[a] *Lehrstuhl für Anorganische Chemie II – Organometallics and Materials, Ruhr-University Bochum, Universitätsstraße 150, D-44801 Bochum (Germany).*

[b] *Functional Inorganics and Hybrid Materials Group, Department of Materials Science and Metallurgy, University of Cambridge, 27 Charles Babbage Road, Cambridge CB3 0FS (UK).*

[c] *Diamond Light Source Ltd. Diamond House, Harwell Science & Innovation Campus, Didcot, Oxfordshire, OX11 0DE (UK).*

Content

1 Single Crystal X-ray Diffraction Data

Table S1. Crystallographic data of $Zn_2(DPe\text{-}bdc)_2dabco$ **(4)** determined by single crystal X-ray diffraction at 300 K.

	4
Empirical formula	$C_{21}H_{30}NO_6Zn$
Formula Weight	457.83
T / K	300(3)
λ / Å	0.71073
Crystal size / mm^3	0.382 × 0.199 × 0.156
Crystal system	tetragonal
Space group	*P*4/*nnc*
a [Å]	15.43134(14)
b [Å]	15.43134(14)
c [Å]	19.2746(3)
α [°]	90.00
β [°]	90.00
γ [°]	90.00
V [$Å^3$]	4589.80(10)
Z	8
ρ_{calc} [g cm^{-3}]	1.325
Absorption coefficient [mm^{-1}]	1.104
F(000)	1928.0
2Θ range [°]	4.226 to 55.996
Index ranges	$-19 \leq h \leq 20$, $-20 \leq k \leq 20$, $-25 \leq l \leq 25$
Reflections collected	25509
Independent reflections	2788
R_{int}	0.0445
Data / restrains / parameters	2788/44/155
Data completeness [%]	99.95
Refinement method	Full-matrix least-squares on F^2
Goodness-of-fit on F^2	1.129
R indices [$I \geq 2\sigma(I)$]	R_1 = 0.0585, wR_2 = 0.1961
R indices (all data)	R_1 = 0.0850, wR_2 = 0.2213
Largest diff. peak/hole [e $Å^{-3}$]	0.70/-0.55

2 Powder Diffraction Data

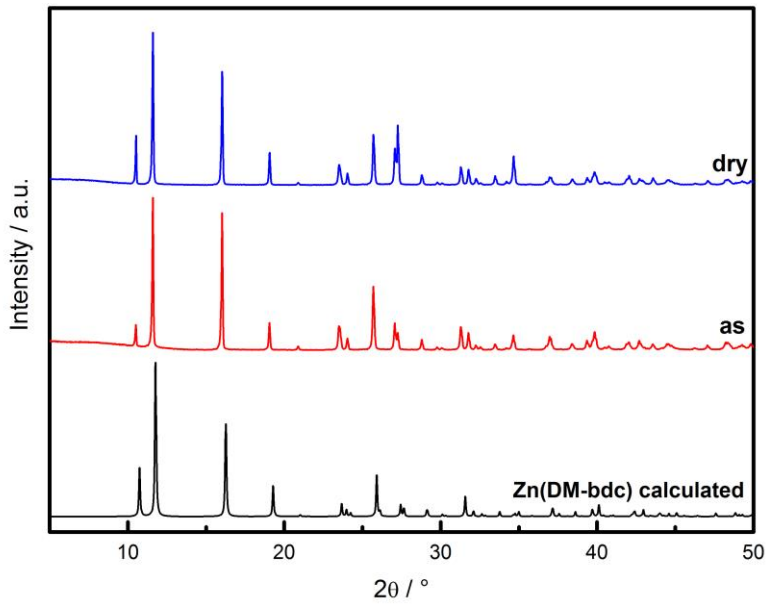

Figure S1: PXRD patterns of Zn(DM-bdc) (synthesized from a standard synthesis batch possessing molar ratios of 2 : 2 : 1 for $Zn(NO_3)_2$: H_2(DM-bdc) : dabco) as synthesized and dry in comparison to the PXRD pattern calculated from single crystal data of Zn(DM-bdc) reported previously.[1] Evidently, applying the standard conditions leads not to the expected pillared-layer Zn_2(DM-bdc)$_2$dabco framework. Incorporation of dabco is not observed and the non-porous 3D coordination polymer Zn(DM-bdc) forms.

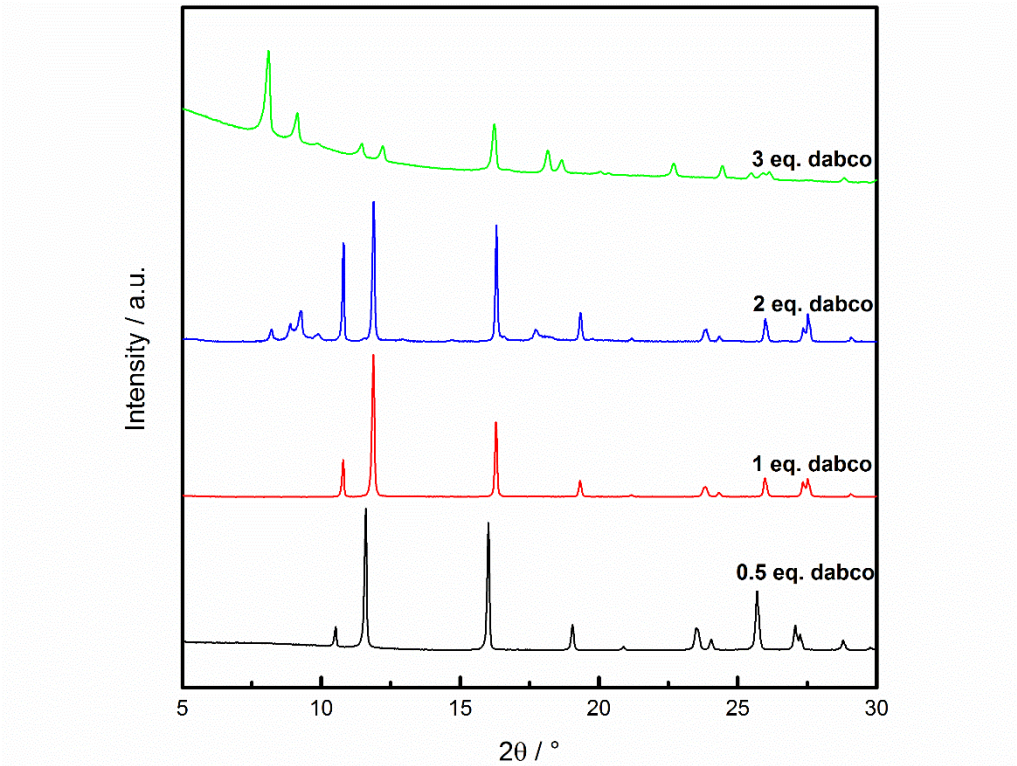

Figure S2: Crystallization study with increasing molar amounts of dabco ranging from 0.5 to 3 equivalents. PXRD patterns of the corresponding as synthesized materials obtained from these synthesis batches show that 0.5 or 1.0 equivalent dabco lead to pure phased Zn(DM-bdc). Increasing the amount to two equivalents of dabco initiates the formation of the desired Zn_2(DM-bdc)$_2$dabco phase, although Zn(DM-bdc) is still the major fraction. Further increasing of the dabco amount to three equivalents finally gave phase pure Zn_2(DM-bdc)$_2$dabco.

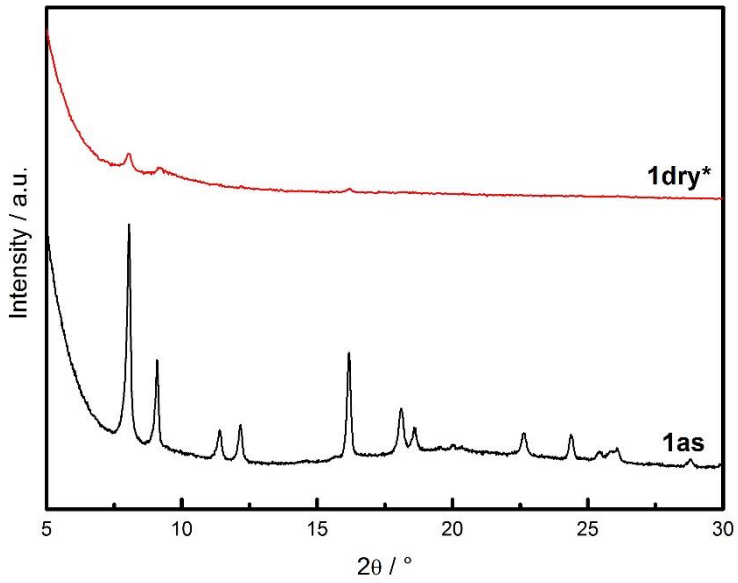

Figure S3: PXRD patterns of as synthesized and activated samples of **1**. Material **1dry*** was immeadiately stored in a glove box under full exclusion of air after activation and a significant loss of crystallinity is observed. Amorphization and collapse of the framework is anticipated when all adsorbed water molecules are removed.

Also for the parent framework $Zn_2(bdc)_2dabco$ water sensitivity is observed.[2] Related Studies show that the water sensitivity in $Zn_2(fu\text{-}bdc)_2dabco$ systems depends on the functionality of the bdc-linker and integration of small polar functional groups renders the MOF water unstable. Compound **1** features only a very small alkyl chain and the methoxy groups increase the hydrophilicity. Water molecules can coordinate to the methoxy group via hydrogen bonding and hence, the framework is more prone to water adsorption, particularly compared to the derivatives featuring longer alkyl chains. Therefore, in case of implementing the small (rather hydrophilic) DM-bdc linker, a certain amount of (stabilizing) water molecules is not only tolerated but rather seems necessary. Note, elemental analysis of **1dry** and **1dry*** was performed and proves that values obtained for **1dry*** fit significantly better to the expected values for guest-free **1** suggesting adsorption of water molecules in case of **1dry**.

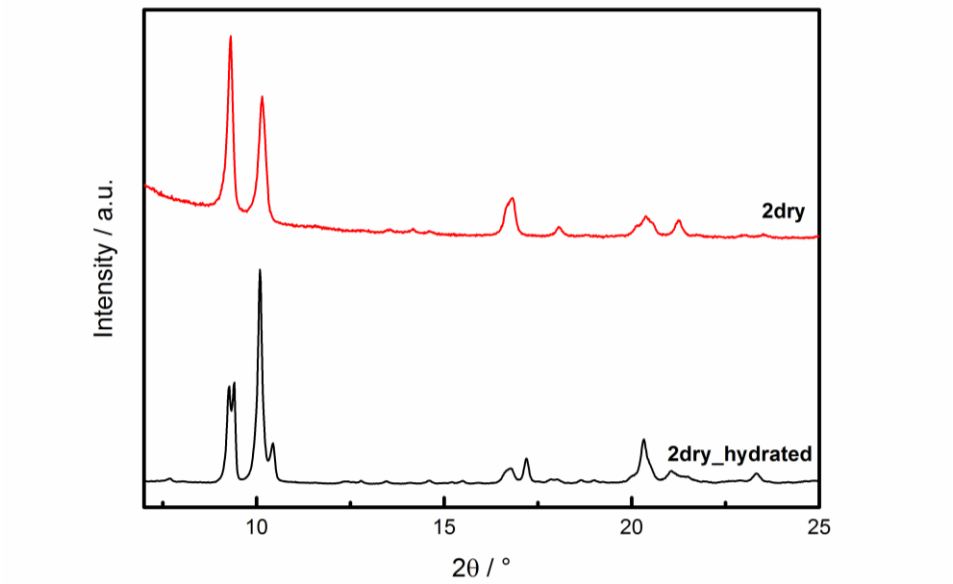

Figure S4: PXRD patterns of of activated samples **2**. Material **2dry_hydrated** war stored under air after activation, while the sample **2dry** was immeadiately stored in a glove box under full exclusion of air. Apparently, minor adsorption of water (when stored under air) leads to significant structural changes. In case of **2dry**, the pattern is identical to the reported pattern of activated $Zn_2(DE\text{-}bdc)_2dabco$.[3] Sample **2dry** was used throughout the whole studie.

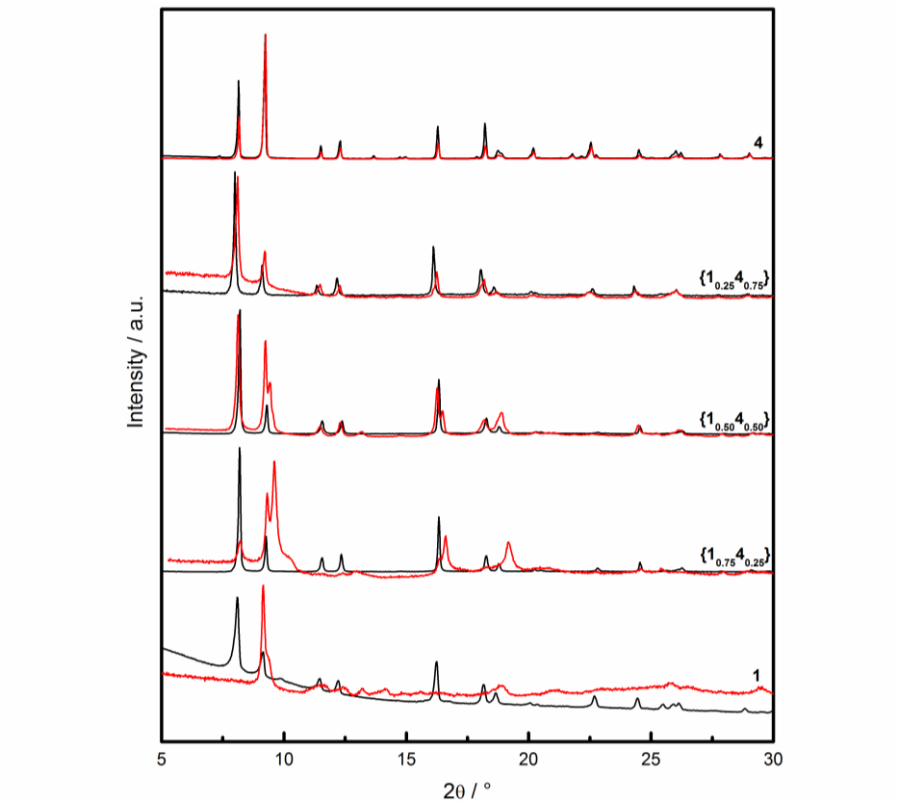

Figure S5: PXRD patterns of as synthesized (black) and dried (red) solid solutions **{1$_x$4$_{1-x}$}** in comparison to the respective single-component MOFs **1** and **4**.

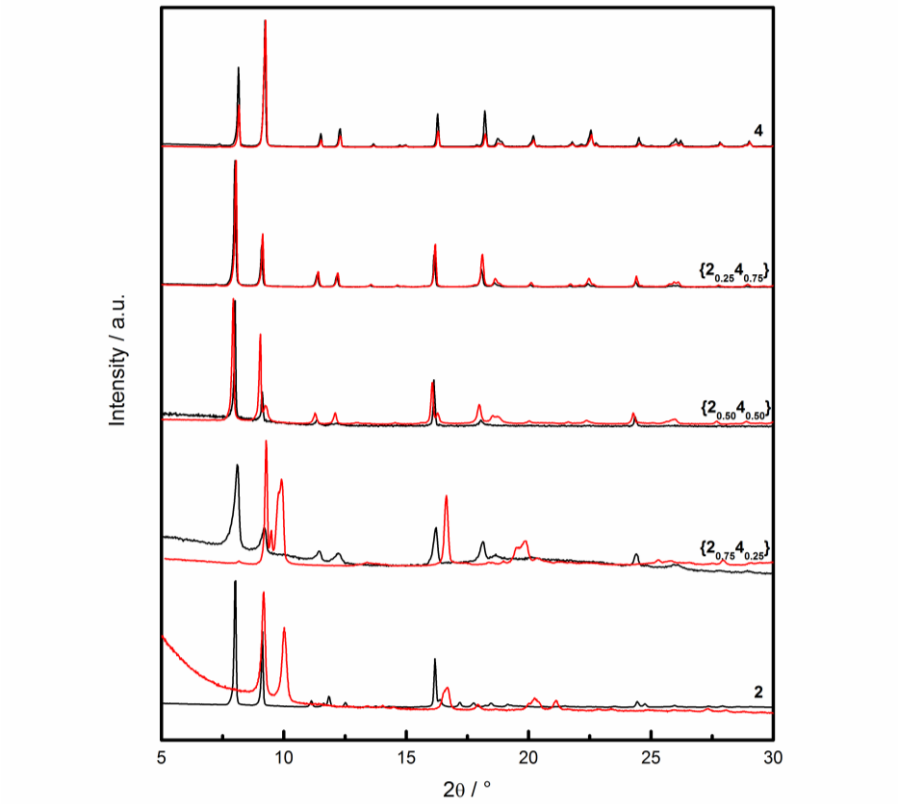

Figure S6: PXRD patterns of as synthesized (black) and dried (red) solid solutions **{2$_x$4$_{1-x}$}** in comparison to the respective single-component MOFs **2** and **4**.

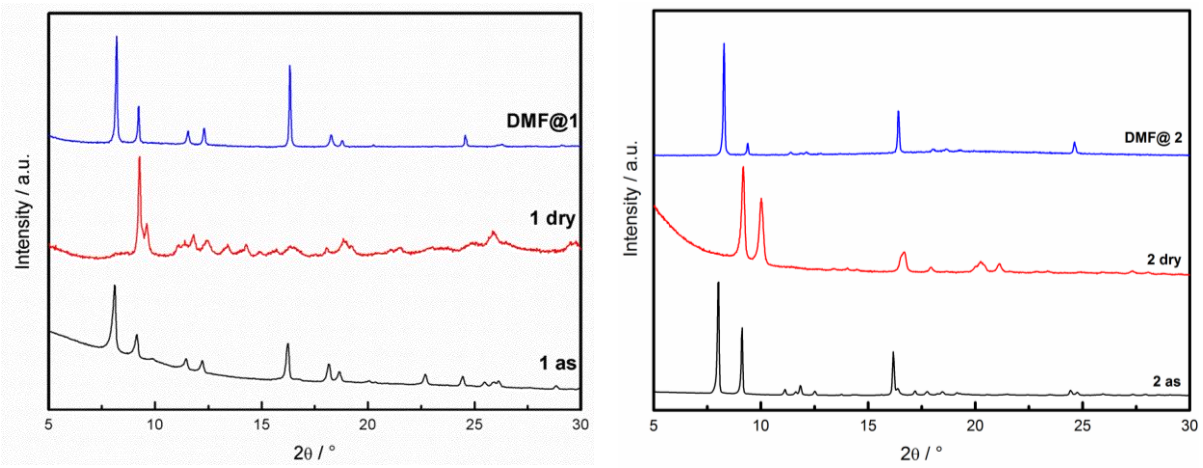

Figure S7: PXRD patterns of **1** (left) and **2** (right) in the as synthesized and dry form and after re-infiltration of DMF molecules

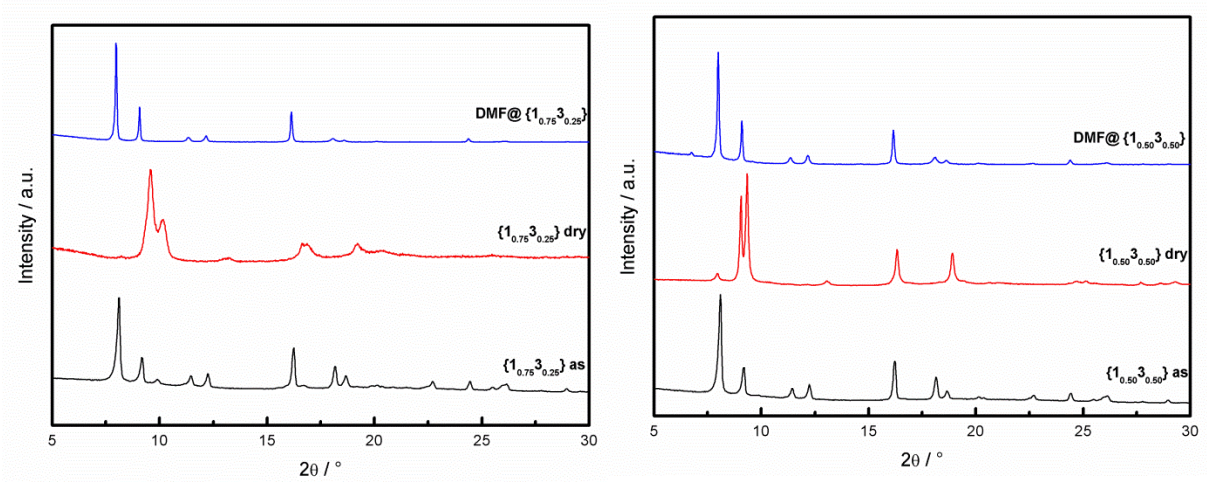

Figure S8: PXRD patterns of **{1$_{0.75}$3$_{0.25}$}** (left) and **{1$_{0.50}$3$_{0.50}$}** (right) in the as synthesized and dry form and after re-infiltration of DMF molecules.

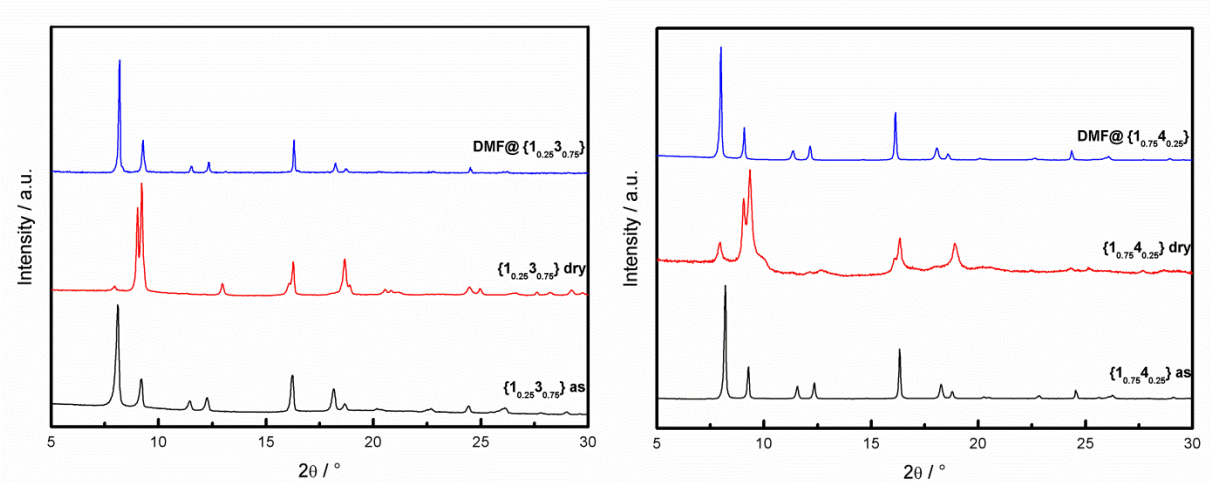

Figure S9: PXRD patterns of **{1$_{0.25}$3$_{0.75}$}** (left) and **{1$_{0.75}$4$_{0.25}$}** (right) in the as synthesized and dry form and after re-infiltration of DMF molecules.

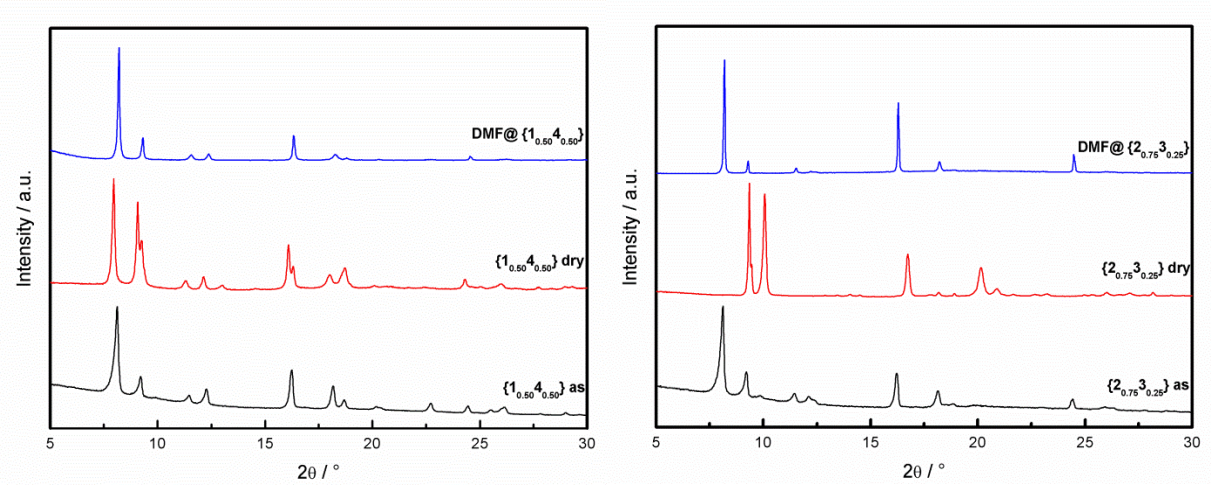

Figure S10: PXRD patterns of **{1$_{0.50}$4$_{0.75}$}** (left) and **{2$_{0.75}$3$_{0.25}$}** (right) in the as synthesized and dry form and after re-infiltration of DMF molecules.

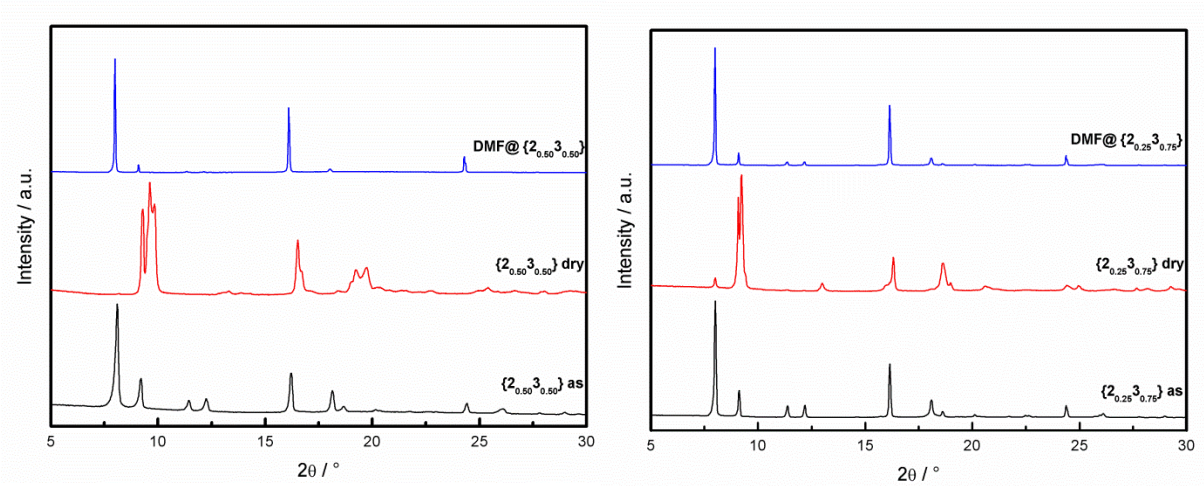

Figure S11: PXRD patterns of **{2$_{0.50}$3$_{0.50}$}** (left) and **{2$_{0.25}$3$_{0.75}$}** (right) in the as synthesized and dry form and after re-infiltration of DMF molecules.

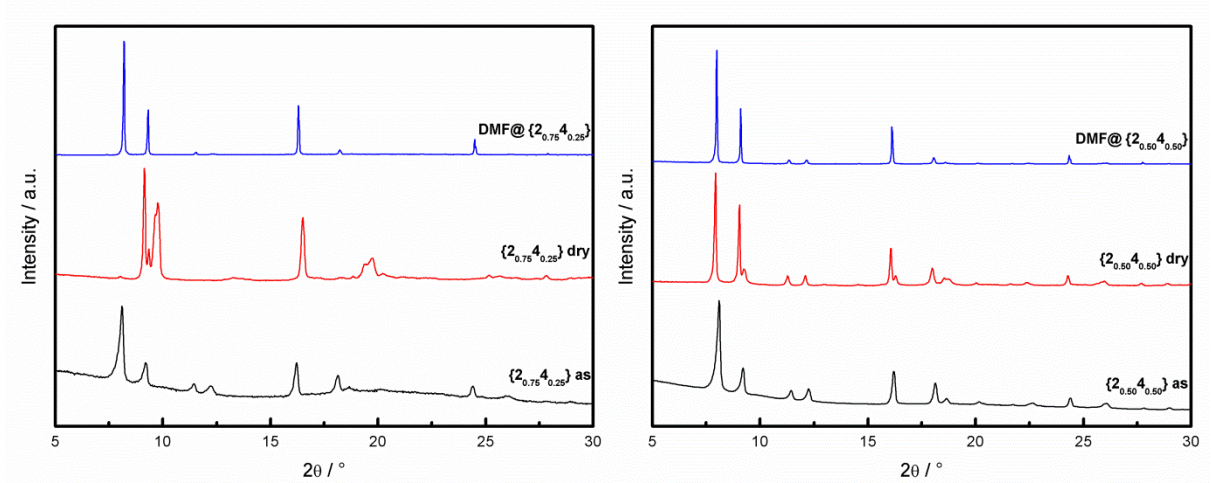

Figure S12: PXRD patterns of **{2$_{0.75}$4$_{0.25}$}** (left) and **{2$_{0.50}$4$_{0.75}$}** (right) in the as synthesized and dry form and after re-infiltration of DMF molecules.

2.1 Cell Parameter Refinement of Single-Component MOFs

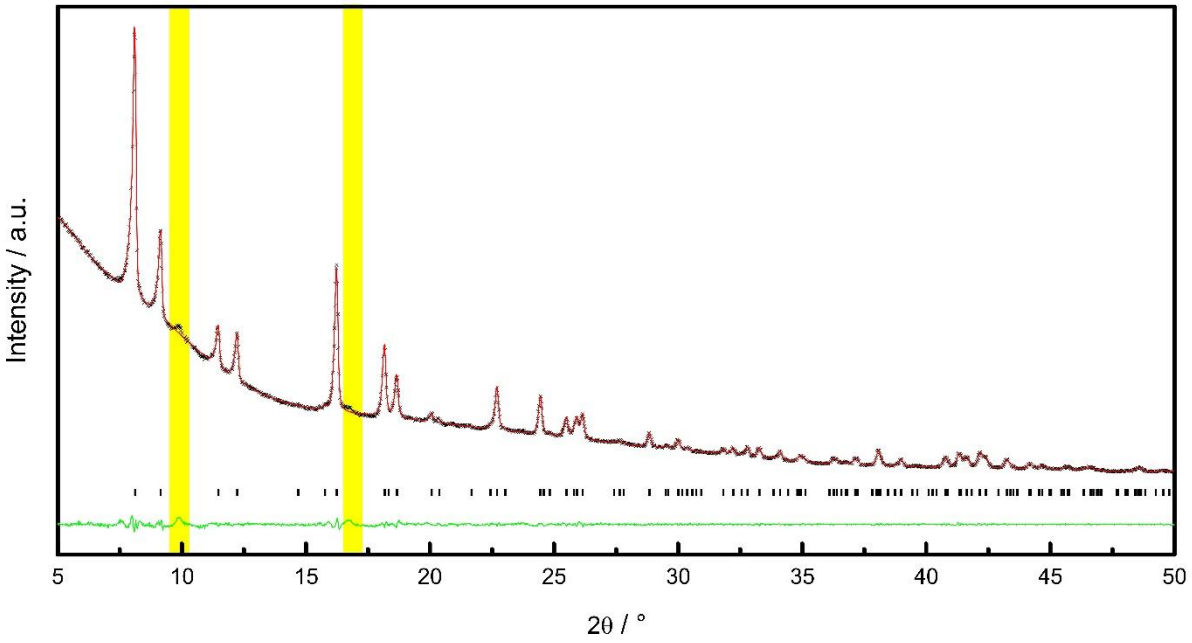

Figure S13: Pawley fit to the PXRD pattern of solvated Zn_2(DM-bdc)$_2$dabco **(1as)** collected at room temperature. The black crosses, red and green lines represent the experimental, calculated and difference profile, respectively. The black markers indicate positions of allowed Bragg reflections in the space group *P*4/*nbm*. The space group has been determined by the indexing routine of the TOPAS program package.[4] The regions shaded in yellow are excluded from the Pawley fit and are assigned to an impurity of an already partly desolvated framework structure. Cell parameters are refined to a = 15.4456(5) Å, c = 9.6822(4) Å and V = 2309.85(18) Å^3. The final R values are R_{exp}= 0.78 and R_{wp} = 1.43.

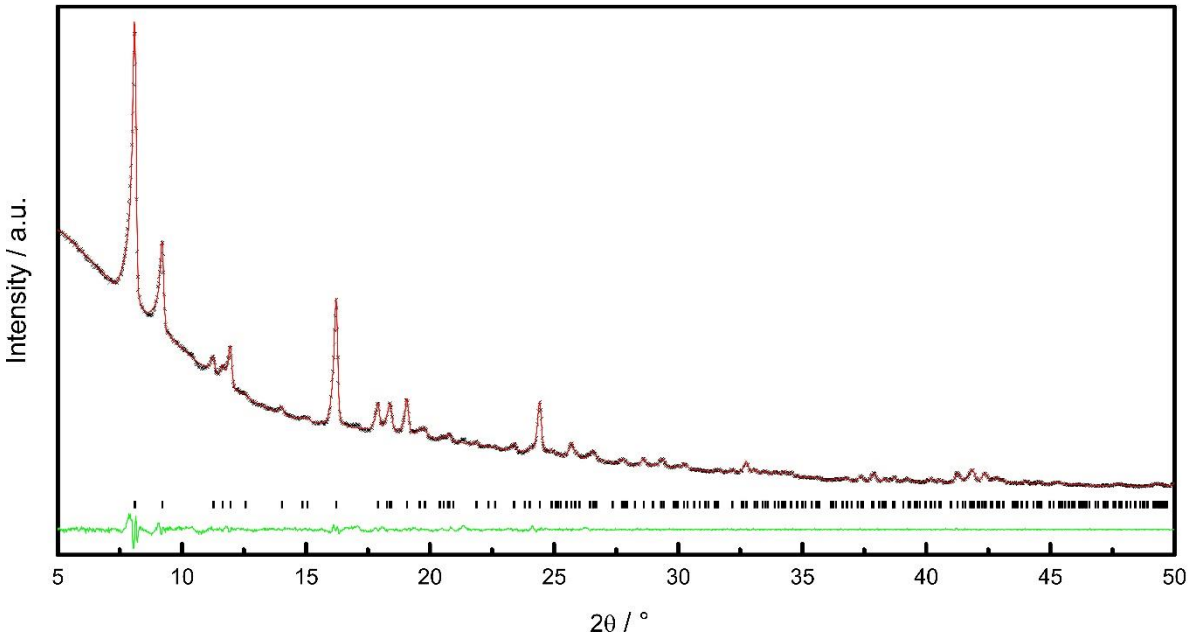

Figure S14: Pawley fit to the PXRD pattern of solvated Zn_2(DE-bdc)$_2$dabco **(2as)** collected at room temperature. The black crosses, red and green lines represent the experimental, calculated and difference profile, respectively. The black markers indicate positions of allowed Bragg reflections in the space group *C*2/*m*. Cell parameters are refined to a = 15.7698(19) Å, b = 15.2203(18) Å, c = 9.6466(9) Å, β = 94.144(11) ° and V = 2309.3(4) Å^3. The final R values are R_{exp} = 0.87 and R_{wp} = 1.63. The results are in accordance to published data.[3]

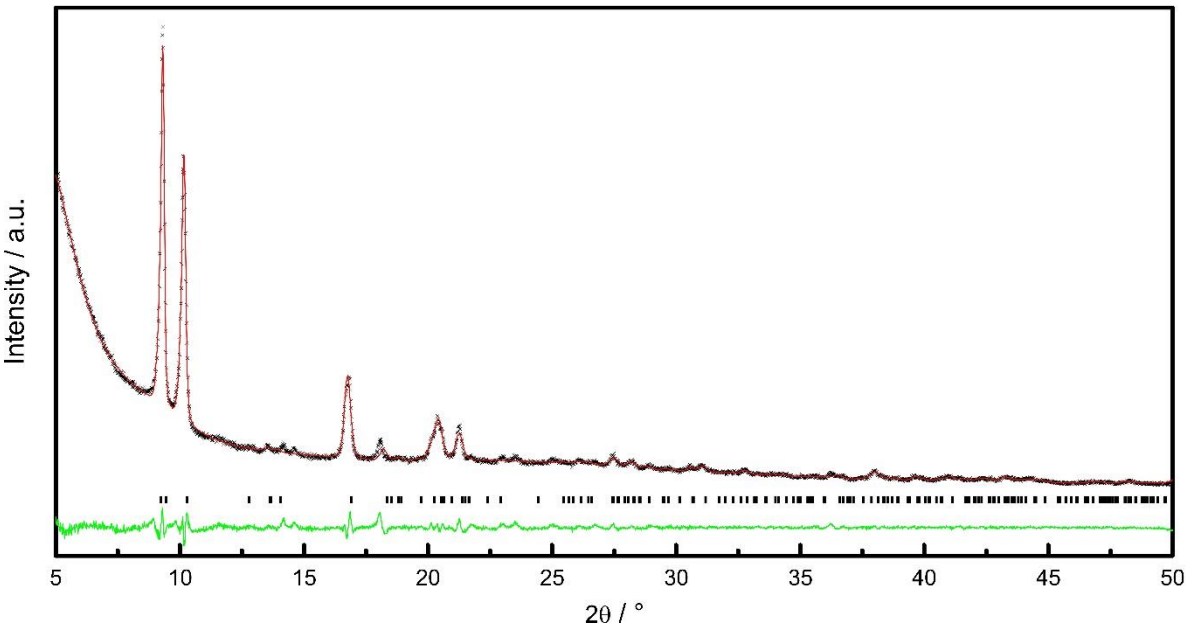

Figure S15: Pawley fit to the PXRD pattern of desolvated Zn_2(DE-bdc)$_2$dabco **(2dry)** collected at room temperature. The black crosses, red and green lines represent the experimental, calculated and difference profile, respectively. The black markers indicate positions of allowed Bragg reflections in the space group *C*2/*m*. Cell parameters are refined to a = 18.801(4) Å, b = 9.682(2) Å, c = 9.606(6) Å, β = 93.80(6° and V = 1745(1) Å^3. The final R values are R_{exp} = 2.38 and R_{wp} = 3.10. The results are in accordance to published data.[3]

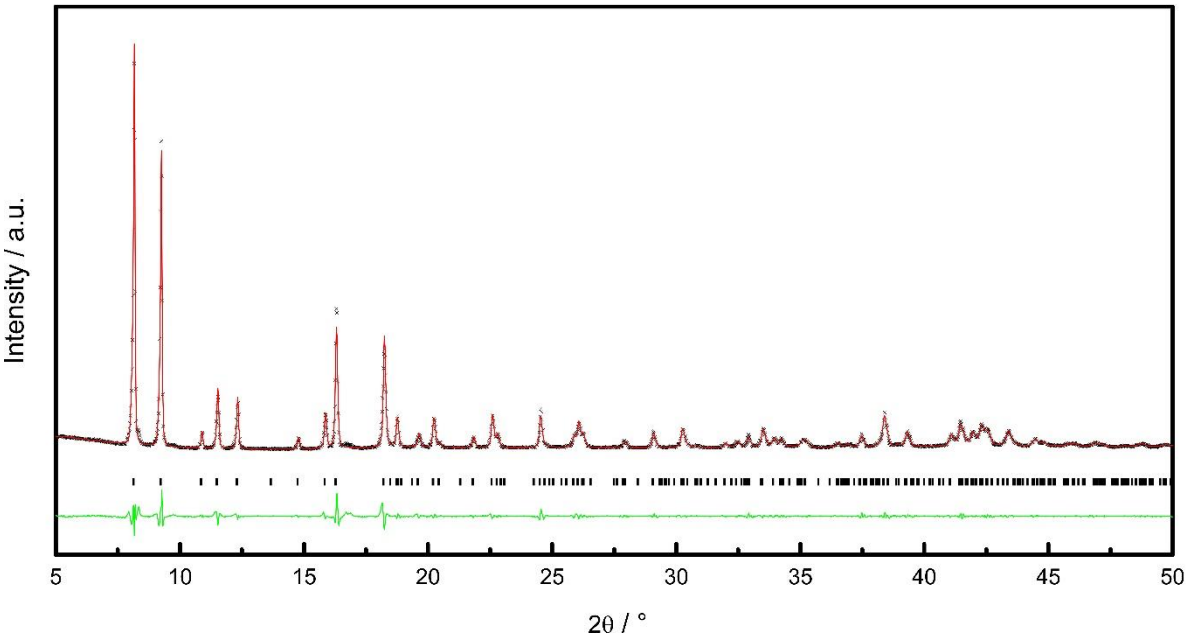

Figure S16: Pawley fit to the PXRD pattern of solvated Zn_2(DB-bdc)$_2$dabco **(3as)** collected at room temperature. The black crosses, red and green lines represent the experimental, calculated and difference profile, respectively. The black markers indicate positions of allowed Bragg reflections in the space group *P4/ncc*. The space group has been determined by the indexing routine of the TOPAS program package.[4] Cell parameters are refined to a = 15.4180(6) Å, c = 19.2234(9) Å and V = 4569.7(4) Å^3. The final R values are R_{exp} = 3.08 and R_{wp} = 8.80.

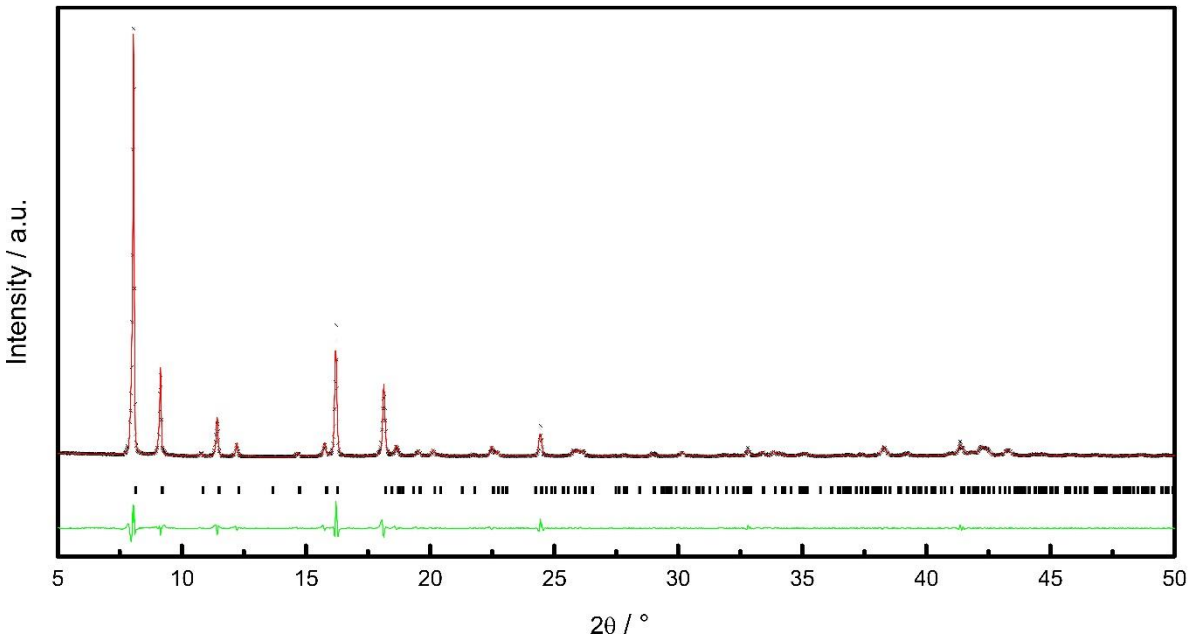

Figure S17: Pawley fit to the PXRD pattern of desolvated Zn_2(DB-bdc)$_2$dabco **(3dry)** collected at room temperature. The black crosses, red and green lines represent the experimental, calculated and difference profile, respectively. The black markers indicate positions of allowed Bragg reflections in the space group *P4/ncc*. Cell parameters are refined to a = 15.4172(6) Å, c = 19.231(1) Å and V = 4570.9(5) Å^3. The final R values are R_{exp} = 2.88 and R_{wp} = 11.37.

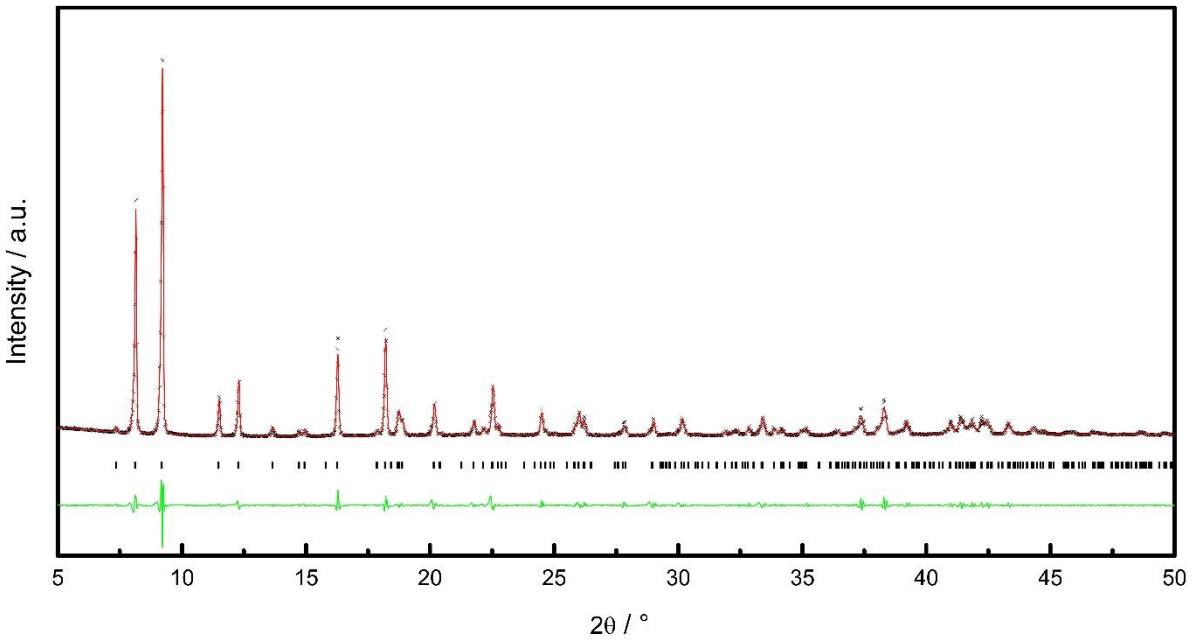

Figure S18: Pawley fit to the PXRD pattern of solvated Zn_2(DPe-bdc)$_2$dabco **(4as)** collected at room temperature. The black crosses, red and green lines represent the experimental, calculated and difference profile, respectively. The black markers indicate positions of allowed Bragg reflections in the space group *P4/nnc*. The space group and the starting values for the refinement have been taken from the single crystal structure analysis. Cell parameters are refined to a = 15.4363(6) Å, c = 19.2745(9) Å and V = 4592.7 (4) Å^3. The final R values are R_{exp} = 2.93 and R_{wp} = 9.36.

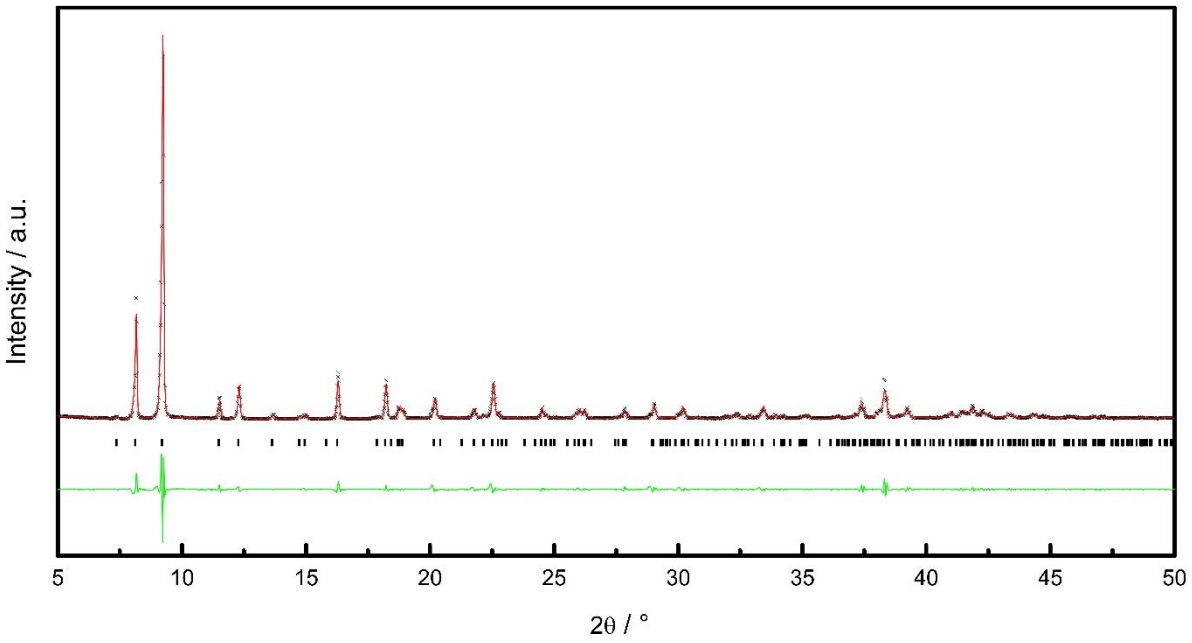

Figure S19: Pawley fit to the PXRD pattern of desolvated Zn_2(DPe-bdc)$_2$dabco **(4dry)** collected at room temperature. The black crosses, red and green lines represent the experimental, calculated and difference profile, respectively. The black markers indicate positions of allowed Bragg reflections in the space group *P4/nnc*. Cell parameters are refined to a = 15.4322(8) Å, c = 19.2679(12) Å and V = 4588.7(5) Å^3. The final R values are R_{exp} = 2.8 and R_{wp} = 12.47

2.2 Cell Parameter Refinement of Mixed-Component MOFs

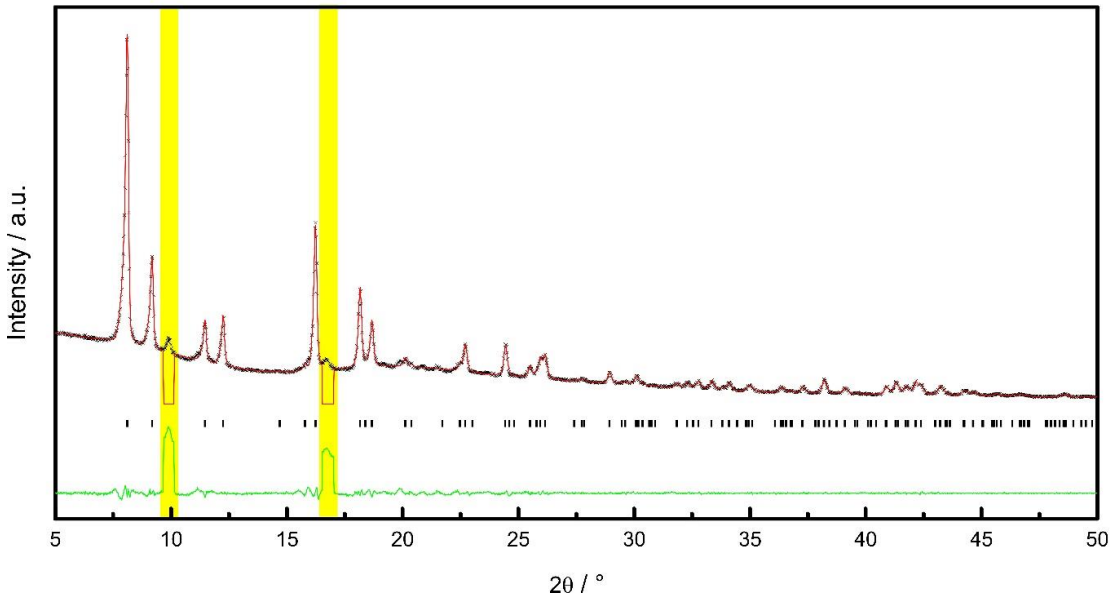

Figure S20: Pawley fit to the PXRD pattern of solvated Zn_2(DM-bdc)$_{1.5}$(DB-bdc)$_{0.5}$dabco, **{1$_{0.75}$3$_{0.25}$}as**, collected at room temperature. The black crosses, red and green lines represent the experimental, calculated and difference profile, respectively. The black markers indicate positions of allowed Bragg reflections in the space group *P4/nbm*. The same space group as for compound **1** was chosen. The regions shaded in yellow are excluded from the Pawley fit and are presumably dedicated to an already partly desolvated framework structure. Cell parameters are refined to a = 15.4603(7) Å, c = 9.6534(6) Å and V = 2307.4(2) Å^3. The final R values are R_{exp} = 1.61 and R_{wp} = 2.91.

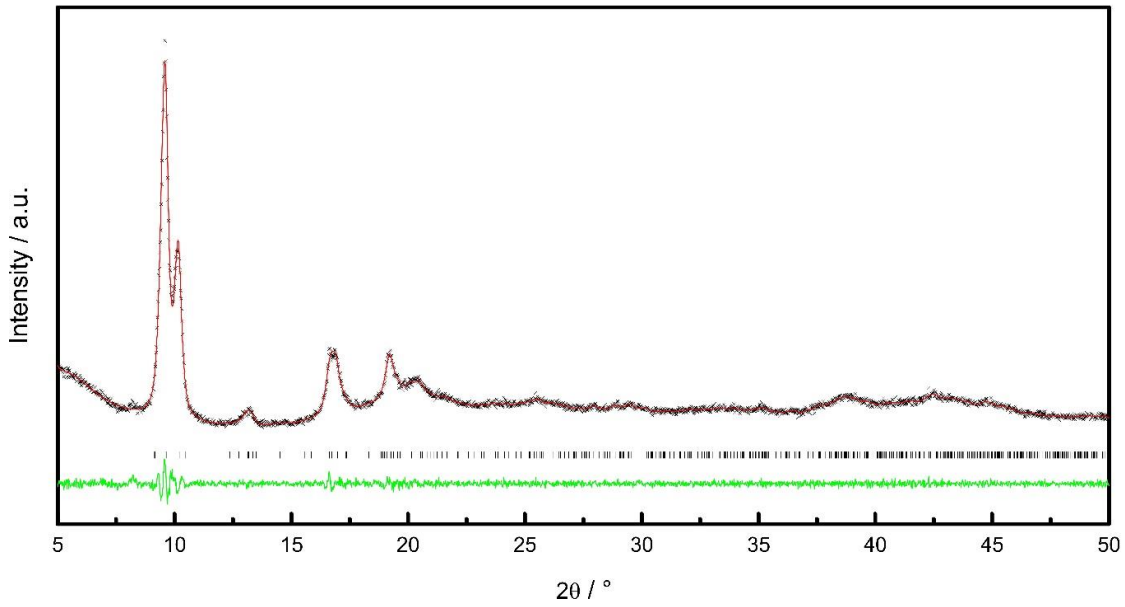

Figure S21: Pawley fit to the PXRD pattern of desolvated Zn_2(DM-bdc)$_{1.5}$(DB-bdc)$_{0.5}$dabco, **{1$_{0.75}$3$_{0.25}$}dry**, collected at room temperature. The black crosses, red and green lines represent the experimental, calculated and difference profile, respectively. The black markers indicate positions of allowed Bragg reflections in the space group $P2_1/m$. Cell parameters are refined to a = 18.33(3) Å, b = 10.67(8) Å, c = 9.69(3) Å, β = 91.5(2)° and V = 1895(15) Å^3. The final R values are R_{exp} = 3.13 and R_{wp} = 3.79. The space group symmetry was chosen on the basis of other breathing Zn_2(fu-bdc)$_2$dabco derivatives published elsewhere.[3] Note, due to the lower crystallinity and the poor quality of the pattern, the cell parameter refinement is less precise and the error in cell parameter is significantly higher.

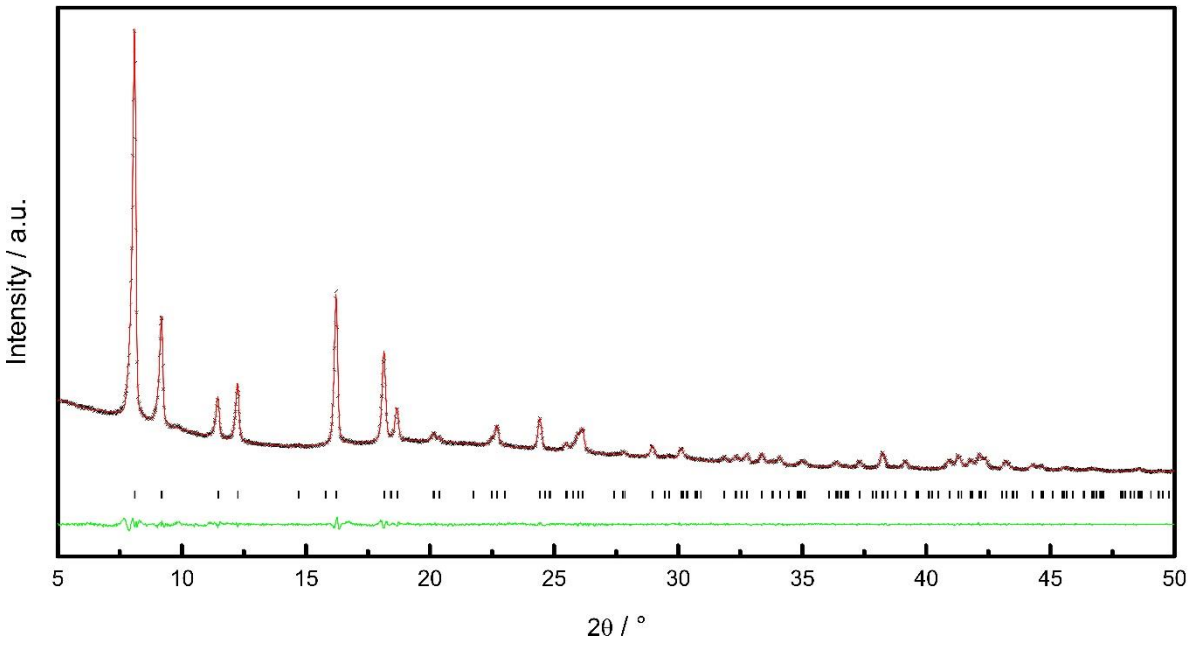

Figure S22: Pawley fit to the PXRD pattern of solvated Zn_2(DM-bdc)$_{1.0}$(DB-bdc)$_{1.0}$dabco, **{1$_{0.50}$3$_{0.50}$}as**, collected at room temperature. The black crosses, red and green lines represent the experimental, calculated and difference profile, respectively. The black markers indicate positions of allowed Bragg reflections in the space group *P4/nbm*. Cell parameters are refined to a = 15.4582(5) Å, c = 9.6365(5) Å and V = 2302.7(2) Å^3. The final R values are R_{exp} = 1.55 and R_{wp} = 2.26.

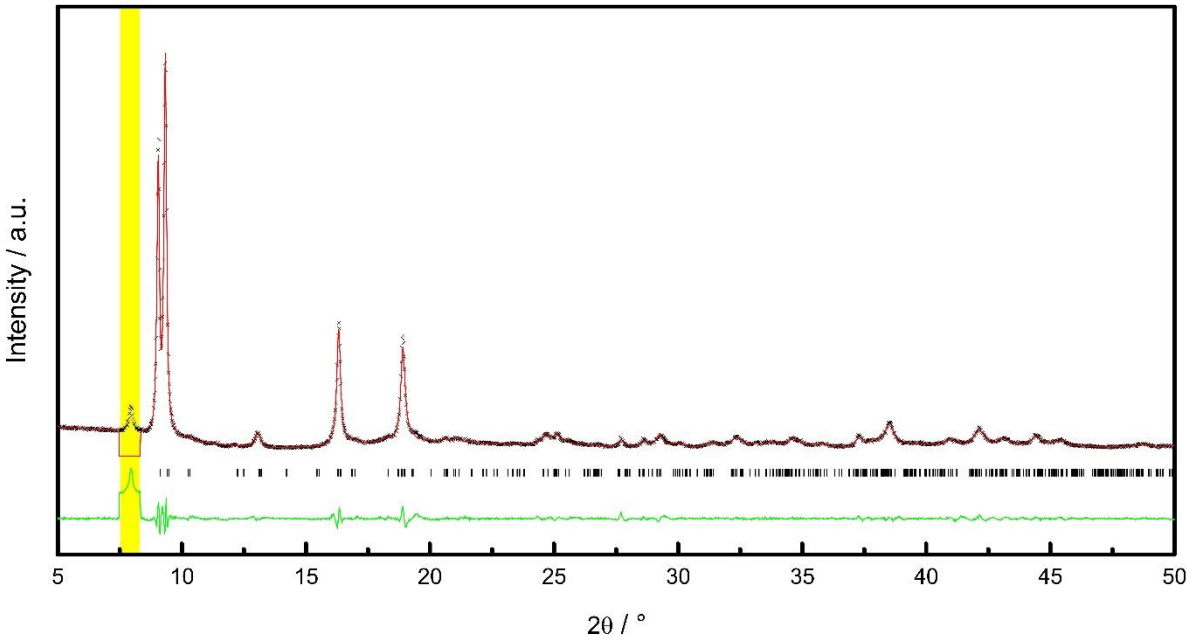

Figure S23: Pawley fit to the PXRD pattern of desolvated Zn_2(DM-bdc)$_{1.0}$(DB-bdc)$_{1.0}$dabco, **{1$_{0.50}$3$_{0.50}$}dry**, collected at room temperature. The black crosses, red and green lines represent the experimental, calculated and difference profile, respectively. The black markers indicate positions of allowed Bragg reflections in the space group *P2$_1$/m*. The space group symmetry was chosen on the basis of other breathing Zn_2(fu-bdc)$_2$dabco derivatives published elsewhere.[3, 5] The region shaded in yellow is excluded from the Pawley fit and is presumably dedicated to the minor presence of the **lp** form. Cell parameters are refined to a = 18.704 (9) Å, b = 10.89(1) Å, c = 9.69(1) Å, β = 90.48(9)° and V = 1975(4) Å^3. The final R values are R_{exp} = 3.07 and R_{wp} = 5.93.

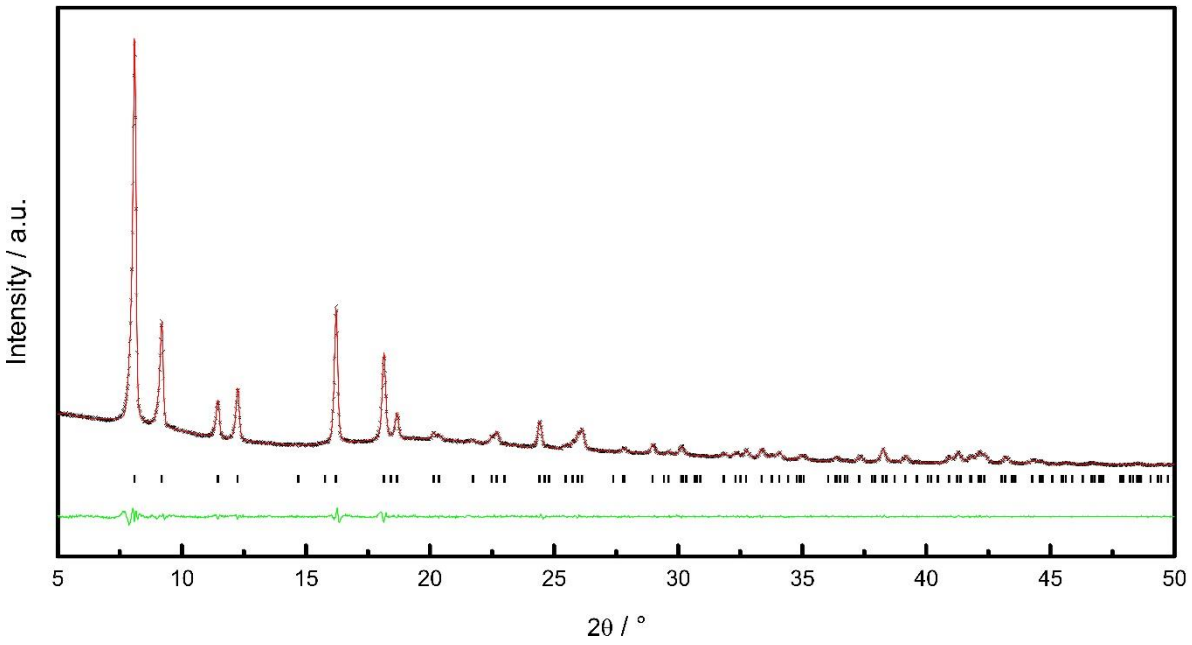

Figure S24: Pawley fit to the PXRD pattern of solvated Zn_2(DM-bdc)$_{0.5}$(DB-bdc)$_{1.5}$dabco, **{1$_{0.25}$3$_{0.75}$}as**, collected at room temperature. The black crosses, red and green lines represent the experimental, calculated and difference profile, respectively. The black markers indicate positions of allowed Bragg reflections in the space group *P4/nbm*. Cell parameters are refined to a = 15.4743(5) Å, c = 9.6389(5) Å and V = 2308.1(2) Å^3. The final R values are R_{exp} = 1.58 and R_{wp} = 2.50

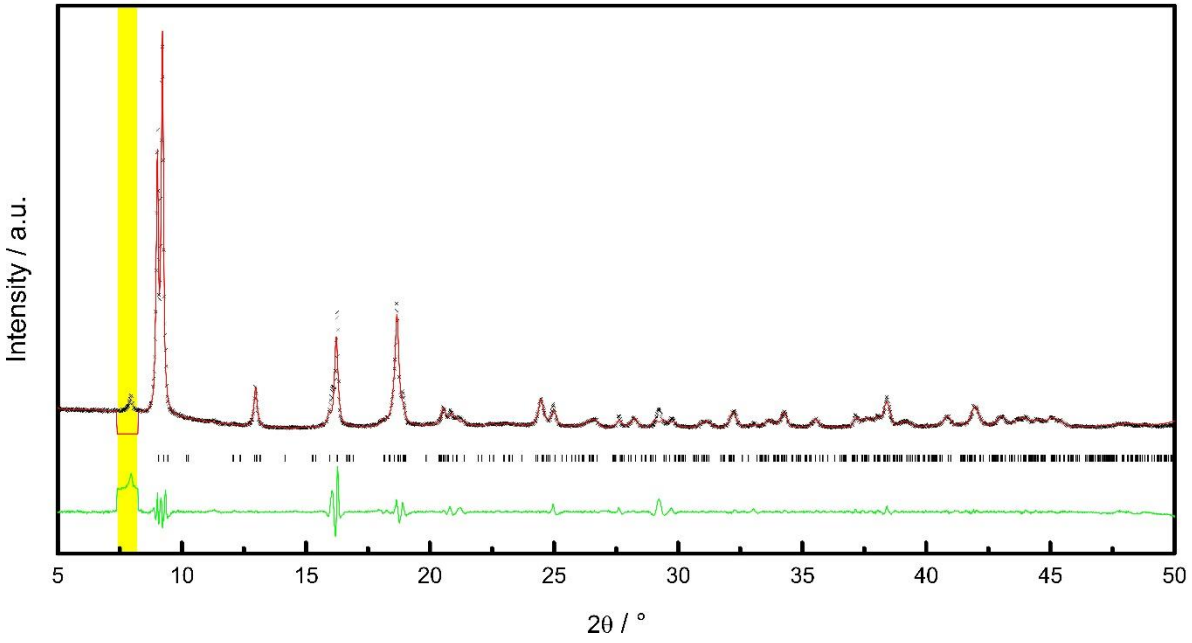

Figure S25: Pawley fit to the PXRD pattern of desolvated Zn_2(DM-bdc)$_{0.5}$(DB-bdc)$_{1.5}$dabco, **{1$_{0.25}$3$_{0.75}$}dry**, collected at room temperature. The black crosses, red and green lines represent the experimental, calculated and difference profile, respectively. The black markers indicate positions of allowed Bragg reflections in the space group $P2_1/m$ (see above). The region shaded in yellow is excluded from the Pawley fit and is presumably dedicated to the minor presence of the **lp** form. Cell parameters are refined to a = 18.782(5) Å, b = 11.111(7) Å, c = 9.778(5) Å, β = 90.56(5)° and V = 2040(2) Å^3. The final R values are R_{exp} = 3.02 and R_{wp} = 10.97.

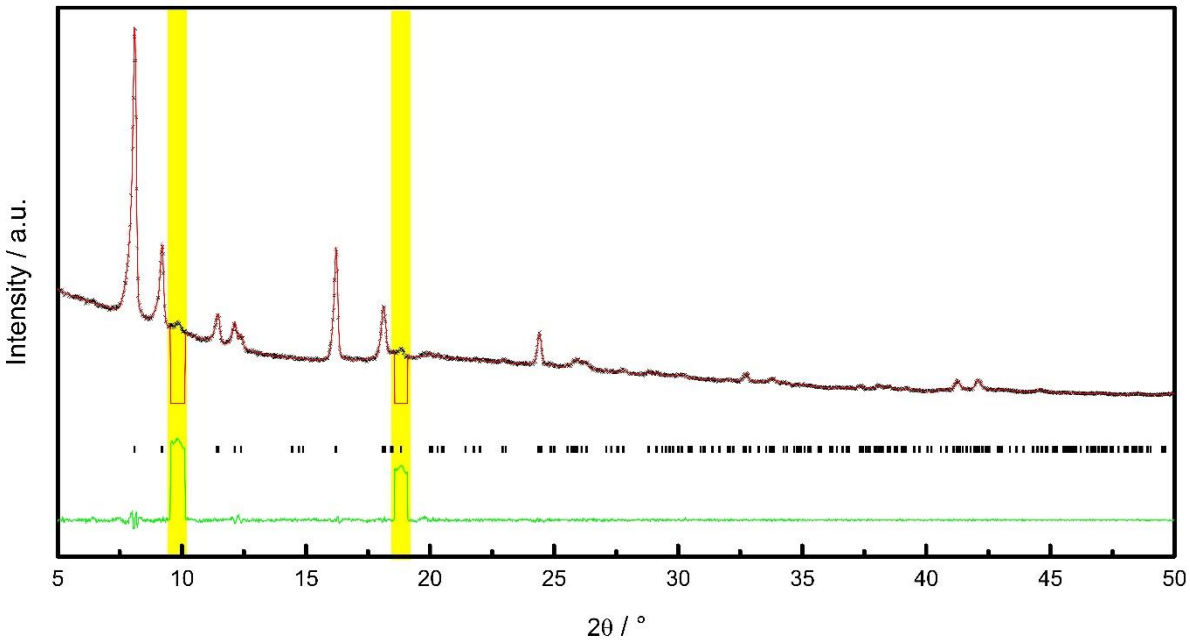

Figure S26: Pawley fit to the PXRD pattern of solvated Zn_2(DE-bdc)$_{1.5}$(DB-bdc)$_{0.5}$dabco, **{2$_{0.75}$3$_{0.25}$}as**, collected at room temperature. The black crosses, red and green lines represent the experimental, calculated and difference profile, respectively. The black markers indicate positions of allowed Bragg reflections in the space group *C*2/*m*. The region shaded in yellow is excluded from the Pawley fit and is presumably dedicated to the minor presence of the **np** form. Cell parameters are refined to a = 15.528(2) Å, b = 15.435(2) Å, c = 9.637(1) Å, β = 91.74(2)° and V = 2308.6(5) Å^3. The final R values are R_{exp} = 1.68 and R_{wp} = 2.09.

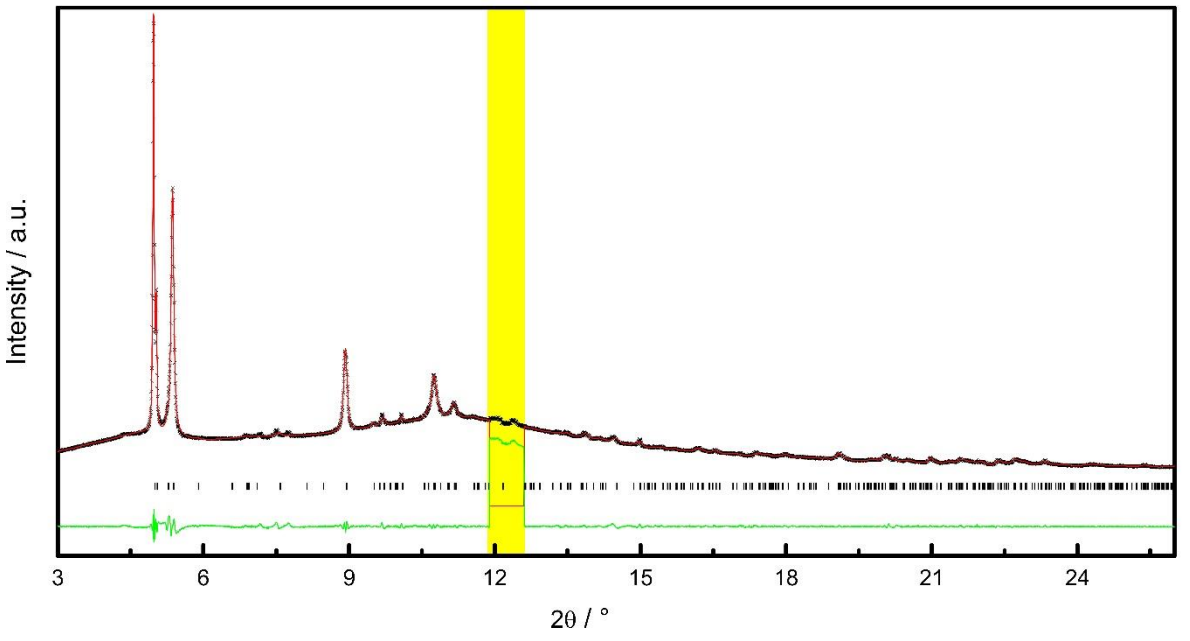

Figure S27: Pawley fit to the PXRD pattern of desolvated Zn_2(DE-bdc)$_{1.5}$(DB-bdc)$_{0.5}$dabco, **{2$_{0.75}$3$_{0.25}$}dry**, collected at room temperature. The pattern was collected at the synchrotron (Diamond Light Source, Oxon., UK, λ = 0.826952 Å). The black crosses, red and green lines represent the experimental, calculated and difference profile, respectively. The black markers indicate positions of allowed Bragg reflections in the space group $P2_1/m$. The region shaded in yellow is excluded from the Pawley fit due to artefacts originating from summation errors during data collection. Cell parameters are refined to a = 18.9890(3) Å, b = 9.9809(15) Å, c = 9.6014(17) Å, β = 97.946(15)° and V = 1802.3(5) Å^3. The final R values are R_{exp} = 0.40 and R_{wp} = 1.35.

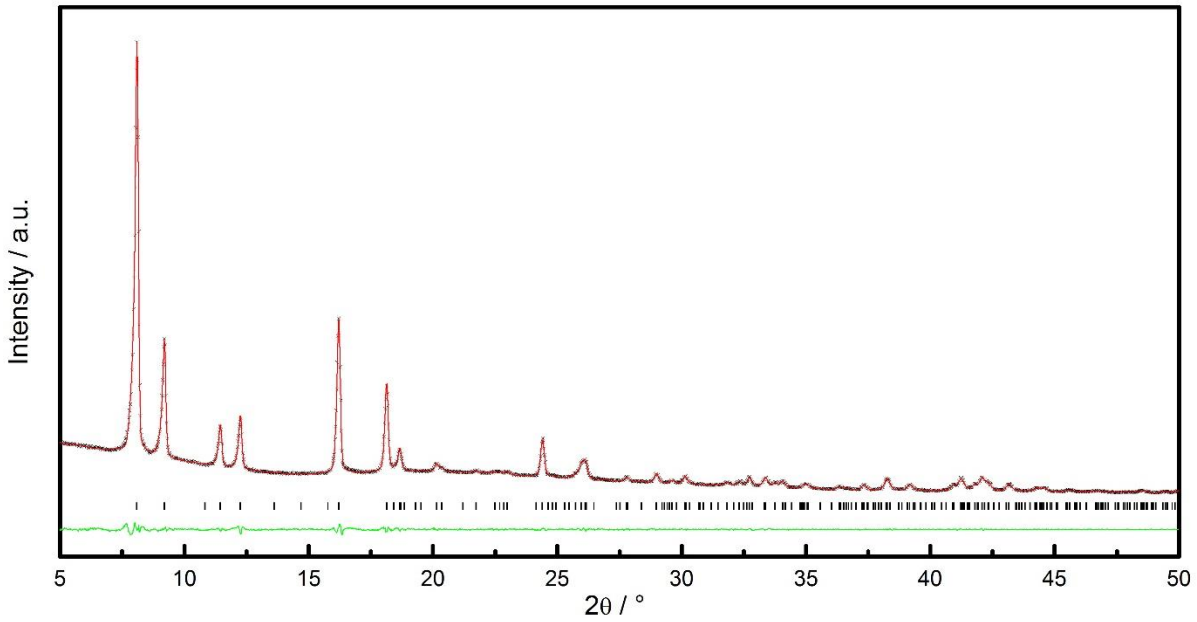

Figure S28: Pawley fit to the PXRD pattern of solvated $Zn_2(DE\text{-}bdc)_{1.0}(DB\text{-}bdc)_{1.0}dabco$, **{2$_{0.50}3_{0.50}$}as**, collected at room temperature. The black crosses, red and green lines represent the experimental, calculated and difference profile, respectively. The black markers indicate positions of allowed Bragg reflections in the space group *P4/ncc*. Cell parameters are refined to a = 15.4794(5) Å, c = 19.2650(11) Å and V = 4616.2(4) Å^3. The final R values are R_{exp} = 1.52 and R_{wp} = 2.38.

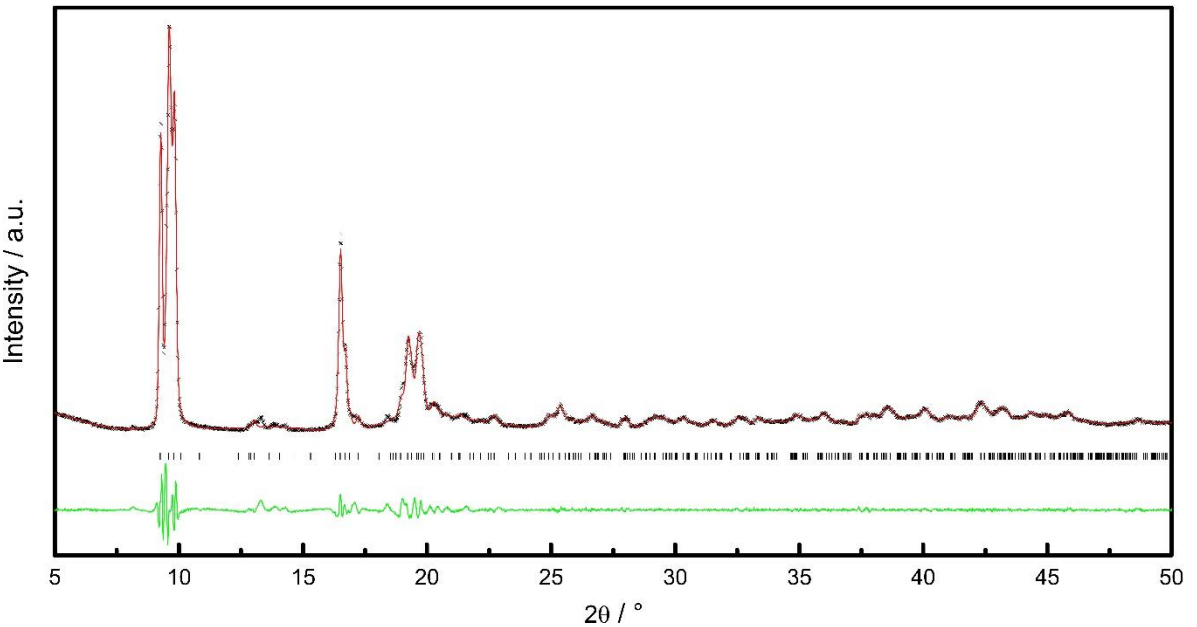

Figure S29: Pawley fit to the PXRD pattern of desolvated $Zn_2(DE\text{-}bdc)_{1.0}(DB\text{-}bdc)_{1.0}dabco$, **{2$_{0.50}3_{0.50}$}dry**, collected at room temperature. The black crosses, red and green lines represent the experimental, calculated and difference profile, respectively. The black markers indicate positions of allowed Bragg reflections in the space group $P2_1/m$. Cell parameters are refined to a = 18.15(5) Å, b = 10.75(3) Å, c = 9.62(2) Å, β = 94.95(2)° and V = 1870(8) Å^3. The final R values are R_{exp} = 3.01 and R_{wp} = 10.53.

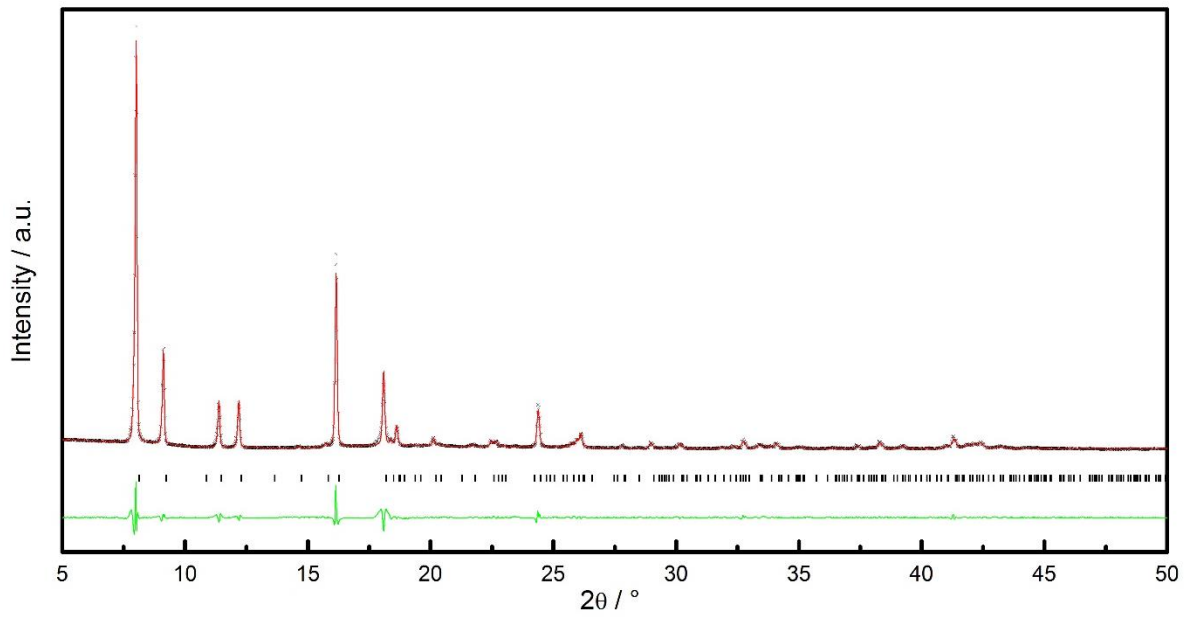

Figure S30: Pawley fit to the PXRD pattern of solvated Zn_2(DE-bdc)$_{0.5}$(DB-bdc)$_{1.5}$dabco, **{2$_{0.25}$3$_{0.75}$}as**, collected at room temperature. The black crosses, red and green lines represent the experimental, calculated and difference profile, respectively. The black markers indicate positions of allowed Bragg reflections in the space group *P4/ncc*. Cell parameters are refined to a = 15.4221(7) Å, c = 19.19013(13) Å and V = 4564.2(5) Å^3. The final R values are R_{exp} = 2.19 and R_{wp} = 9.35.

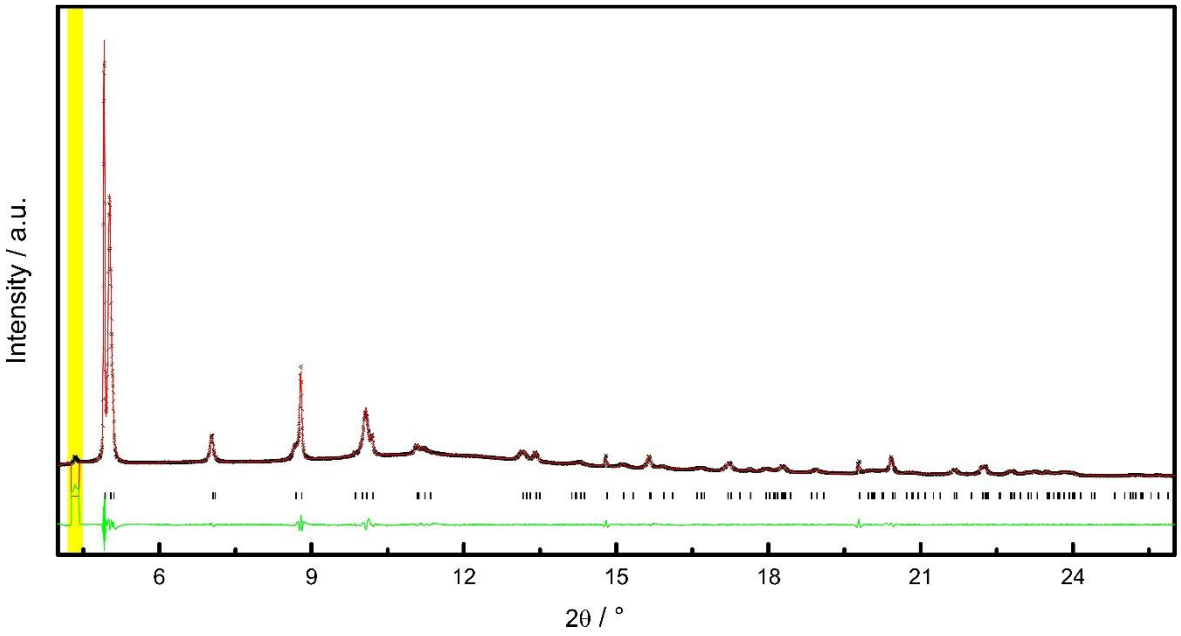

Figure S31: Pawley fit to the PXRD pattern of desolvated Zn_2(DE-bdc)$_{0.5}$(DB-bdc)$_{1.5}$dabco, **{2$_{0.25}$3$_{0.75}$}dry**, collected at room temperature. The pattern was collected at the synchrotron (Diamond Light Source, Oxon., UK, λ = 0.826952 Å). The black crosses, red and green lines represent the experimental, calculated and difference profile, respectively. The black markers indicate positions of allowed Bragg reflections in the space group *Cmmm*. The region shaded in yellow is excluded from the Pawley fit due to the minor presence of the **lp** form. Cell parameters are refined to a = 18.6070(5) Å, b = 10.9171(5) Å, c = 9.6244(4) Å, and V = 1955.07(13) Å^3. The final R values are R_{exp} = 0.46 and R_{wp} = 1.83.

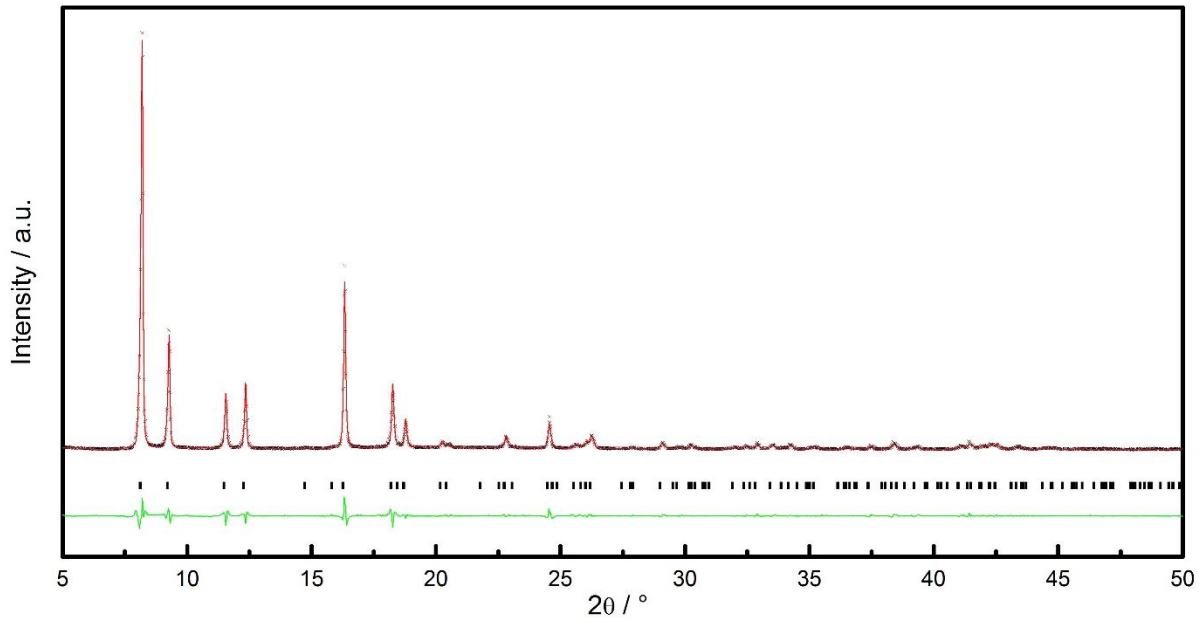

Figure S32: Pawley fit to the PXRD pattern of solvated Zn_2(DM-bdc)$_{1.5}$(DPe-bdc)$_{0.5}$dabco, **{1$_{0.75}$4$_{0.25}$}as**, collected at room temperature. The black crosses, red and green lines represent the experimental, calculated and difference profile, respectively. The black markers indicate positions of allowed Bragg reflections in the space group *P*4/*nbm*. Cell parameters are refined to a = 15.4328(6) Å, c = 9.6260(6) Å, and V = 2292.6(2) Å^3. The final R values are R_{exp} = 4.14 and R_{wp} = 9.70.

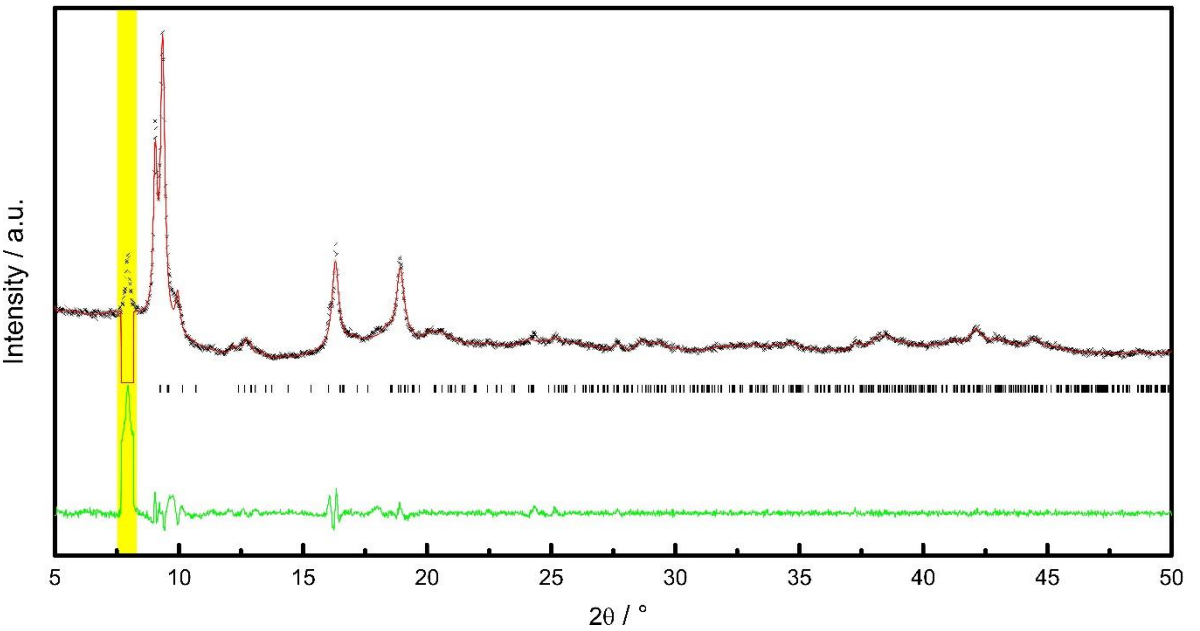

Figure S33: Pawley fit to the PXRD pattern of desolvated Zn_2(DM-bdc)$_{1.5}$(DPe-bdc)$_{0.5}$dabco, **{1$_{0.75}$4$_{0.25}$}dry**, collected at room temperature. The black crosses, red and green lines represent the experimental, calculated and difference profile, respectively. The black markers indicate positions of allowed Bragg reflections in the space group $P2_1/m$. The region shaded in yellow is excluded from the Pawley fit due to the minor presence of the **lp** form. Cell parameters are refined to a = 18.50(9) Å, b = 10.75(5) Å, c = 9.60(4) Å, β = 93.59(8)° and V = 1906(16) Å^3. The final R values are R_{exp} = 3.24 and R_{wp} = 5.20.

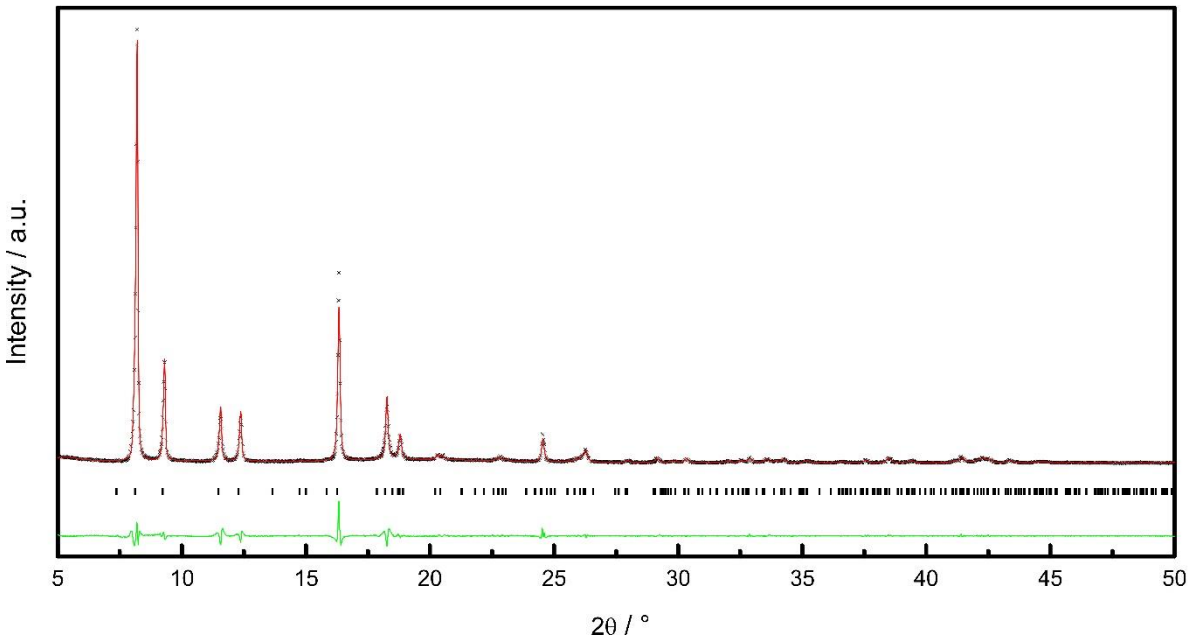

Figure S34: Pawley fit to the PXRD pattern of solvated Zn_2(DM-bdc)$_{1.0}$(DPe-bdc)$_{1.0}$dabco, **{1$_{0.50}$4$_{0.50}$}as**, collected at room temperature. The black crosses, red and green lines represent the experimental, calculated and difference profile, respectively. The black markers indicate positions of allowed Bragg reflections in the space group *P4/nnc*. Cell parameters are refined to a = 15.4329(8) Å, c = 19.2028(16) Å, and V = 4573.6(6) Å^3. The final R values are R_{exp} = 3.68 and R_{wp} = 9.67.

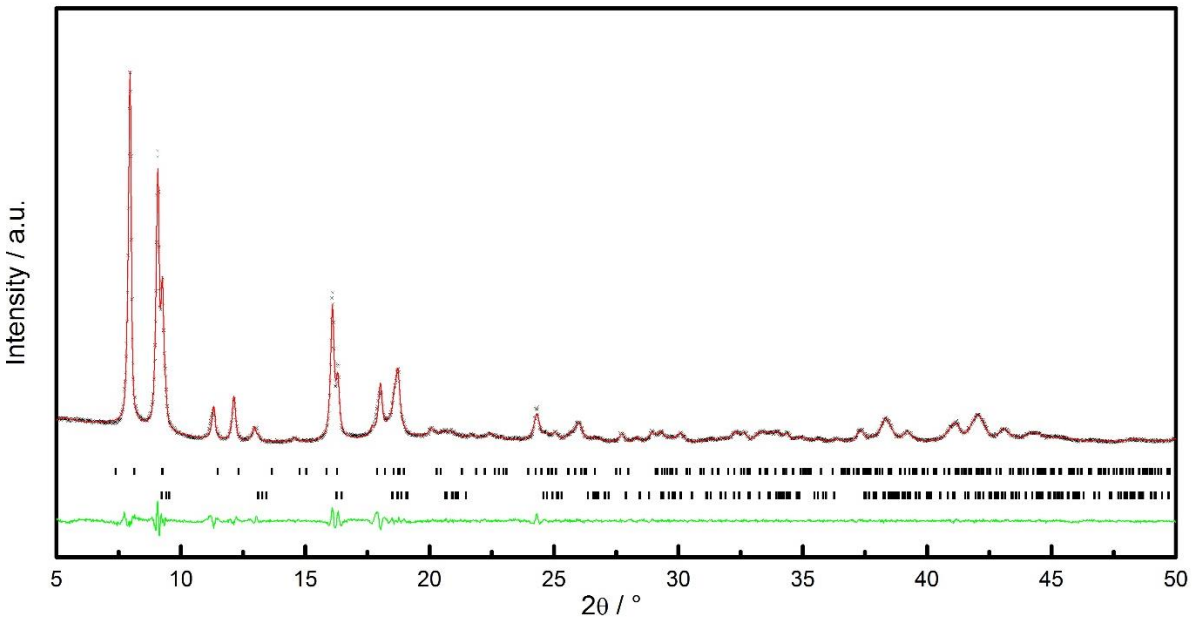

Figure S35: Pawley fit to the PXRD pattern of desolvated Zn_2(DM-bdc)$_{1.0}$(DPe-bdc)$_{1.0}$dabco, **{1$_{0.50}$4$_{0.50}$}dry**, collected at room temperature. The black crosses, red and green lines represent the experimental, calculated and difference profile, respectively. A two-phase model was applied. The black markers indicate positions of allowed Bragg reflections of the **lp** phase in the space group *P4/nnc* (top) and of the **np** phase in the space group *C*2/*m* (bottom). The final R values are R_{exp} = 3.05 and R_{wp} = 5.51. See Table S4 for cell parameters.

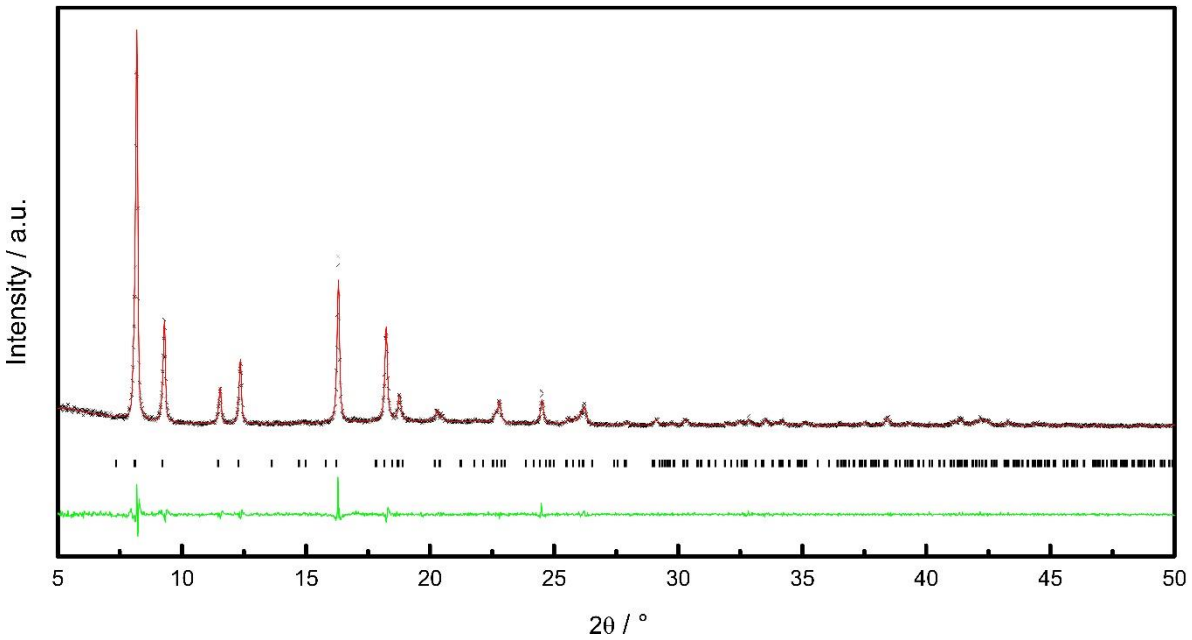

Figure S36: Pawley fit to the PXRD pattern of solvated Zn_2(DM-bdc)$_{0.5}$(DPe-bdc)$_{1.5}$dabco, **{1$_{0.25}$4$_{0.75}$}as**, collected at room temperature. The black crosses, red and green lines represent the experimental, calculated and difference profile, respectively. The black markers indicate positions of allowed Bragg reflections in the space group *P4/nnc*. Cell parameters are refined to a = 15.4627(11) Å, c = 19.223(2) Å, and V = 4596.1(8) Å^3. The final R values are R_{exp} = 8.57 and R_{wp} = 10.06.

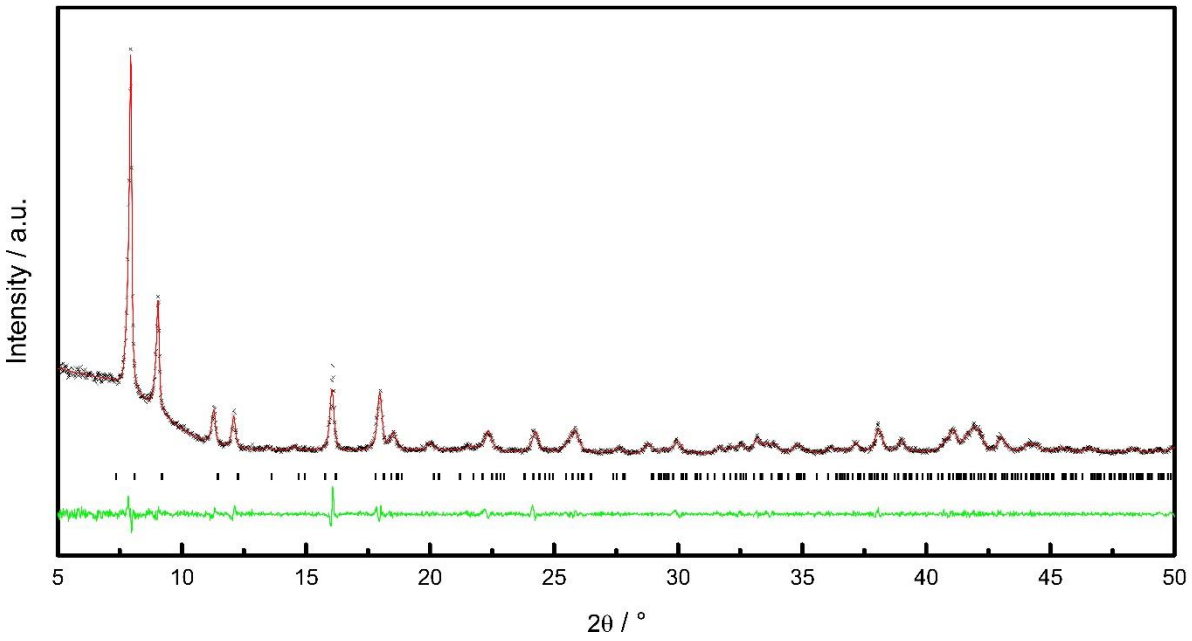

Figure S37: Pawley fit to the PXRD pattern of desolvated Zn_2(DM-bdc)$_{0.5}$(DPe-bdc)$_{1.5}$dabco, **{1$_{0.25}$4$_{0.75}$}dry**, collected at room temperature. The black crosses, red and green lines represent the experimental, calculated and difference profile, respectively. The black markers indicate positions of allowed Bragg reflections in the space group *P4/nnc*. Cell parameters are refined to a = 15.478(2) Å, c = 19.261(4) Å, and V = 4614(2) Å^3. The final R values are R_{exp} = 5.11 and R_{wp} = 6.58.

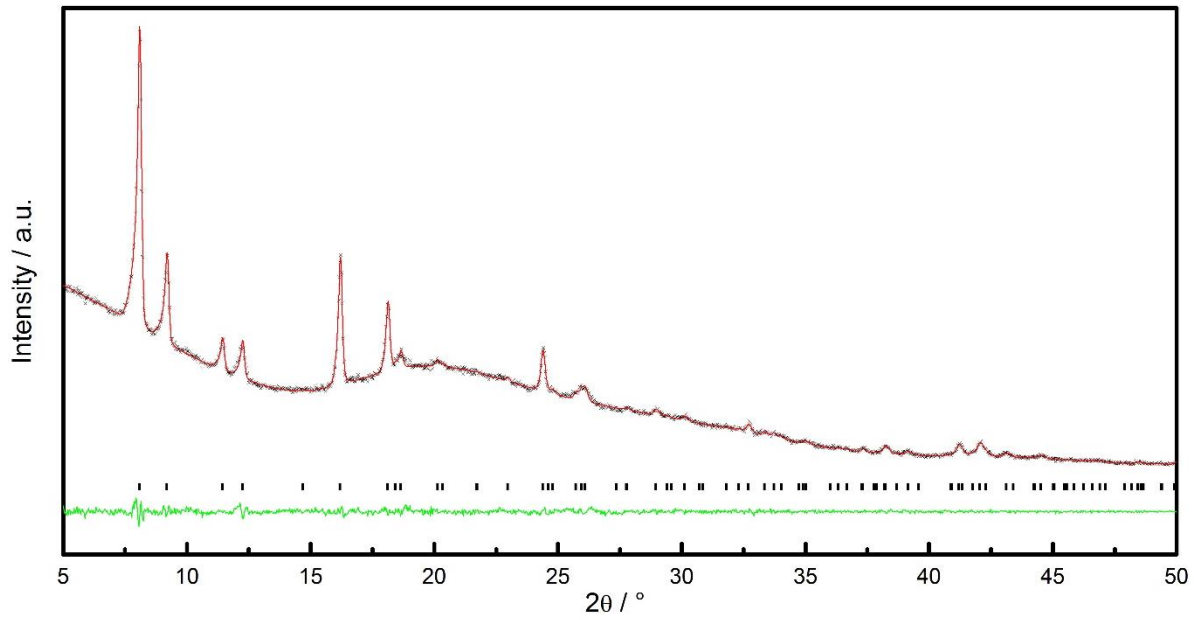

Figure S38: Pawley fit to the PXRD pattern of solvated Zn_2(DE-bdc)$_{1.5}$(DPe-bdc)$_{0.5}$dabco, **{2$_{0.75}$4$_{0.25}$}as**, collcted at room temperature. The black crosses, red and green lines represent the experimental, calculated and difference profile, respectively. The black markers indicate positions of allowed Bragg reflections in the space group *P*4/*mmm*. Cell parameters are refined to a = 10.9562(10) Å, c = 9.6383(16) Å, and V = 1157.0(3) Å^3. The final R values are R_{exp} = 1.64 and R_{wp} = 2.00.

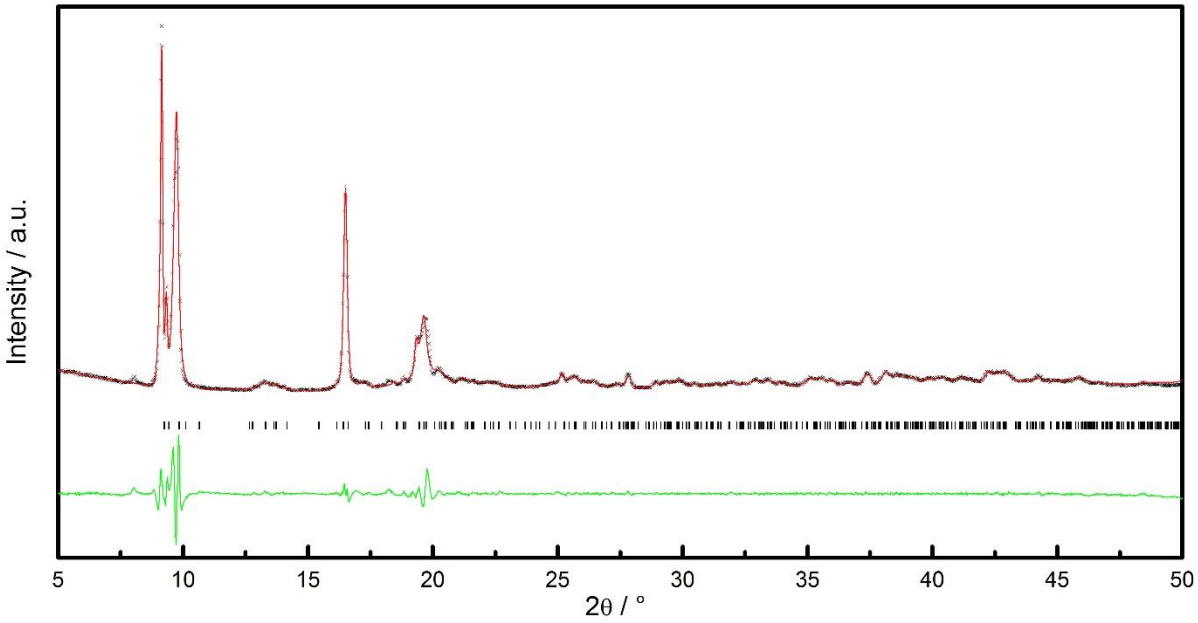

Figure S39: Pawley fit to the PXRD pattern of desolvated Zn_2(DE-bdc)$_{1.5}$(DPe-bdc)$_{0.5}$dabco, **{2$_{0.75}$4$_{0.25}$}dry**, collected at room temperature. The black crosses, red and green lines represent the experimental, calculated and difference profile, respectively. The black markers indicate positions of allowed Bragg reflections in the space group *P*2$_1$/*m*. Cell parameters are refined to a = 18.812(5) Å, b = 10.253(4) Å, c = 9.595(4) Å, β = 93.73(7)° and V = 1846(1) Å^3. The final R values are R_{exp} = 3.14 and R_{wp} = 10.43.

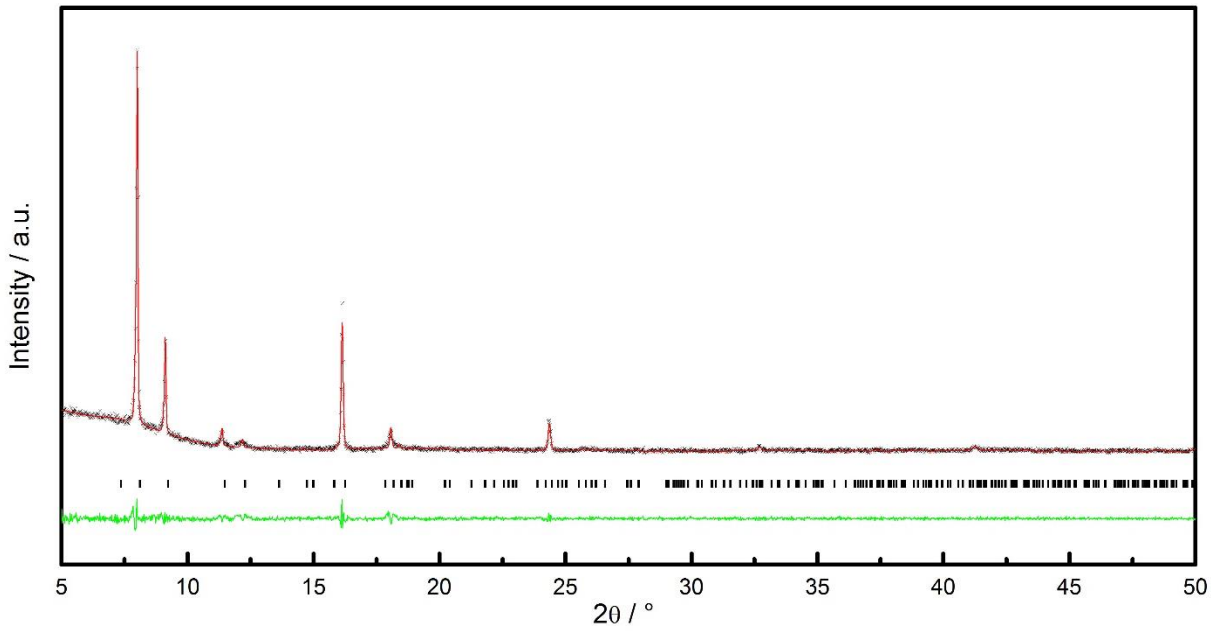

Figure S40: Pawley fit to the PXRD pattern of solvated Zn_2(DE-bdc)$_{1.0}$(DPe-bdc)$_{1.0}$dabco, **{2$_{0.50}$4$_{0.50}$}as**, collected at room temperature. The black crosses, red and green lines represent the experimental, calculated and difference profile, respectively. The black markers indicate positions of allowed Bragg reflections in the space group *P4/nnc*. Cell parameters are refined to a = 15.4387(14) Å, c = 19.196(3) Å, and V = 4575(1) Å^3. The final R values are R_{exp} = 10.61 and R_{wp} = 12.73.

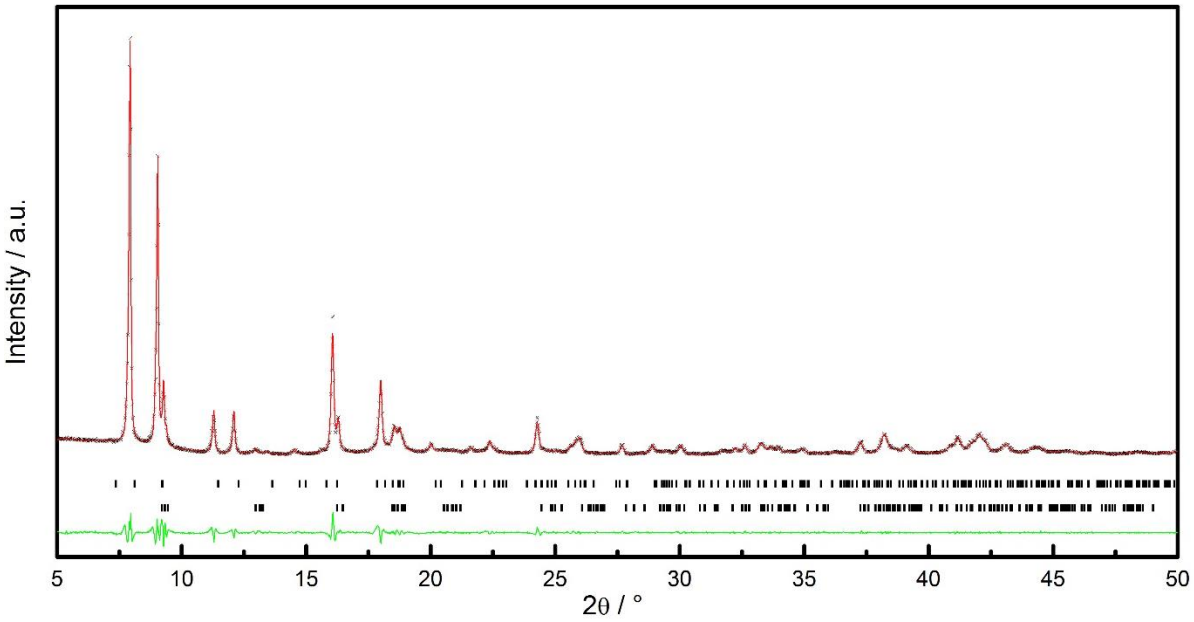

Figure S41: Pawley fit to the PXRD pattern of desolvated Zn_2(DE-bdc)$_{1.0}$(DPe-bdc)$_{1.0}$dabco, **{2$_{0.50}$4$_{0.50}$}dry**, collected at room temperature. The black crosses, red and green lines represent the experimental, calculated and difference profile, respectively. A two-phase model was applied. The black markers indicate positions of allowed Bragg reflections of the **lp** phase in the space group *P4/nnc* (top) and of the **np** phase in the space group *C*2/*m* (bottom). The final R values are R_{exp} = 3.11and R_{wp} = 6.97. See Table S5 for cell parameters.

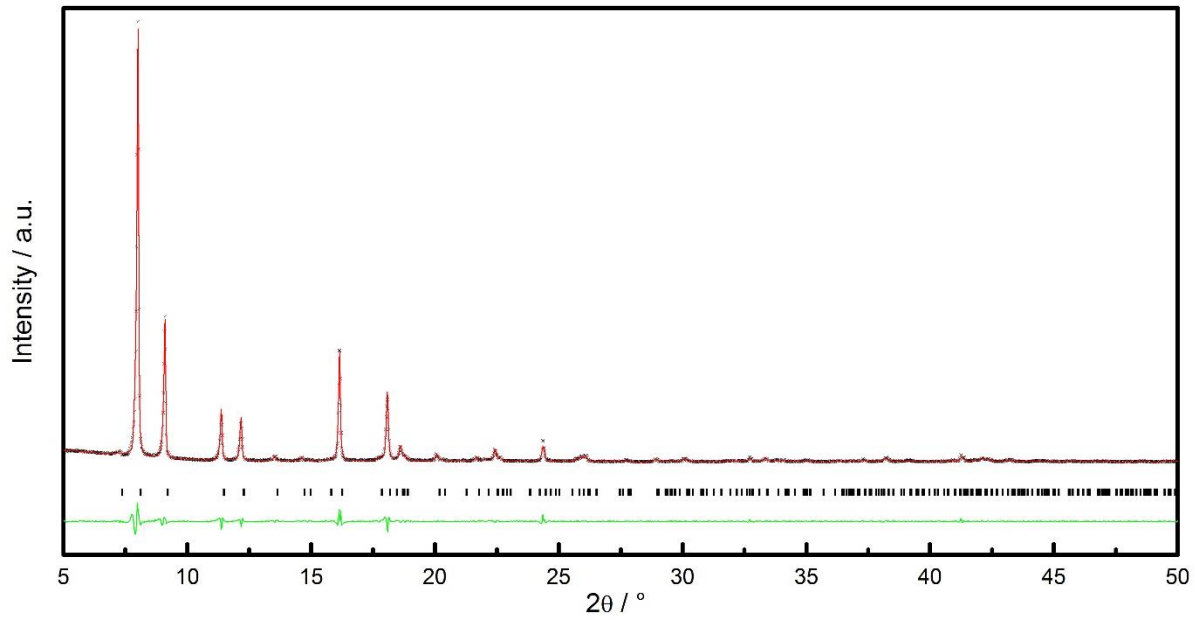

Figure S42: Pawley fit to the PXRD pattern of solvated $Zn_2(DE\text{-}bdc)_{0.5}(DPe\text{-}bdc)_{1.5}dabco$, **{2$_{0.25}4_{0.75}$}as**, collected at room temperature. The black crosses, red and green lines represent the experimental, calculated and difference profile, respectively. The black markers indicate positions of allowed Bragg reflections in the space group *P4/nnc*. Cell parameters are refined to a = 15.4268(7) Å, c = 19.2327(12) Å, and V = 4577.1(5) Å^3. The final R values are R_{exp} = 4.11 and R_{wp} = 8.86.

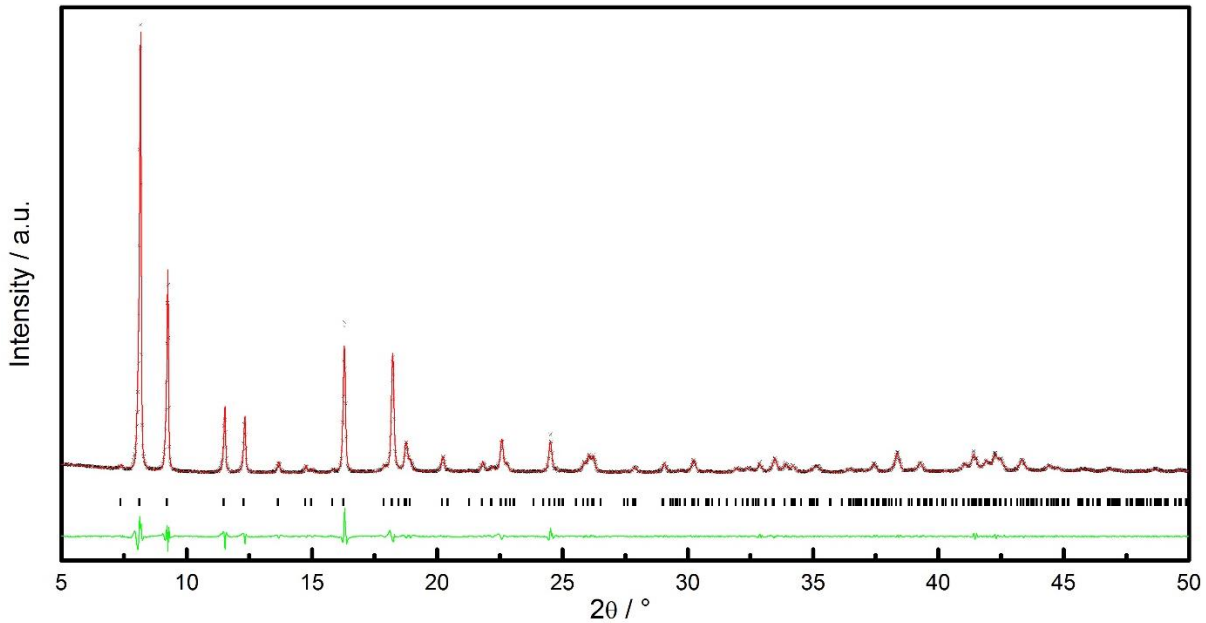

Figure S43: Pawley fit to the PXRD pattern of desolvated $Zn_2(DE\text{-}bdc)_{0.5}(DPe\text{-}bdc)_{1.5}dabco$. **{2$_{0.25}4_{0.75}$}dry**, collected at room temperature. The black crosses, red and green lines represent the experimental, calculated and difference profile, respectively. The black markers indicate positions of allowed Bragg reflections in the space group *P4/nnc*. Cell parameters are refined to a = 15.4319(6) Å, c = 19.2362(9) Å, and V = 4581.0(4) Å^3. The final R values are R_{exp} = 2.95 and R_{wp} = 8.05.

Table S2: Crystallographic data of as synthesized and dried solid solutions **{1_x3_{1-x}}** in comparison to the single-component parent MOFs **1** and **3** obtained via Pawley refinement of PXRD data.

	1		**{$1_{0.75}3_{0.25}$}**		**{$1_{0.50}3_{0.50}$}**		**{$1_{0.25}3_{0.75}$}**		**3**	
	as	**dry**	**as**	**dry**	**as**	**dry**	**as**	**dry**	**as**	**dry**
Space group	*P*4/*nbm*	–	*P*4/*nbm*	*P*2$_1$/*m*	*P*4/*nbm*	*P*2$_1$/*m*	*P*4/*nbm*	*P*2$_1$/*m*	*P*4/*ncc*	*P*4/*ncc*
a [Å]	15.4456(5)	–	15.4603(7)	18.33(3)	15.4582(5)	18.704(9)	15.4743(5)	18.782(5)	15.4180(6)	15.4172(6)
b [Å]	15.4456(5)	–	15.4603(7)	10.67(8)	15.4582(5)	10.89(1)	15.4743(5)	11.111(7)	15.4180(6)	15.4172(6)
c [Å]	9.6822(4)	–	9.6534(6)	9.69(3)	9.6365(5)	9.69(1)	9.6389(5)	9.778(5)	19.2234(9)	19.231(1)
β [°]	90	–	90	91.5(2)	90	90.48(9)	90	90.56(5)	90	90
V [Å^3]	2309.85(18)	–	2307.4(2)	1895(15)	2302.7(2)	1975(4)	2308.1(2)	2040(2)	4569.7(4)	4570.9(5)
V [%]	100	–	100	82.1	100	85.8	100	88.4	100	100
Z	2	–	2	2	2	2	2	2	4	4

Table S3: Crystallographic data of as synthesized and dried solid solutions **{2_x3_{1-x}}** in comparison to the single-component parent MOFs **2** and **3** obtained via Pawley refinement of PXRD data. The pattern of activated samples **{$2_{0.75}3_{0.25}$}** and **{$2_{0.25}3_{0.75}$}** were collected at Diamond Light Source, Oxon., UK.

	2		**{$2_{0.75}3_{0.25}$}**		**{$2_{0.50}3_{0.50}$}**		**{$2_{0.25}3_{0.75}$}**		**3**	
	as	**dry**	**as**	**dry**	**as**	**dry**	**as**	**dry**	**as**	**dry**
Space group	*C*2/*m*	*C*2/*m*	*C*2/*m*	*P*2$_1$/*m*	*P*4/*ncc*	*P*2$_1$/*m*	*P*4/*ncc*	*Cmmm*	*P*4/*ncc*	*P*4/*ncc*
a [Å]	15.7698(19)	18.801(4)	15.528(2)	18.9890(3)	15.4794(5)	18.15(5)	15.4221(7)	18.6070(5)	15.4180(6)	15.4172(6)
b [Å]	15.2203(18)	9.682(2)	15.435(2)	9.9809(15)	15.4794(5)	10.75(3)	15.4221(7)	10.9171(5)	15.4180(6)	15.4172(6)
c [Å]	9.6466(9)	9.606(6)	9.637(1)	9.6014(17)	19.2650(11)	9.62(2)	19.1901(13)	9.6244(4)	19.2234(9)	19.231(1)
β [°]	94.144(11)	93.80(6)	91.74(2)	97.946(15)	90	94.95(2)	90	90	90	90
V [Å^3]	2309.3(4)	1745(1)	2308.6(5)	1802.3(5)	4616.2(4)	1870(8)	4564.2(5)	1955.07(13)	4569.7(4)	4570.9(5)
V [%]	100	75.6	100	78.1	100	81.0	100	85.7	100	100
Z	2	2	2	2	4	2	4	2	4	4

Table S4: Crystallographic data of as synthesized and dried solid solutions **{1_x4_{1-x}}** in comparison to the single-component parent MOFs **1** and **4** obtained via Pawley refinement of PXRD data.The **lp** form is only present as a minor phase in **{$1_{0.75}4_{0.25}$}dry** and hence excluded from the fit. For sample **{$1_{0.50}4_{0.50}$}dry** a two-phase model was used but only parameters of the **np** phase are listed here, although this is the minor phase (*).

	1		**{$1_{0.75}4_{0.25}$}**		**{$1_{0.50}4_{0.50}$}**		**{$1_{0.25}4_{0.75}$}**		**4**	
	as	**dry**	**as**	**dry**	**as**	**dry***	**as**	**dry**	**as**	**dry**
Space group	*P*4/*nbm*	–	*P4/nbm*	*P*2$_1$/*m*	*P4/nnc*	*C*2/*m*	*P4/nnc*	*P4/nnc*	*P4/nnc*	*P4/nnc*
a [Å]	15.4456(5)	–	15.4328(6)	18.50(9)	15.4329(8)	18.593(10)	15.4627(11)	15.478(2)	15.4363(6)	15.4322(8)
b [Å]	15.4456(5)	–	15.4328(6)	10.75(5)	15.4329(8)	10.913(3)	15.4627(11)	15.478(2)	15.4363(6)	15.4322(8)
c [Å]	9.6822(4)	–	9.6260(6)	9.60(4)	19.2028(16)	9.60(3)	19.223(2)	19.261(4)	19.2745(9)	19.2679(12)
β [°]	90	–	90	93.59(8)	90	91.4(4)	90	90	90	90
V [Å^3]	2309.85(18)	–	2292.6(2)	1906(16)	4573.6(6)	1947(7)	4596.1(8)	4614(2)	4592.7(4)	4588.7(6)
V [%]	100	–	100	83.1	100	85.1	100	101	100	100
Z	2	–	2	2	4	2	4	4	4	4

Table S5: Crystallographic data of as synthesized and dried solid solutions **{2_x4_{1-x}}** in comparison to the single-component parent MOFs **2** and **4** obtained via Pawley refinement of the PXRD data. For sample **{$2_{0.50}4_{0.50}$}dry** a two-phase model was used but only parameters of the **np** phase are listed here, although this is the minor phase (*).

	2		**{$2_{0.75}4_{0.25}$}**		**{$2_{0.50}4_{0.50}$}**		**{$2_{0.25}4_{0.75}$}**		**4**	
	as	**dry**	**as**	**dry**	**as**	**dry***	**as**	**dry**	**as**	**dry**
Space group	*C*2/*m*	*C*2/*m*	*P4/mmm*	*P*2$_1$/*m*	*P4/nnc*	*C*2/*m*	*P4/nnc*	*P4/nnc*	*P4/nnc*	*P4/nnc*
a [Å]	15.7698(19)	18.801(4	10.9562(10)	18.812(5)	15.4387(14)	18.741(3)	15.4268(7)	15.4319(6)	15.4363(6)	15.4322(8)
b [Å]	15.2203(18)	9.682(2)	10.9562(10)	10.253(4)	15.4387(14)	10.643(4)	15.4268(7)	15.4319(6	15.4363(6)	15.4322(8)
c [Å]	9.6466(9)	9.606(6)	9.6383(16)	9.595(4)	19.196(3)	9.610(10)	19.2327(12)	19.2362(9)	19.2745(9)	19.2679(12)
β [°]	94.144(11)	93.80(6)	90	93.73(8)	90	92.4(1)	90	90	90	90
V [Å^3]	2309.3(4)	1745(1)	1157.0(3)	1846(1)	4575(1)	1915(2)	4577.1(5)	4581.0(4)	4592.7(4)	4588.7(6)
V [%]	100	75.6	100	79.8	100	83.7	100	100	100	100
Z	2	2	1	2	4	2	4	4	4	4

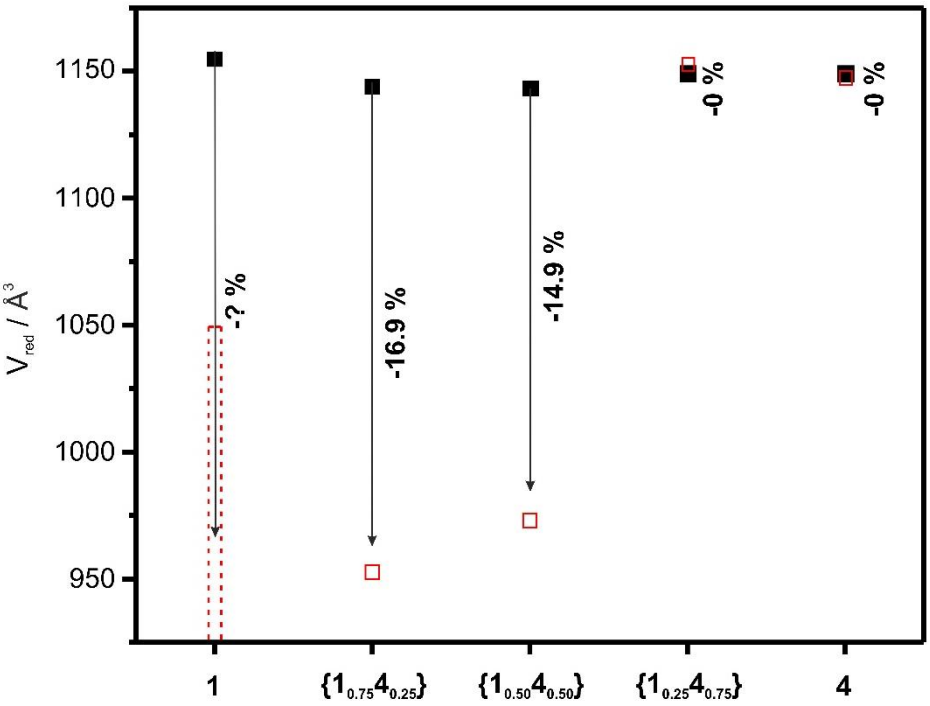

Figure S44: Comparison of the reduced volumes of the as synthesized (black, filled symbols) and the activated (red, open symbols) MOFs **{1$_x$4$_{1-x}$}** in comparison to the single component MOFs **1** and **4** determined by Pawley refinement of PXRD data. Note, the reduced volume V_{red} is obtained by dividing the cell volume by the number of formula units per unit cell (Z).

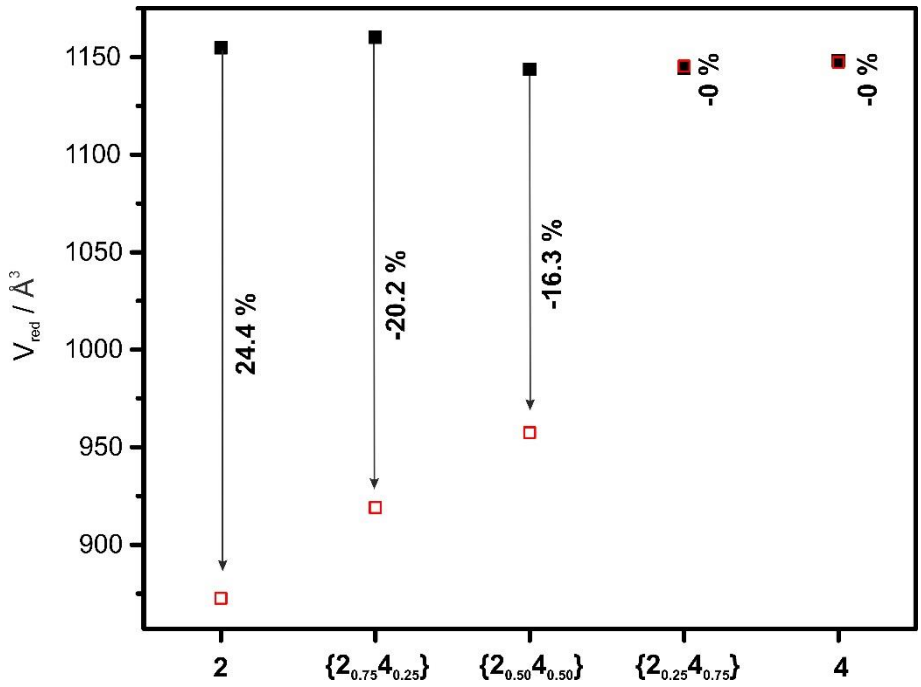

Figure S45: Comparison of the reduced volumes of the as synthesized (black, filled symbols) and the activated (red, open symbols) MOFs **{2$_x$4$_{1-x}$}** in comparison to the single component MOFs **2** and **3** determined by Pawley refinement of the PXRD data. Note, the reduced volume V_{red} is obtained by dividing the cell volume by the number of formula units per unit cell (Z).

3 VT PXRD and Thermal Expansion

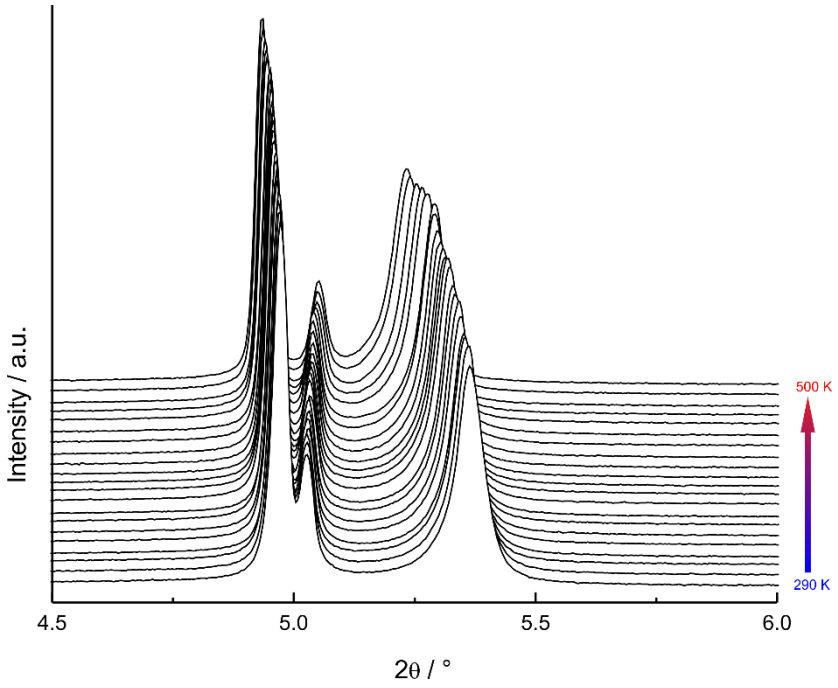

Figure S46: Close-up view of the low angle reflections of dried **{2$_{0.75}$3$_{0.25}$}** as a function of temperature. Data were recorded at Diamond Light Source (Oxon., UK) using X-rays of a wavelength of 0.826952 Å.

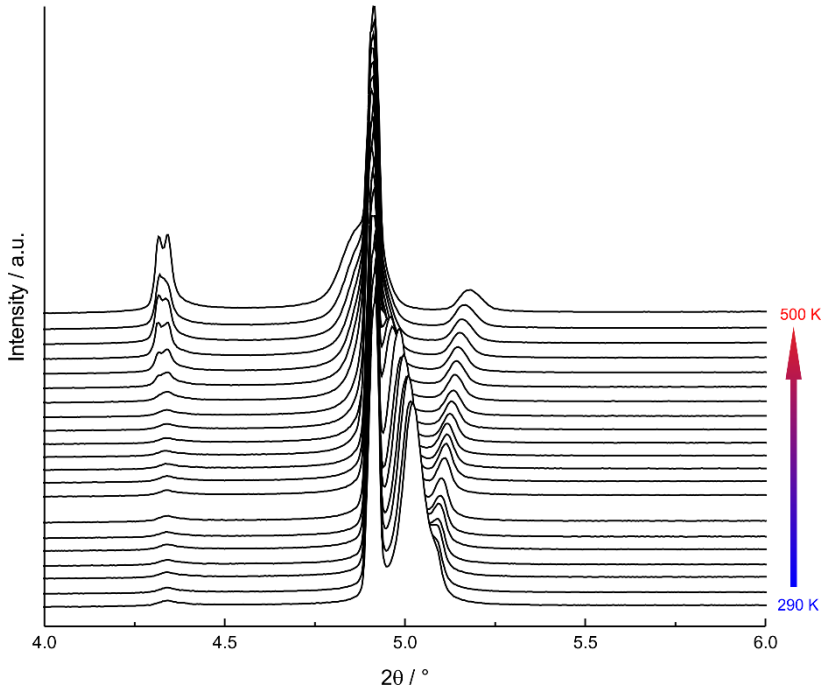

Figure S47: Close-up view of the low angle reflections of dried **{2$_{0.25}$3$_{0.75}$}** as a function of temperature. Data were recorded at Diamond Light Source (Oxon., UK) using X-rays of a wavelength of 0.826952 Å.

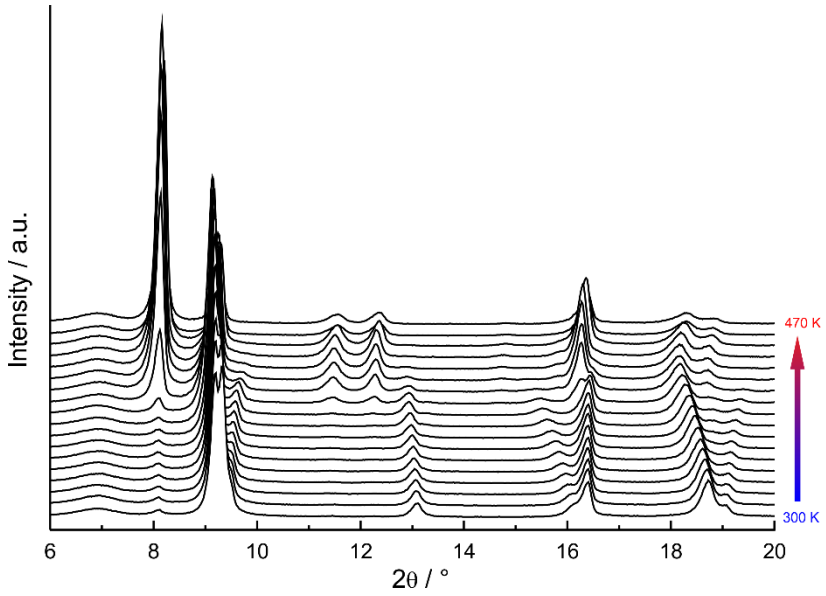

Figure S48: VT-PXRD patterns of dried **{$1_{0.25}3_{0.75}$}** recorded .on a Bruker D8 Advance diffractometer at the Department of Earth Sciences, University of Cambridge.

Table S6: Temperature dependent crystallographic data of **{$2_{0.75}3_{0.25}$}** extracted from VT-PXRD. Note, in the whole temperature range only the **np** is present and no **np** → **lp** tansformation occurs upon heating.

T **/ K**	**Space group**	***a*** **/ Å**	***b*** **/ Å**	***c*** **/ Å**	***β*** **/ °**	***V*** **/ Å^3**	R_{wp} **/ %**
290	$P2_1/m$	18.9890(3)	9.9809(15)	9.6014(17)	97.946(15)	1802.3(5)	1.35
300	$P2_1/m$	18.9872(3)	9.9907(13)	9.6037(15)	97.960(14)	1804.2(5)	1.39
310	$P2_1/m$	18.974(3)	10.0004(12)	9.6006(12)	97.815(16)	1804.7(4)	1.35
320	$P2_1/m$	18.967(3)	10.0129(14)	9.6018(14)	97.772(16)	1806.8(4)	1.37
330	$P2_1/m$	18.964(3)	10.0247(14)	9.6043(14)	97.753(16)	1809.2(5)	1.39
340	$P2_1/m$	18.955(2)	10.0379(12)	9.6048(11)	97.650(14)	1811.2(4)	1.35
350	$P2_1/m$	18.952(2)	10.0499(11)	9.6072(11)	97.662(14)	1813.5(4)	1.33
360	$P2_1/m$	18.945(2)	10.0685(11)	9.6108(11)	97.632(13)	1817.0(4)	1.33
370	$P2_1/m$	18.9493(19)	10.0822(10)	9.6170(10)	97.676(13)	1820.9(3)	1.31
380	$P2_1/m$	18.946(2)	10.09218(11)	9.6195(11)	97.796(13)	1822.3(4)	1.30
390	$P2_1/m$	18.939(2)	10.1047(10)	9.6212(11)	97.811(13)	1824.2(3)	1.32
400	$P2_1/m$	18.9379(19)	10.1176(10)	9.6254(10)	97.863(13)	1826.9(3)	1.34
410	$P2_1/m$	18.9446(16)	10.1373(9)	9.6343(9)	97.951(14)	1832.5(3)	1.49
420	$P2_1/m$	18.9473(13)	10.1504(7)	9.6406(7)	98.094(12)	1835.6(2)	1.37
430	$P2_1/m$	18.9511(12)	10.1665(7)	9.6479(7)	98.232(13)	1839.7(2)	1.41
440	$P2_1/m$	18.9543(3)	10.1836(13)	9.6558(15)	98.398(10)	1843.8(5)	1.43
450	$P2_1/m$	18.958(3)	10.2082(12)	9.6651(14)	98.467(9)	1850.0(4)	1.39
460	$P2_1/m$	18.9705(15)	10.2339(8)	9.6818(8)	98.996(12)	1856.5(3)	1.34
470	$P2_1/m$	18.952(2)	10.2698(11)	9.6835(12)	98.654(8)	1863.3(4)	1.33
480	$P2_1/m$	18.973(4)	10.311(2)	9.7045(18)	98.830(8)	1875.8(3)	1.33
490	$P2_1/m$	18.9462(19)	10.3197(9)	9.6973(10)	98.775(7)	1873.8(3)	1.29
500	$P2_1/m$	18.9444(2)	10.3382(10)	9.7025(11)	98.817(7)	1877.8(4)	1.30

Table S7: Temperature dependent crystallographic data of **{2$_{0.25}$3$_{0.75}$}** extracted from VT-PXRD. Note, in the whole temperature range both, the **np** and the **lp** form, are present. However, until 440 K the **lp** form is only present as a very small fraction. Therefore single-phase fits were performed. From 440 K on, the **lp**/**np** ratio significantly increases and fitting with a two-phase model seems reasonable (see Table S8). However, all data presented in this table were obtained via single-phase fits.

T **/ K**	**Space Group**	***a*** **/ Å**	***b*** **/ Å**	***c*** **/ Å**	***V*** **/ Å^3**	***R*$_{wp}$** **/ %**
290	*Cmmm*	18.6070(5)	10.9171(5)	9.6244(4)	1955.07(13)	1.83
300	*Cmmm*	18.5963(5)	10.9374(6)	9.6249(5)	1957.66(15)	1.93
310	*Cmmm*	18.5844(5)	10.9597(5)	9.6269(4)	1960.79(14)	1.84
320	*Cmmm*	18.5740(5)	10.9803(5)	9.6277(4)	1963.55(13)	1.87
330	*Cmmm*	18.5611(4)	11.0018(5)	9.6284(3)	1966.18(12)	1.74
340	*Cmmm*	18.5498(5)	11.0239(5)	9.6289(4)	1969.04(13)	1.83
350	*Cmmm*	18.5351(5)	11.0446(5)	9.6285(4)	1971.07(13)	1.74
370	*Cmmm*	18.5051(6)	11.0925(6)	9.6287(5)	1976.46(16)	1.90
380	*Cmmm*	18.4901(14)	11.1077(10)	9.6277(8)	1977.4(3)	1.90
390	*Cmmm*	18.4823(13)	11.1279(10)	9.6305(7)	1980.7(3)	1.96
400	*Cmmm*	18.467(3)	11.1482(17)	9.6304(13)	1982.6(5)	1.90
410	*Cmmm*	18.457(2)	11.1655(12)	9.6323(9)	1985.0(4)	1.80
420	*Cmmm*	18.4497(7)	11.1939(7)	9.6381(4)	1990.53(17)	1.85
430	*Cmmm*	18.436(8)	11.2201(9)	9.6401(4)	1994.1(2)	2.09
440	*Cmmm*	18.3988(9)	11.2842(10)	9.637(6)	2000.8(2)	2.12
450	*Cmmm*	18.3788(9)	11.3113(9)	9.6341(6)	2002.8(2)	2.48
460	*Cmmm*	18.3602(13)	11.3279(12)	9.6317(9)	2003.2(3)	2.46
470	*Cmmm*	18.308(3)	11.385(2)	9.617(2)	2004.6(7)	3.87
480	*Cmmm*	18.288(3)	11.3876(19)	9.6156(16)	2002.5(6)	3.45
490	*Cmmm*	18.263(2)	11.4126(19)	9.6171(14)	2004.5(5)	3.23
500	*Cmmm*	18.2043(19)	11.4951(16)	9.6196(11)	2013.0(5)	3.39

Table S8: Temperature dependent crystallographic data of **{2$_{0.25}$3$_{0.75}$}** extracted via two-phase fits to PXRD data obtained in the range from 440 to 470 K. Both, the **np** and the **lp** form coexist in the temperature range and the **lp**/**np** ratio significantly increases with temperature. From 480 K to 500 K, a two-phase model would also be reasonable, however, refinement was not possible due to (partial) loss of crystallinity and a decrease in quality of the powder pattern.

T / K	**space group**	**a / Å**	**b / Å**	**c / Å**	**V / Å^3**	**Z**	**phase**	**R$_{wp}$**
440	Cmmm	18.3998(9)	11.2809(10)	9.6376(6)	2000.5(2)	2	**np**	2.06
	P4/mmm	10.8970(10)	10.8970(10)	9.6862(11)	1150.2(2)	1	**lp**	
450	Cmmm	18.3848(10)	11.3025(9)	9.6364(6)	2002.4(2)	2	**np**	2.06
	P4/mmm	10.9011(9)	10.9011(9)	9.7324(13)	1156.6(2)	1	**lp**	
460	Cmmm	18.3710(8)	11.3134(9)	9.6358(5)	2002.7(2)	2	**np**	2.02
	P4/mmm	10.9063(7)	10.9063(7)	9.7376(10)	1158.2(2)	1	**lp**	
470	Cmmm	18.3531(9)	11.3268(10)	9.6341(6)	2002.8(2)	2	**np**	2.18
	P4/mmm	10.9122(7)	10.9122(7)	9.7414(1)	1160.0(2)	1	**lp**	

In order to determine the thermal expansion coefficients α_a, α_b, α_c, and α_V of the **np** phases of **{2$_{0.75}$3$_{0.25}$}** and **{2$_{0.25}$3$_{0.75}$}**, the cell parameters *a*, *b*, *c*, and *V* (see Table S6 and S7) have been plotted as a function of temperature and empirically fitted with a linear function of the type:

$$i(T) = i_o + i_1 T$$

with *i* = *a*, *b*, *c* or *V*. The corresponding thermal expansion coefficients α_i have been derived according to the following correlation:

$$\alpha_i = \frac{i_1}{i(290K)}$$

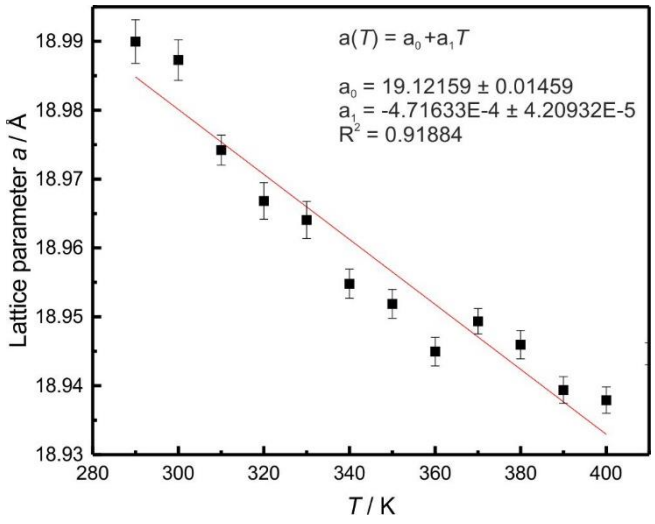

Figure S49: Evolution of the lattice parameter *a* (black) of the **np** of **{2$_{0.75}$3$_{0.25}$}** in the range of 290 K to 400 K. The linear fit is depicted in red.

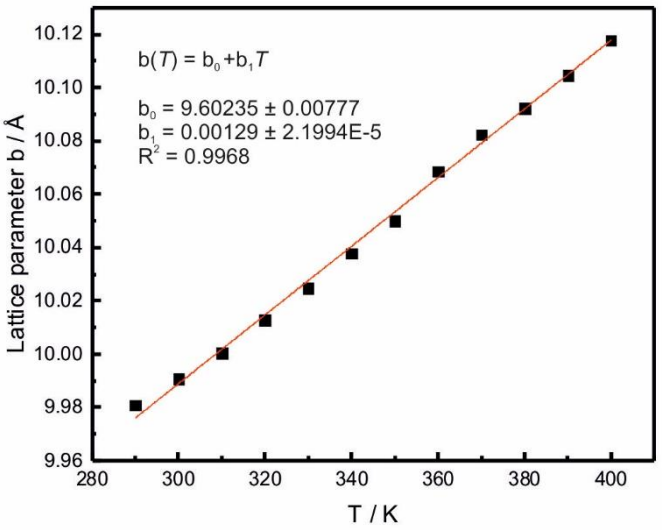

Figure S50: Evolution of the lattice parameter *b* (black) of the **np** of **{2$_{0.75}$3$_{0.25}$}** in the range of 290 K to 400 K. The linear fit is depicted in red. The error bars are not larger than the size of the symbols.

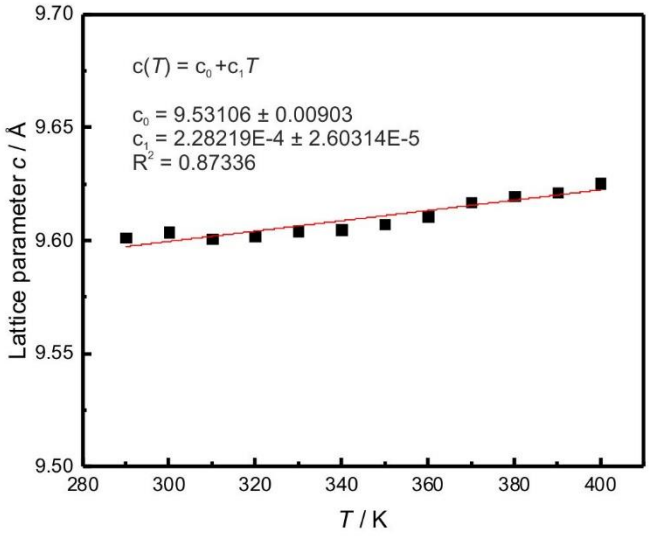

Figure S51: Evolution of the lattice parameter *c* (black) of the **np** of **{2$_{0.75}$3$_{0.25}$}** in the range of 290 K to 400 K. The linear fit is depicted in red. The error bars are not larger than the size of the symbols.

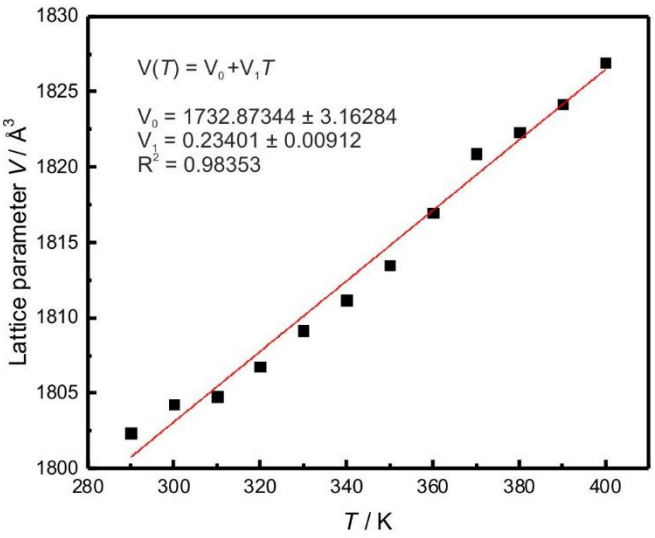

Figure S52: Evolution of the cell volume *V* (black) of the **np** of **{2$_{0.75}$3$_{0.25}$}** in the range of 290 K to 400 K. The linear fit is depicted in red. The error bars are not larger than the size of the symbols.

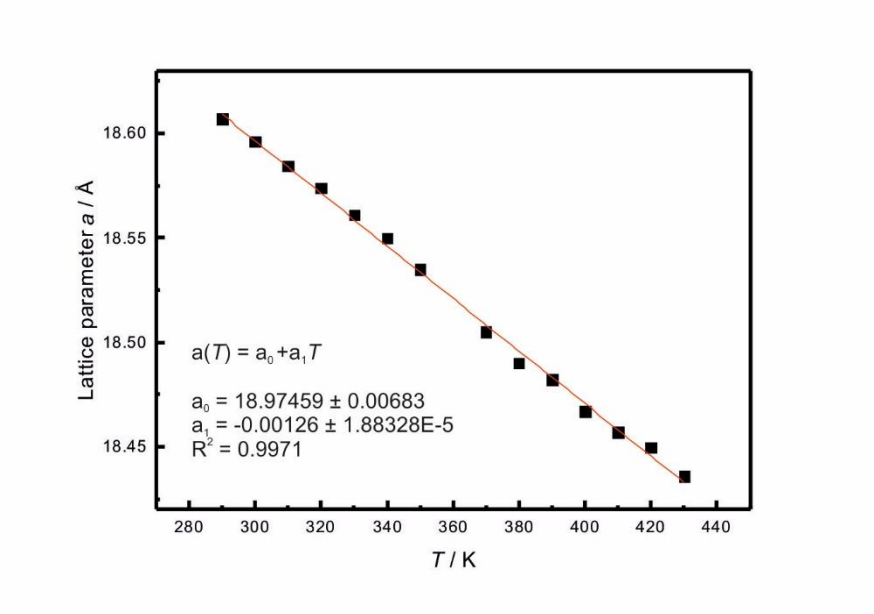

Figure S53: Evolution of the cell parameter *a* (black) of the **np** of **{2$_{0.25}$3$_{0.75}$}** in the range of 290 K to 430 K. The linear fit is depicted in red. The error bars are not larger than the size of the symbols.

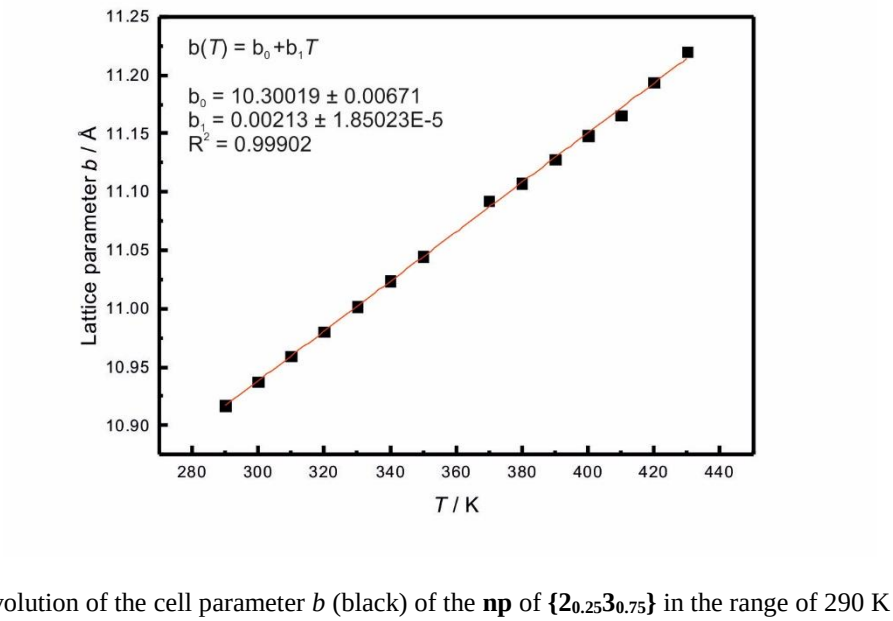

Figure S54: Evolution of the cell parameter *b* (black) of the **np** of **{2$_{0.25}$3$_{0.75}$}** in the range of 290 K to 430 K. The linear fit is depicted in red. The error bars are not larger than the size of the symbols.

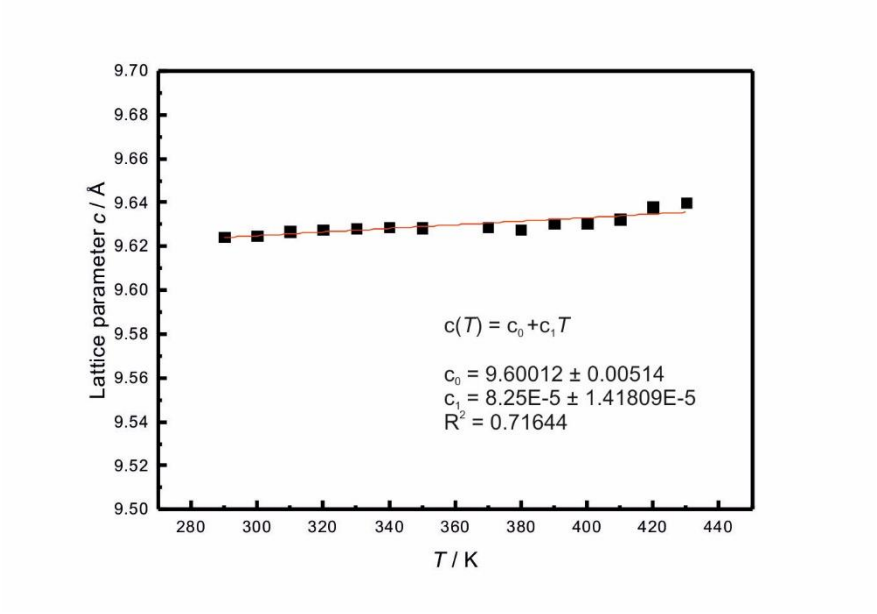

Figure S55: Evolution of the cell parameter *c* (black) of the **np** of **{$2_{0.25}3_{0.75}$}** in the range of 290 K to 430 K. The linear fit is depicted in red. The error bars are not larger than the size of the symbols.

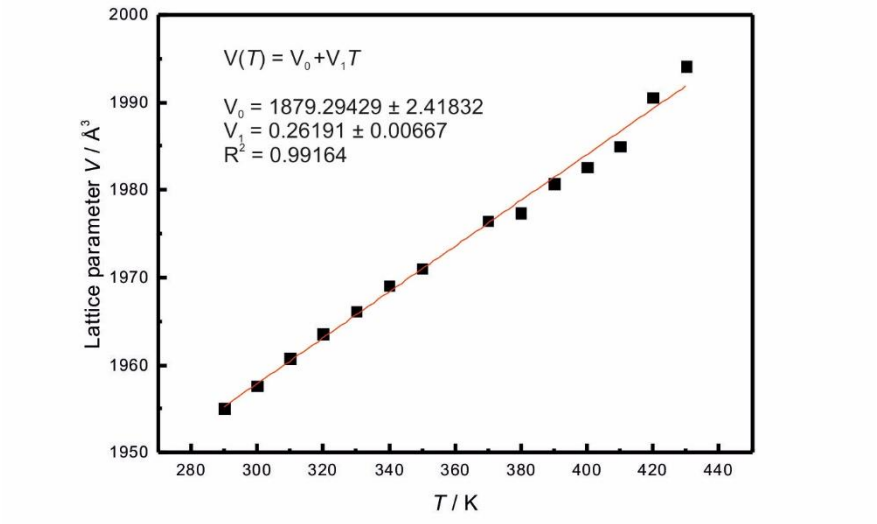

Figure S56: Evolution of the cell parameter *c* (black) of the **np** of **{$2_{0.25}3_{0.75}$}** in the range of 290 K to 430 K. The linear fit is depicted in red. The error bars are not larger than the size of the symbols.

4 Differential Scanning Calorimetry

Table S9: Comparison of the transition temperatures ($T_{np \rightarrow lp}$ and $T_{lp \rightarrow np}$) and the respective transition enthalpies ($\Delta H_{np \rightarrow lp}$ and $\Delta H_{np \rightarrow lp}$) obtained from DSC measurements of all activated solid solutions, which show a thermo-responsive phase transition in the measured temperature range. The relatively small transition enthalpies for **{1$_{0.25}$3$_{0.75}$}dry** and **{2$_{0.50}$3$_{0.50}$}dry** compared to the enthalpies for **{2$_{0.25}$3$_{0.75}$}dry** suggest that **{1$_{0.25}$3$_{0.75}$}dry** and **{2$_{0.50}$3$_{0.50}$}dry** transform only partially to the **lp** form upon heating.[5]

sample	cycle	$T_{np \rightarrow lp}$ / °C	$\Delta H_{np \rightarrow lp}$ / kJ mol^{-1}	$T_{lp \rightarrow np}$ / °C	$\Delta H_{np \rightarrow lp}$ / kJ mol^{-1}
{1$_{0.25}$3$_{0.75}$}dry	1st	170.0	4.83	109.5	- 4.54
	2nd	151.7	4.37	107.0	- 4.49
	3rd	149.7	4.12	107.4	- 3.46
{2$_{0.50}$3$_{0.50}$}dry	1st	202.5	5.32	217.5	- 3.58
	2nd	202.1	5.20	215.0	- 3.32
	3rd	202.9	5.00	212.4	- 3.12
{2$_{0.25}$3$_{0.75}$}dry	1st	165.2	14.43	151.7	- 10.48
	2nd	168.5	14.79	151.6	- 9.97
	3rd	168.8	14.30	150.4	- 9.84

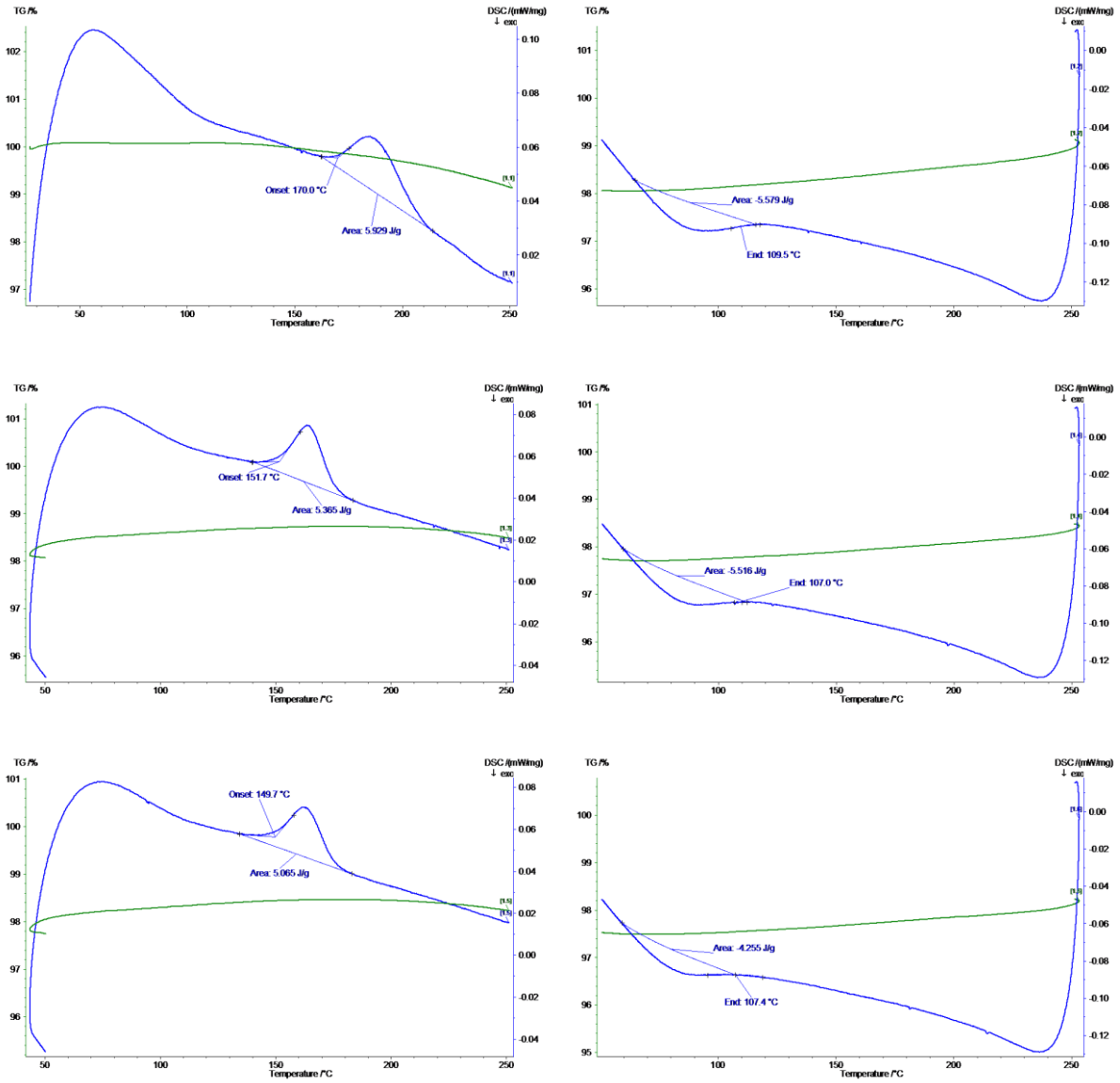

Figure S57: DSC curves of **{1$_{0.25}$3$_{0.75}$}dry** measured from 30 – 250 °C with a heating rate of 5 °C min^{-1}. The first cycle is depicted on top, second cycle in the middle and third cycle at the bottom with the heating and cooling branch left and right, respectively.

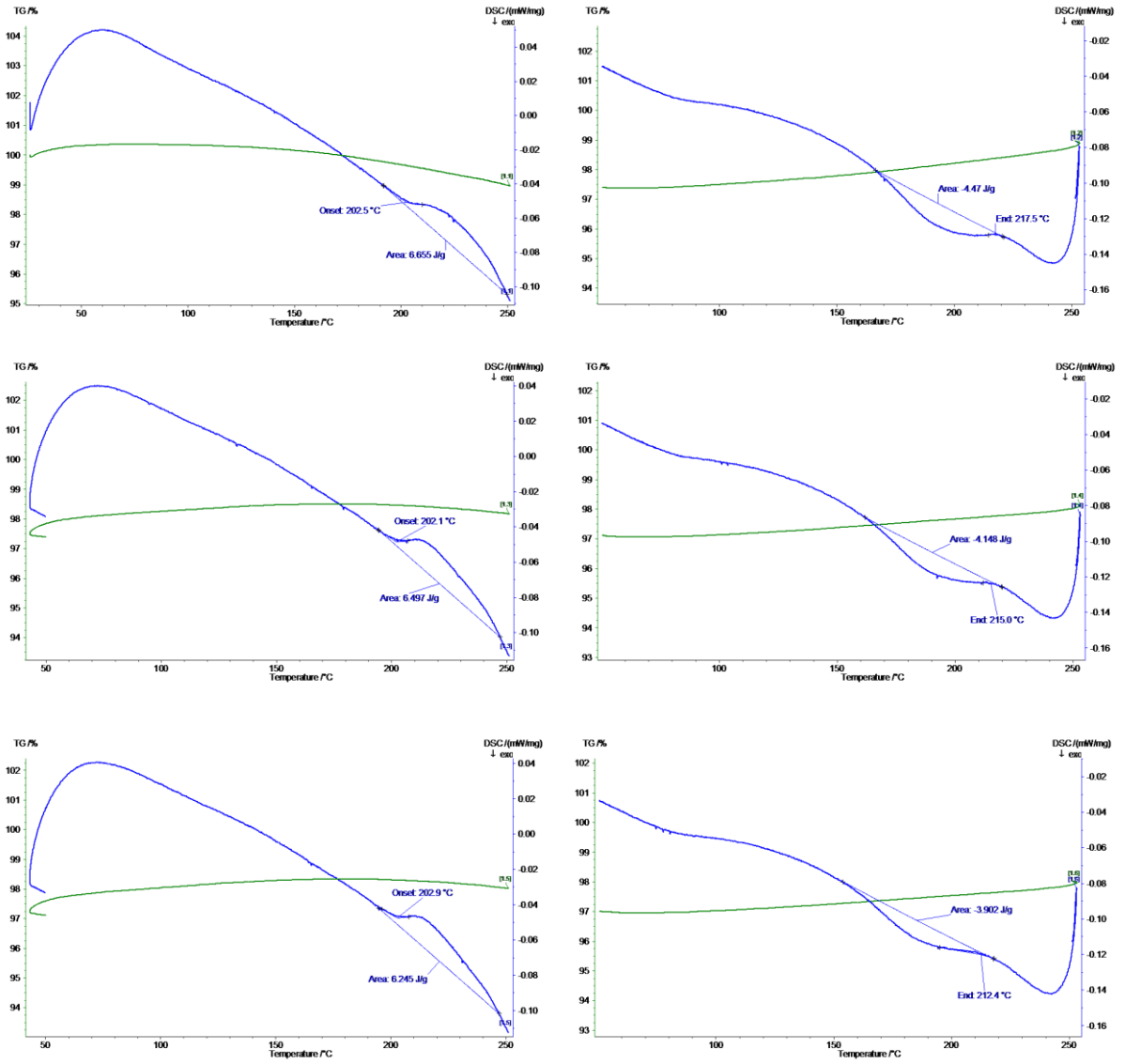

Figure S58: DSC curves of **{$2_{0.50}3_{0.50}$}dry** measured from 30 – 250 °C with a heating rate of 5 °C min^{-1}. The first cycle is depicted on top, second cycle in the middle and third cycle at the bottom with the heating and cooling branch left and right, respectively.

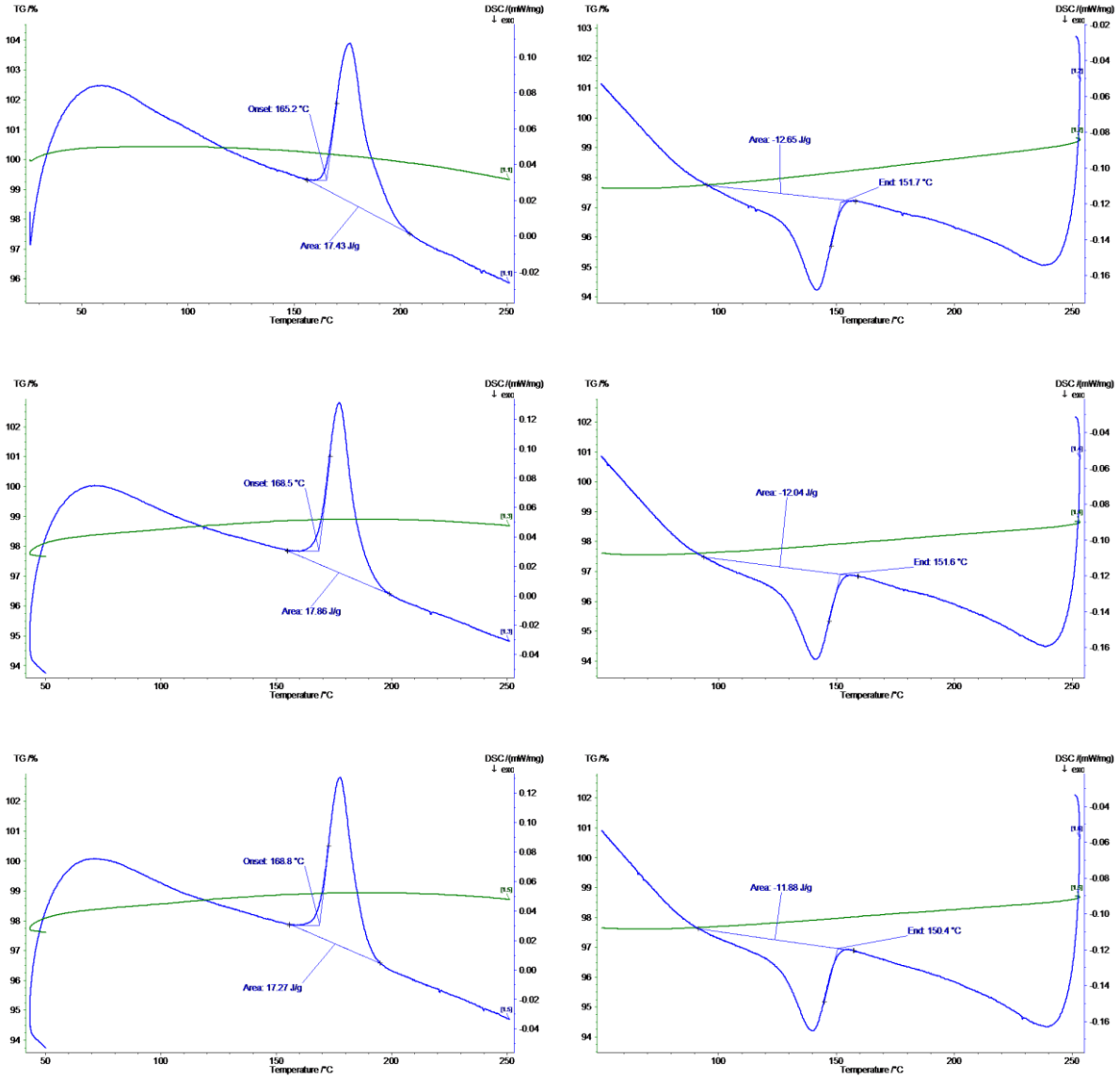

Figure S59: DSC curves of **{$2_{0.25}3_{0.75}$}dry** measured from 30 – 250 °C with a heating rate of 5 °C min^{-1}. The first cycle is depicted on top, second cycle in the middle and third cycle at the bottom with the heating and cooling branch left and right, respectively.

5 Sorption studies

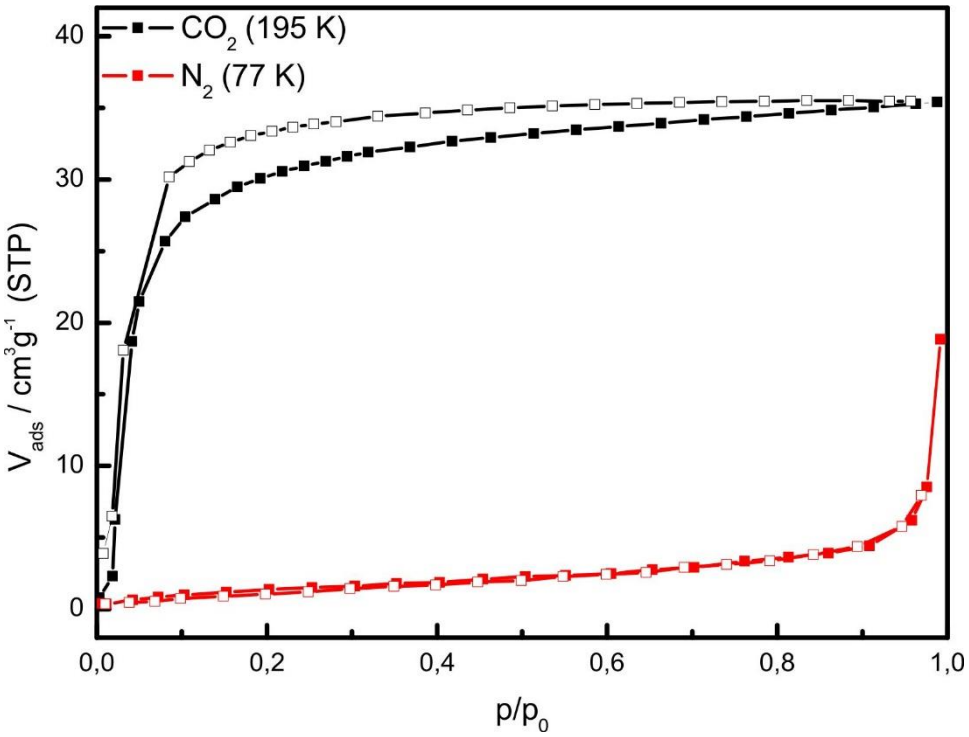

Figure S60: N_2 and CO_2 sorption isotherms of the parent compounds **4dry** measured at 77 K and 195 K. The adsorption and desorption branches are depicted with solid and open symbols, respectively. The connecting lines do not have a physical meaning and are only depicted for visual support.

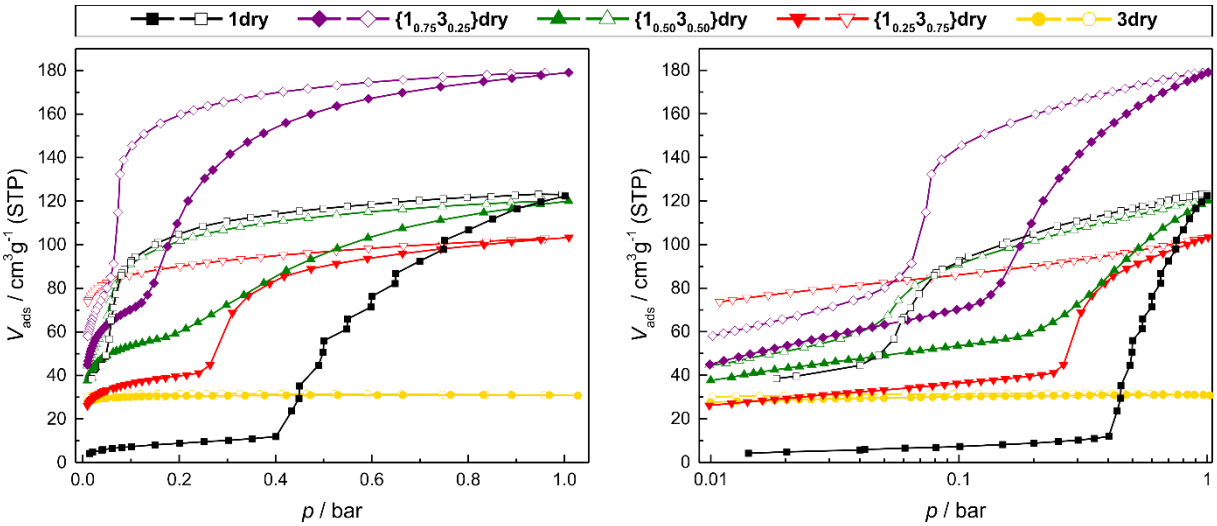

Figure S61: CO_2 sorption isotherms with a linear pressure axis (left) and a logarithmic pressure axis (right) of the parent compounds **1dry** and **3dry** in comparison to the mixed-linker materials **{1$_x$3$_{1-x}$}dry** (x = 0.75, 0.50, 0.25). The adsorption and desorption branches are depicted with solid and open symbols, respectively. The connecting lines do not have a physical meaning and are only depicted for visual support.

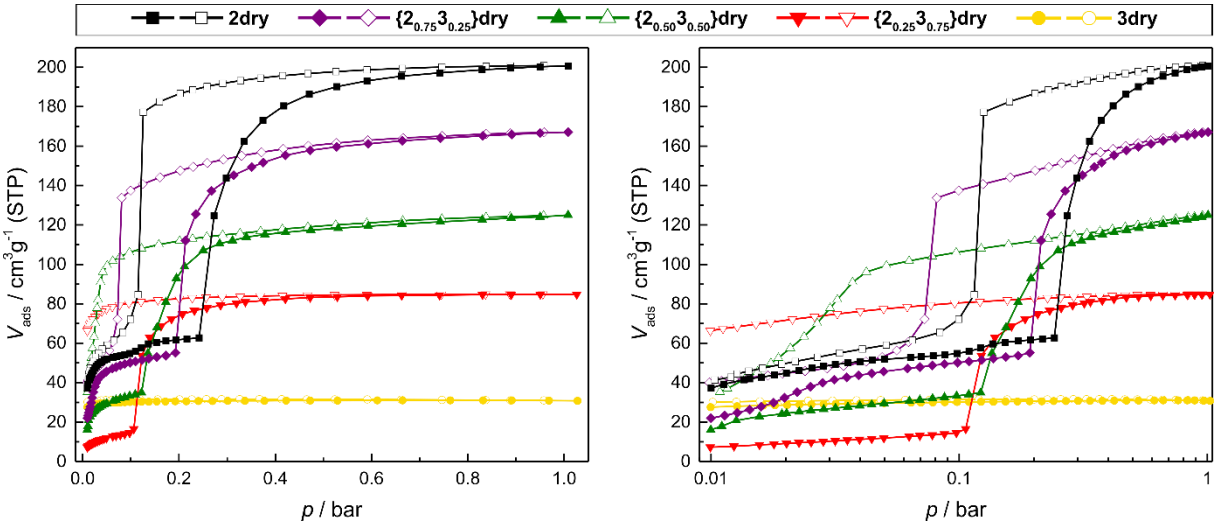

Figure S62: CO_2 sorption isotherms with a linear pressure axis (left) and a logarithmic pressure axis (right) of the parent compounds **2dry** and **3dry** in comparison to the mixed-linker materials **{2$_x$3$_{1-x}$}dry** (x = 0.75, 0.50, 0.25). The adsorption and desorption branches are depicted with solid and open symbols, respectively. The connecting lines do not have a physical meaning and are only depicted for visual support.

6 Thermogravimetric Analysis

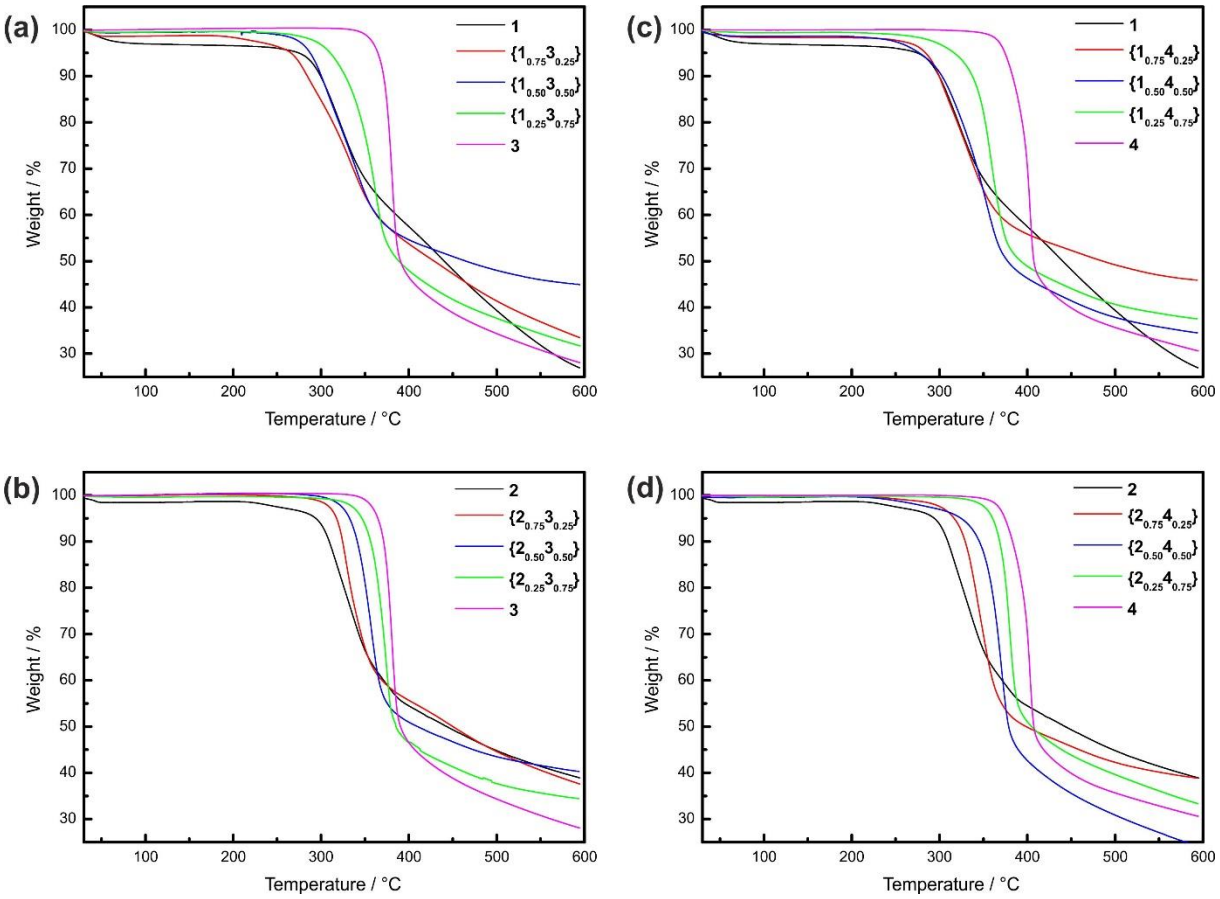

Figure S63: TG curves of dried samples **{1$_x$3$_{1-x}$}** (a), **{2$_x$3$_{1-x}$}** (b), **{1$_x$4$_{1-x}$}** (c), **{2$_x$4$_{1-x}$}** (d) in comparison to their respective parent frameworks **1**, **2**, **3** and **4**. In case of **1dry**, **{1$_{0.75}$3$_{0.25}$}dry** and **2dry**, a small weight loss is observed at temperatures below 250 °C. Presence of DMF molecules from the synthesis can be excluded due to ^{1}H NMR spectroscopic data (see Figure S65, S66, S69). Since the activated materials were stored under air, small amounts of water may have been adsorbed, which is in accordance with results obtained from elemental analysis.

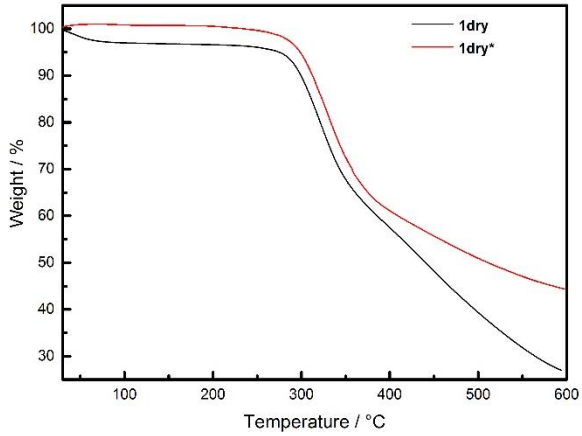

Figure S64: TG curves of dried samples **1dry** and **1dry***. **1dry*** was immediately stored in a glove box under fully exclusion of air, while **1dry** was stored in air after activation

7 ^{1}H and ^{13}C NMR spectra of activated MOFs

Figure S65: ^{1}H and ^{13}C NMR spectra (top and bottom respectively) of a digested sample of **1dry** in DMSO-d_6/DCl(20%)/D_2O. Signals originating from dabco are assigned with a hash (#), the solvent signals are marked with an asterisk (*). The ratio of DM-bdc:dabco is as expected 2:1. Furthermore, the NMR spectra confirm the absence of any guest molecules (DMF or CH_2Cl_2).

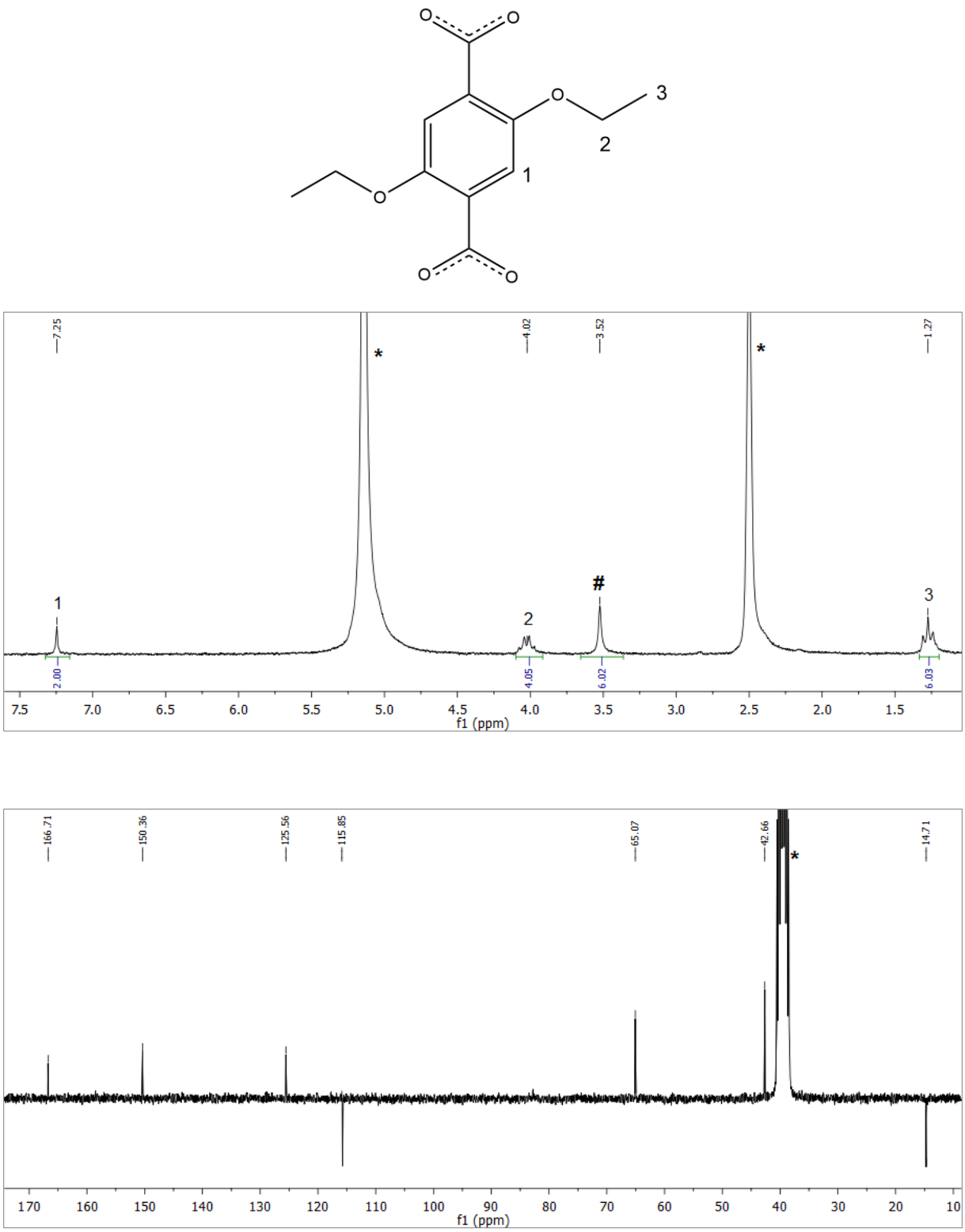

Figure S66: ^{1}H and ^{13}C NMR spectra (top and bottom respectively) of a digested sample of **2dry** in DMSO-d_6/DCl(20%)/D_2O. Signals originating from dabco are assigned with a hash (#), the solvent signals are marked with an asterisk (*). The ratio of DE-bdc:dabco is as expected 2:1. Furthermore, the NMR spectra confirm the absence of any guest molecules (DMF or CH_2Cl_2).

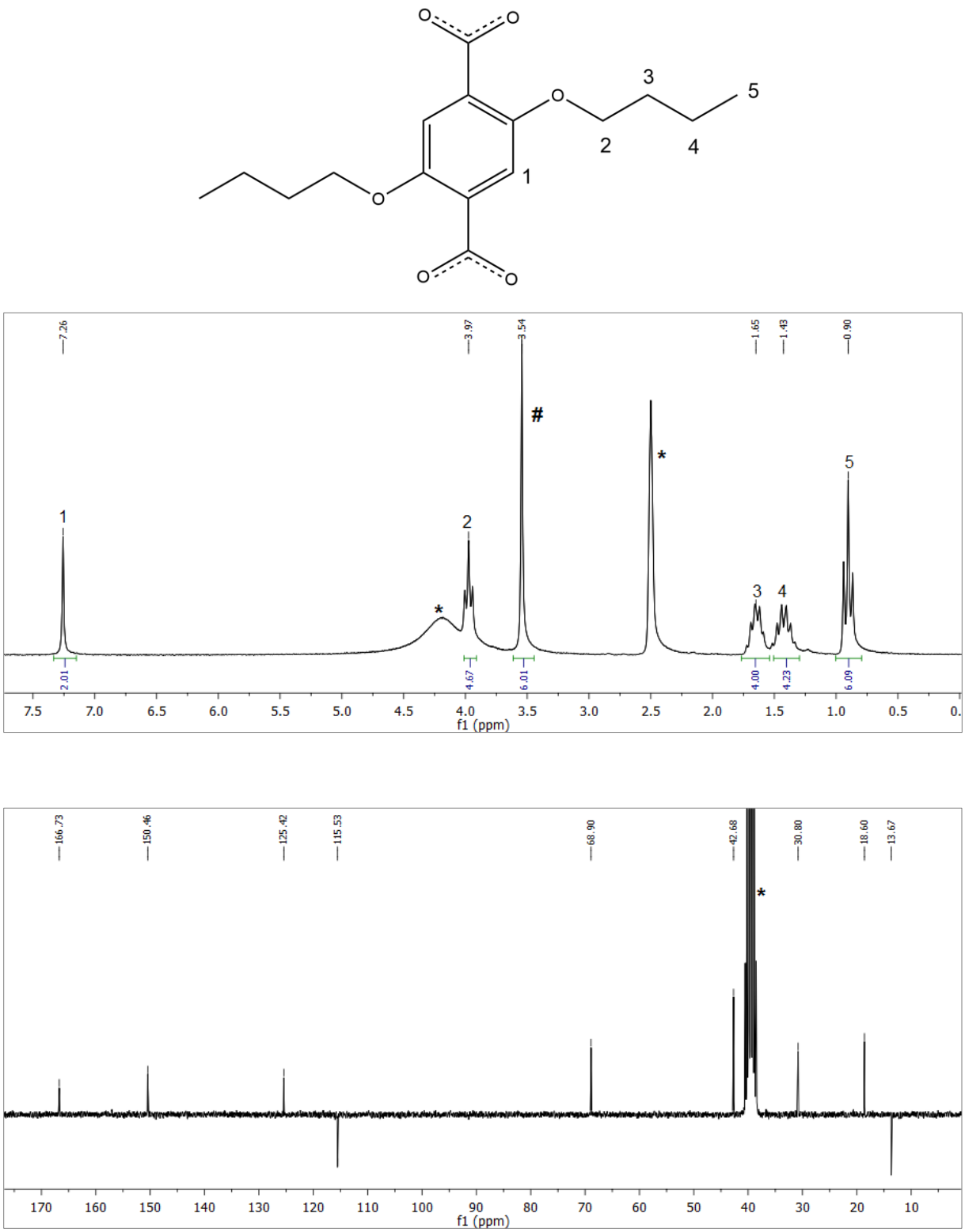

Figure S67: ^{1}H and ^{13}C NMR spectra (top and bottom respectively) of a digested sample of **3dry** in DMSO-d_6/DCl(20%)/D_2O. Signals originating from dabco are assigned with a hash (#), the solvent signals are marked with an asterisk (*). The ratio of DB-bdc:dabco is as expected 2:1. Furthermore, the NMR spectra confirm the absence of any guest molecules (DMF or CH_2Cl_2).

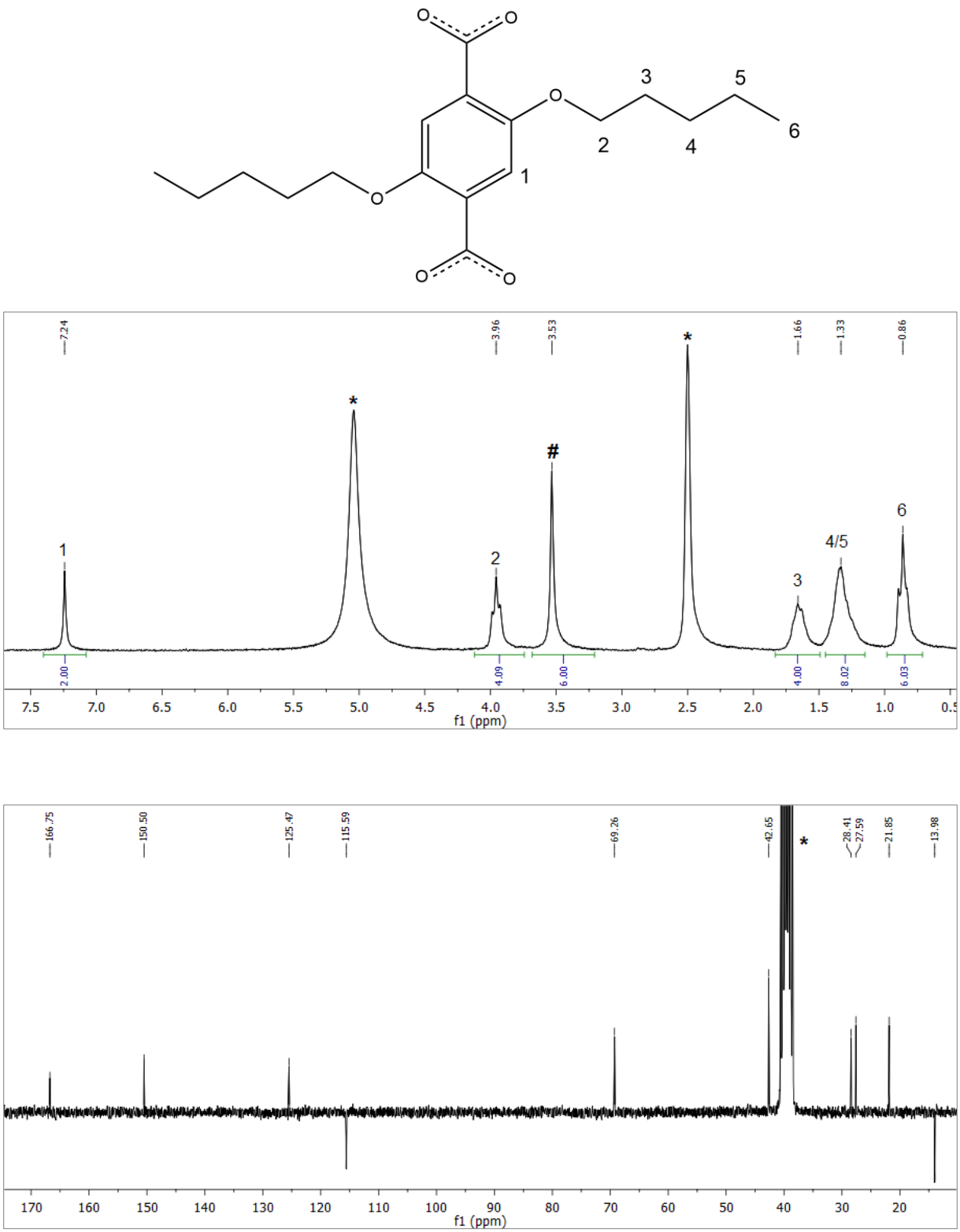

Figure S68: ^{1}H and ^{13}C NMR spectra (top and bottom respectively) of a digested sample of **4dry** in DMSO-d_6/DCl(20%)/D_2O. Signals originating from dabco are assigned with a hash (#), the solvent signals are marked with an asterisk (*). The ratio of DPe-bdc:dabco is as expected 2:1. Furthermore, the NMR spectra confirm the absence of any guest molecules (DMF or CH_2Cl_2).

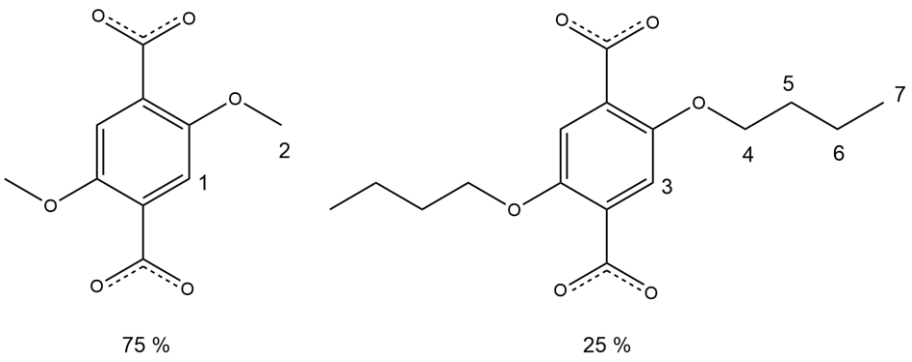

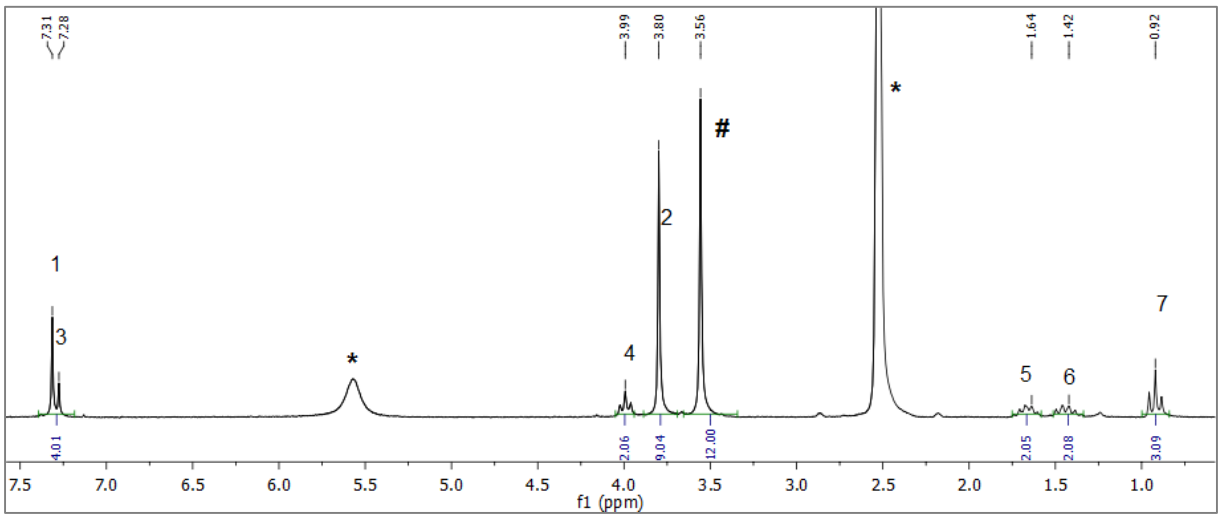

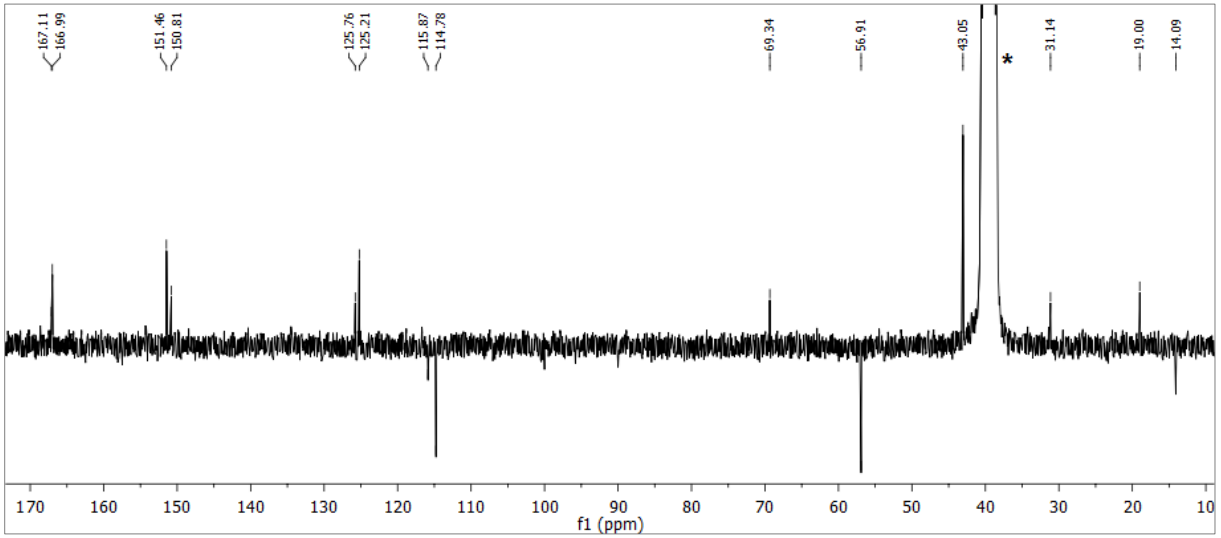

Figure S69: ^{1}H and ^{13}C NMR spectra (top and bottom respectively) of a digested sample of **{$1_{0.75}3_{0.25}$}dry** in DMSO-d_6/DCl(20%)/D_2O. Signals originating from dabco are assigned with a hash (#), the solvent signals are marked with an asterisk (*). Integration of the signals shows that the ratio of DM-bdc:DB-bdc:dabco is as expected and approximatively equal to 1.5:0.5:1.0. Furthermore, the NMR spectra confirm the absence of any guest molecules (DMF or CH_2Cl_2).

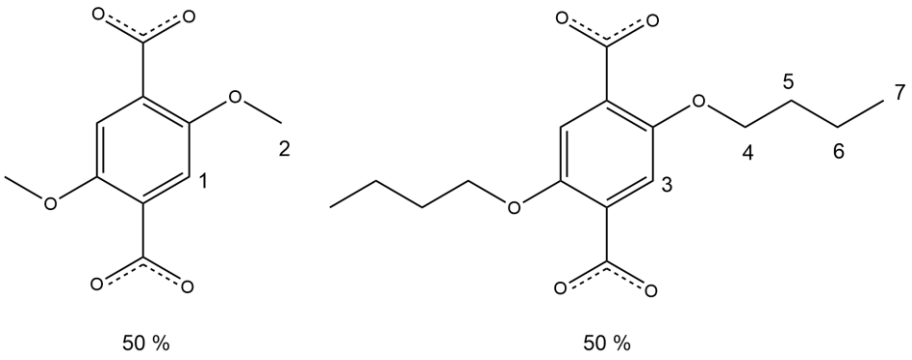

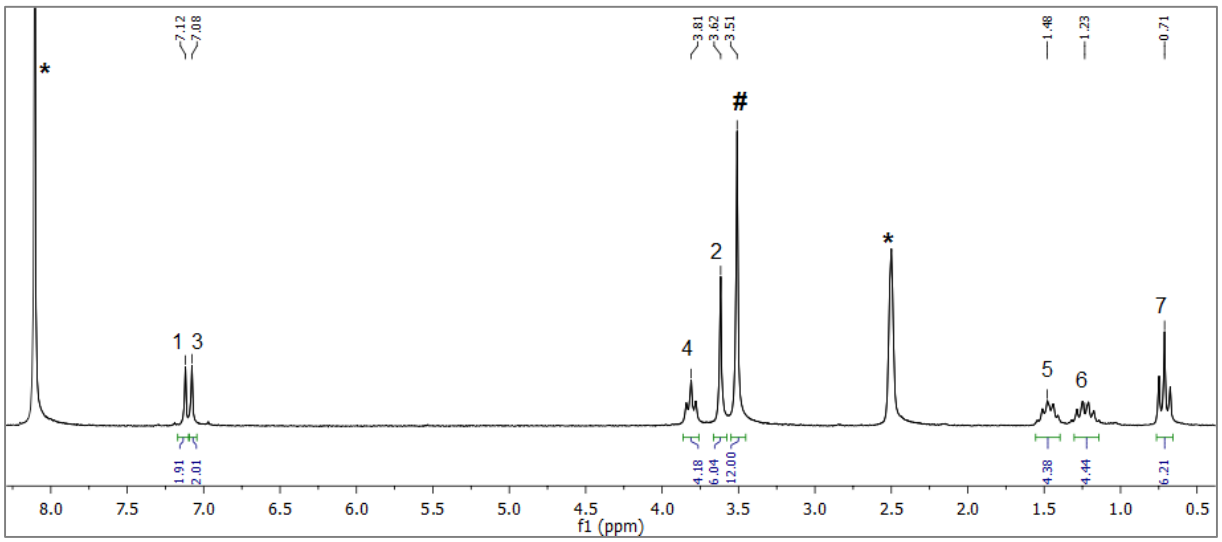

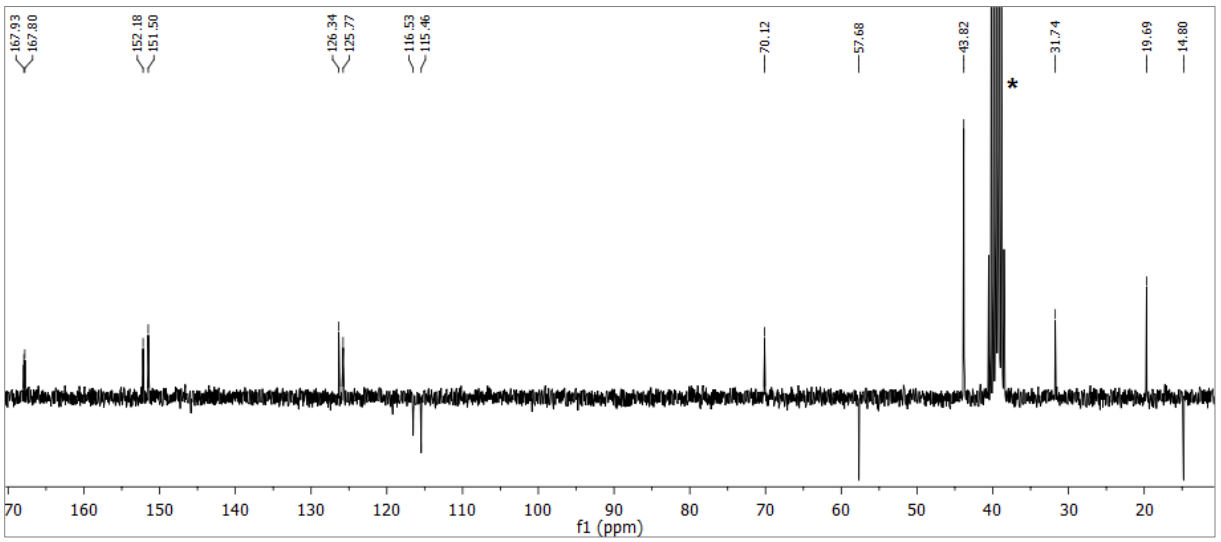

Figure S70: ^{1}H and ^{13}C NMR spectra (top and bottom respectively) of a digested sample of **{$1_{0.50}3_{0.50}$}dry** in DMSO-d_6/DCl(20%)/D_2O. Signals originating from dabco are assigned with a hash (#), the solvent signals are marked with an asterisk (*). Integration of the signals shows that the ratio of DM-bdc:DB-bdc:dabco is as expected and approximatively equal to 1.0:1.0:1.0. Furthermore, the NMR spectra confirm the absence of any guest molecules (DMF or CH_2Cl_2).

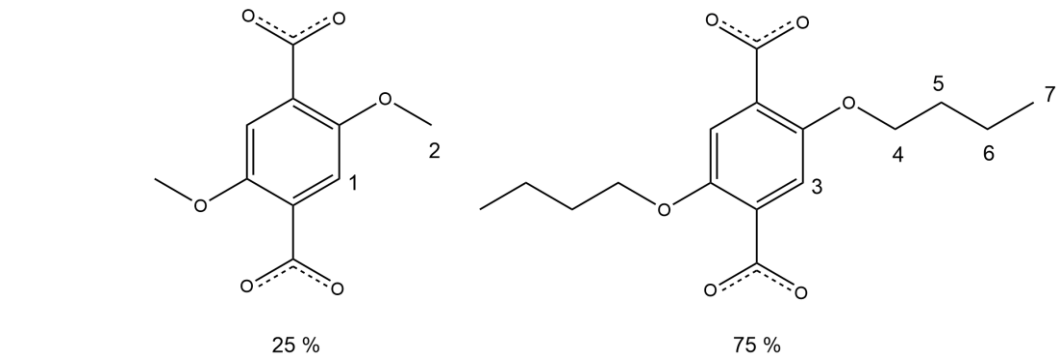

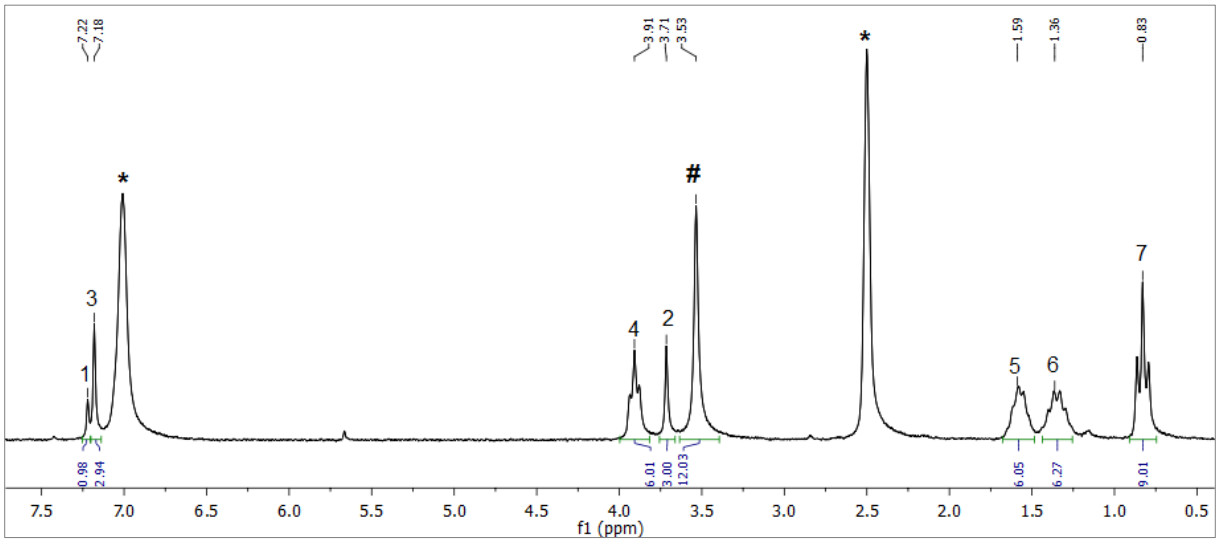

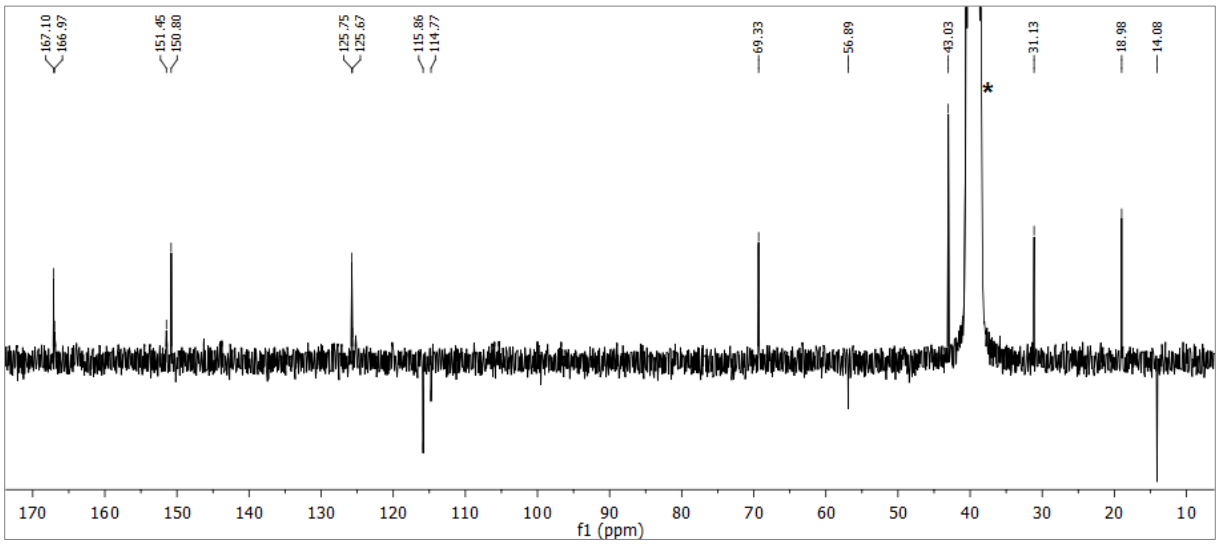

Figure S71: ^{1}H and ^{13}C NMR spectra (top and bottom respectively) of a digested sample of **{1$_{0.25}$3$_{0.75}$}dry** in DMSO-d_6/DCl(20%)/D_2O. Signals originating from dabco are assigned with a hash (#), the solvent signals are marked with an asterisk (*). Integration of the signals shows that the ratio of DM-bdc:DB-bdc:dabco is as expected and approximatively equal to 0.5:1.5:1.0. Furthermore, the NMR spectra confirm the absence of any guest molecules (DMF or CH_2Cl_2).

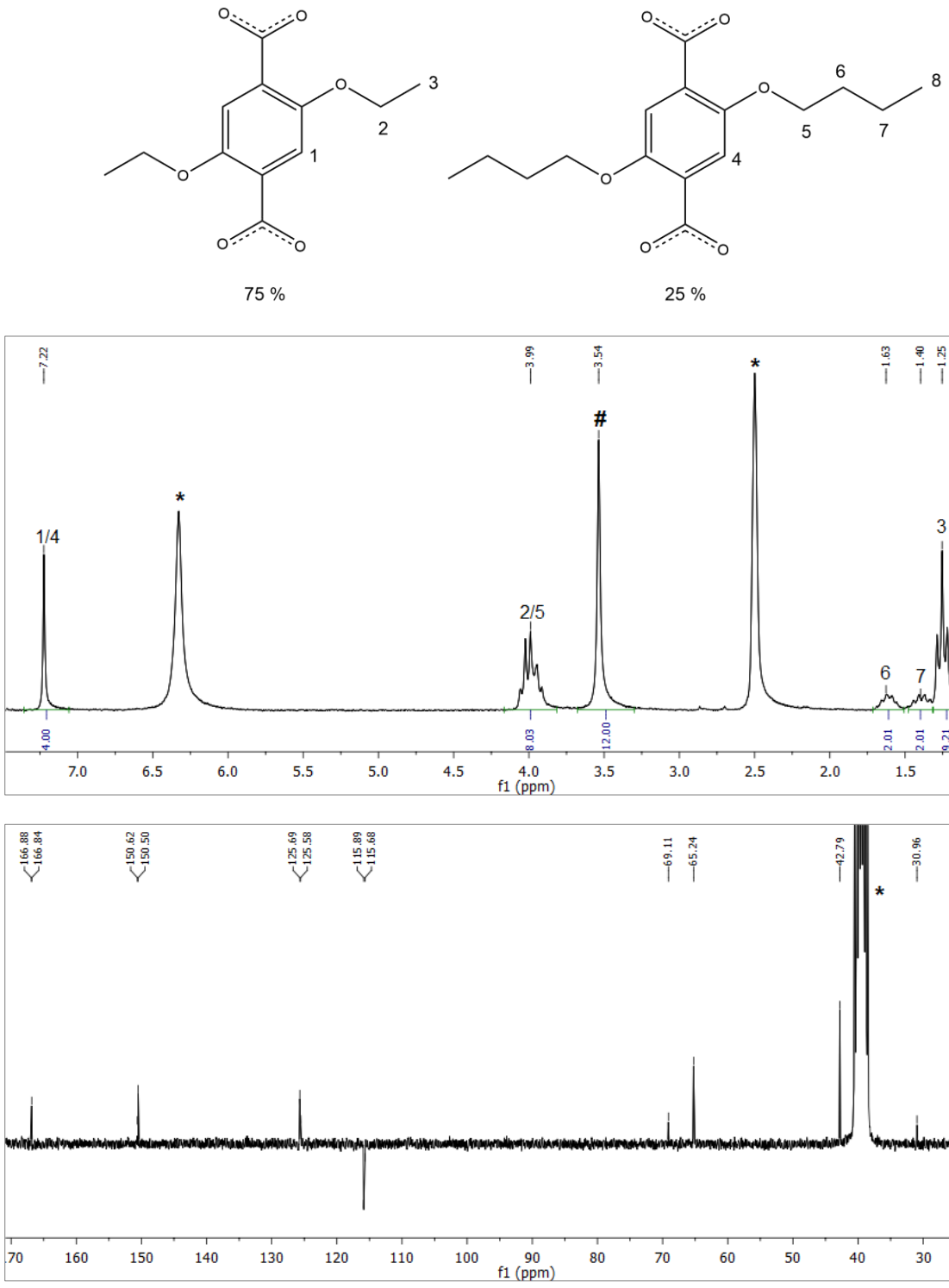

Figure S72: ^{1}H and ^{13}C NMR spectra (top and bottom respectively) of a digested sample of **{2$_{0.75}$3$_{0.25}$}dry** in DMSO-d_6/DCl(20%)/D_2O. Signals originating from dabco are assigned with a hash (#), the solvent signals are marked with an asterisk (*). The aromatic signals 1 and 4 feature a very similar shift and therefore only one signal is observed in the ^{1}H NMR spectrum. Also signals 2 and 5 are very similar and overlay to a multiplet. The ratio of DE-bdc:DB-bdc:dabco is as expected 1.5:0.5:1.0. Furthermore, the NMR spectra confirm the absence of any guest molecules (DMF or CH_2Cl_2).

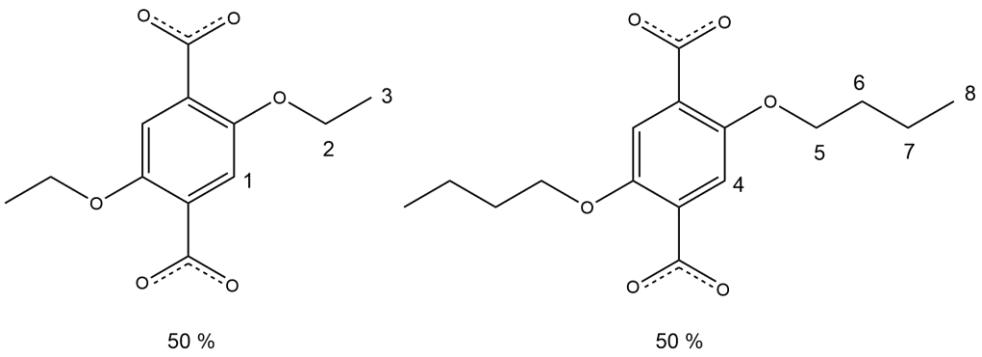

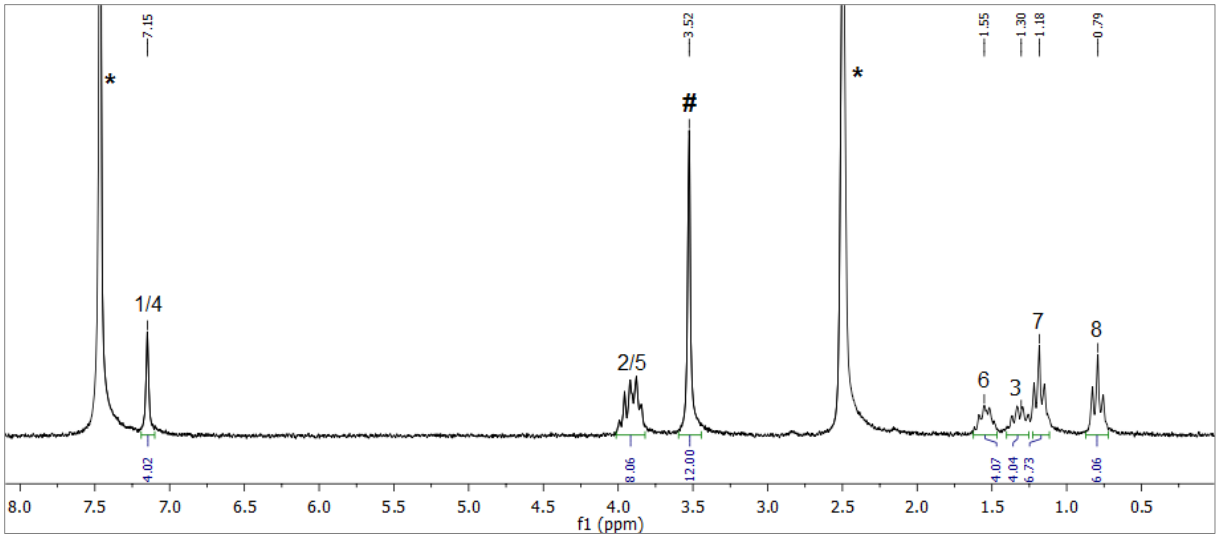

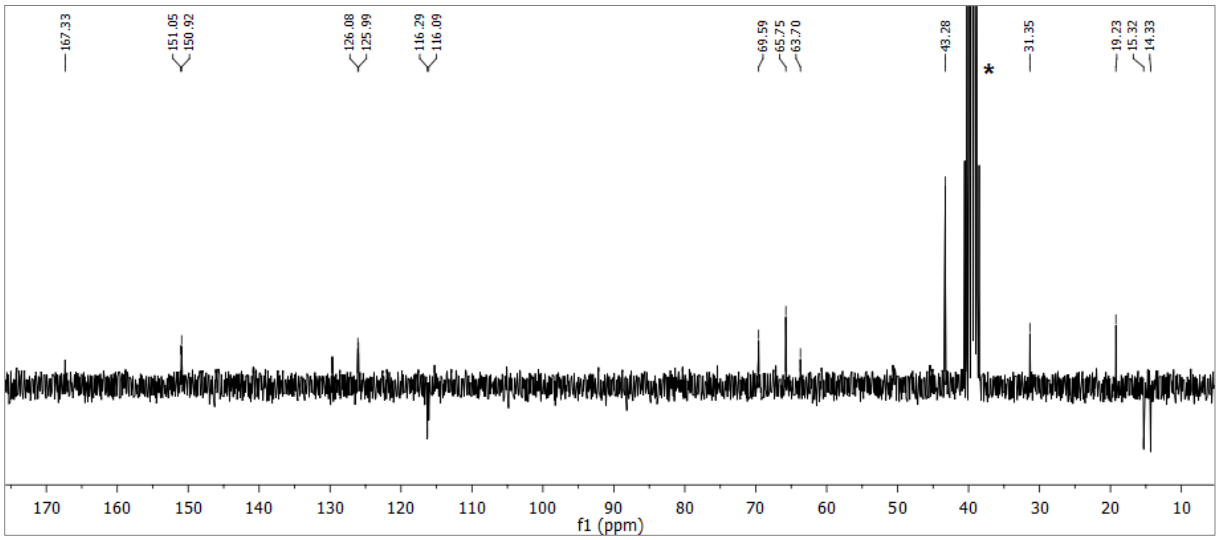

Figure S73: ^{1}H and ^{13}C NMR spectra (top and bottom respectively) of a digested sample of **{$2_{0.50}3_{0.50}$}dry** in DMSO-d_6/DCl(20%)/D_2O. Signals originating from dabco are assigned with a hash (#), the solvent signals are marked with an asterisk (*). The aromatic signals 1 and 4 feature a very similar shift and therefore only one signal is observed in the ^{1}H NMR spectrum. Also signals 2 and 5 are very similar and overlay to a multiplet. The ratio of DE-bdc:DB-bdc:dabco is as expected 1.0:1.0:1.0. Furthermore, the NMR spectra confirm the absence of any guest molecules (DMF or CH_2Cl_2).

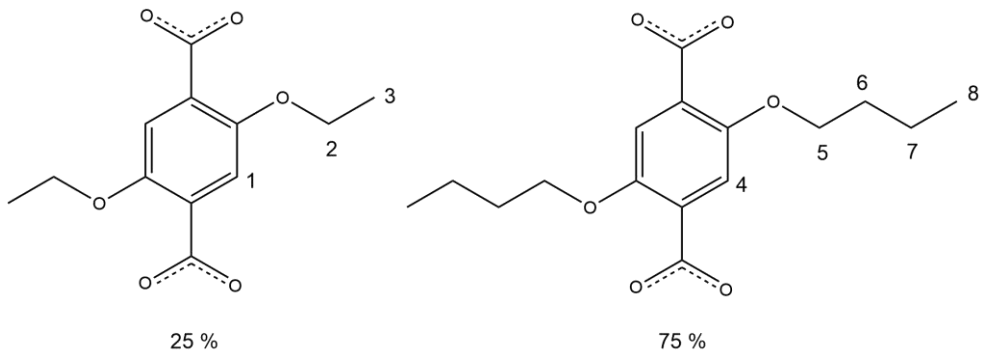

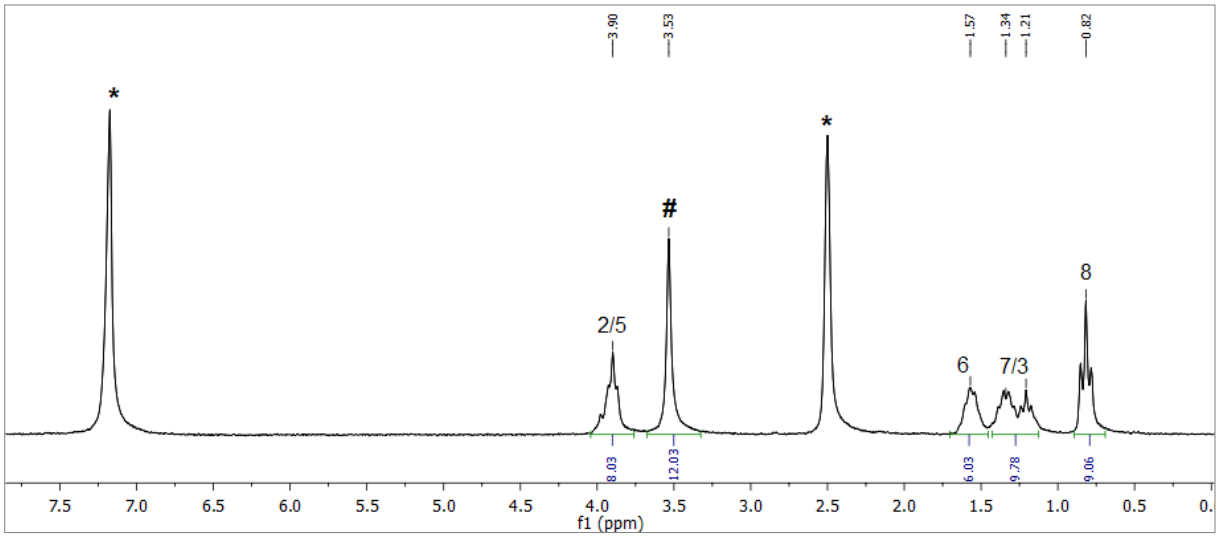

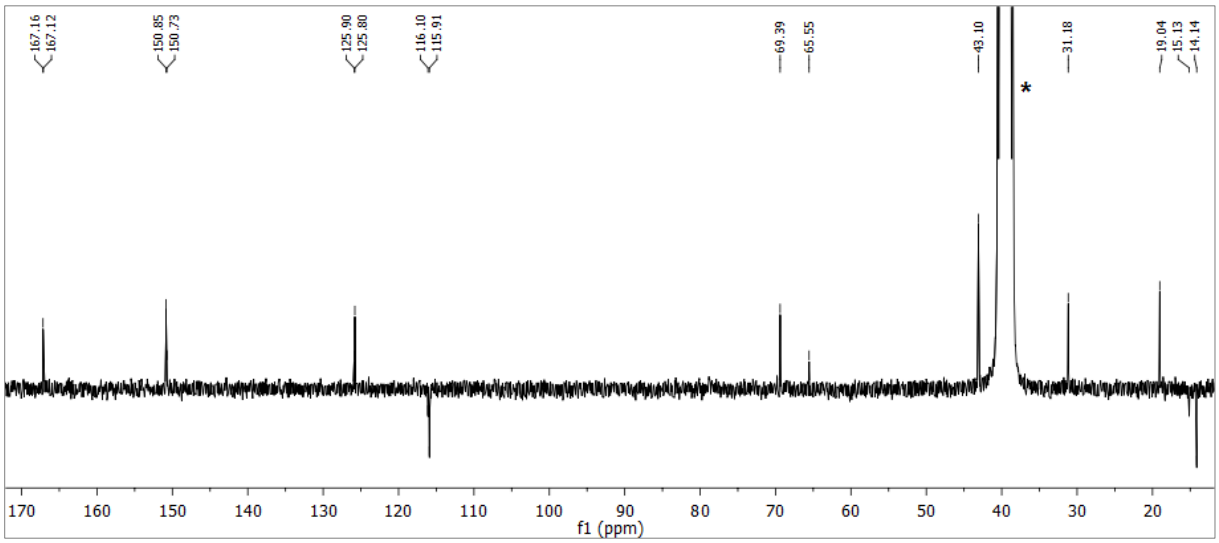

Figure S74: ^{1}H and ^{13}C NMR spectra (top and bottom respectively) of a digested sample of **{2$_{0.25}$3$_{0.75}$}dry** in DMSO-d_6/DCl(20%)/D_2O. Signals originating from dabco are assigned with a hash (#), the solvent signals are marked with an asterisk (*). The aromatic signals 1 and 4 are overlaid by the D_2O/DCl peak at 7.2 ppm in the ^{1}H NMR spectrum. Also signals 2 and 5 are very similar and overlay to a multiplet. The ratio of DE-bdc:DB-bdc:dabco is as expected 0.5:1.5:1.0. Furthermore, the NMR spectra confirm the absence of any guest molecules (DMF or CH_2Cl_2).

8 References

1. T. Boehle, F. Eissmann, E. Weber and F. O. R. L. Mertens, *Acta Cryst.*, 2011, **C67**, m5-m8.
2. K. Tan, N. Nijem, P. Canepa, Q. Gong, J. Li, T. Thonhauser and Y. J. Chabal, *Chem. Mater.*, 2012, **24**, 3153-3167.
3. S. Henke, A. Schneemann, A. Wütscher and R. A. Fischer, *J. Am. Chem. Soc.*, 2012, **134**, 9464-9474.
4. A. Coelho, *TOPAS-Academic v5*, Coehlo Software, Brisbane, Australia, 2012.
5. S. Henke, A. Schneemann and R. A. Fischer, *Adv. Funct. Mater.*, 2013, **23**, 5966-5966.